

**Regulation of nuclear factor kappa-light-chain-enhancer of activated B cells
(NF-κB) by protein Kinase C theta (PKC-θ) and cylindromatosis (CYLD) in
murine listeriosis and toxoplasmosis**

**Dissertation
zur Erlangung des akademischen Grades**

**doctor rerum naturalium
(Dr. rer. nat.)**

**genehmigt durch die Fakultät für Naturwissenschaften
der Otto-von-Guericke-Universität Magdeburg**

**von: M.Sc (Biotechnology) Nishanth Gopala Krishna
geb. am 26.Dezember 1980 in Hyderabad, Indien**

**Gutachter: Prof. Dr. med. Dirk Schlüter
Prof. Dr. rer. nat. Astrid M. Westendorf**

**eingereicht am 27.August 2013
verteidigt am 04.Dezember 2013**

Acknowledgements

I would like to specially thank my supervisor Prof. Dirk Schlüter for providing me the opportunity to do my doctoral thesis under his supervision in his laboratory. His immense patience, support and motivation are commendable. I would like to thank him for giving me the opportunity to attend various conferences and his guidance in helping me to present posters and give presentations.

I would like to thank my second supervisor Prof. Michael Naumann for accepting me to the GRK1167 and also his valuable inputs during the thesis committee meetings. I thank Prof. Martina Deckert and Elena Fischer for their assistance in the preparation, staining and histological evaluation of the preparations.

I express my gratitude to Dr. Katrin Boroucki for her support in the determination of liver enzymes.

These collaborations facilitated the smooth progress and successful completion of the projects. I am grateful to Dr. Monika Sakowicz-Burkiewicz who guided me in the beginning of my work by introducing me to the working techniques and methods in the lab.

I would like to thank all the members of our group and a special mention to our lab technicians Ms. Annette Sohnekind, Ms. Nadja Schlüter and Ms. Dana Zabler for their support and help and also Ms. Anita Marquardt for breeding the mice.

Last but not the least I would like to thank my family and friends for their constant support and encouragement during my entire doctoral thesis period.

Publications

This work is published under the following titles:

Sakowicz-Burkiewicz M, **Nishanth G**, Helmuth U, Drögemüller K, Busch DH, Utermöhlen O, Naumann M, Deckert M, Schlüter D. (2008) Protein kinase C-theta critically regulates the proliferation and survival of pathogen-specific T cells in murine listeriosis. *J Immunol.* Apr 15; 180(8):5601-12.

Nishanth G, Sakowicz-Burkiewicz M, Händel U, Kliche S, Wang X, Naumann M, Deckert M, Schlüter D. (2010) Protective *Toxoplasma gondii*-specific T-cell responses require T-cell-specific expression of protein kinase C-theta. *Infect Immun.* Aug; 78(8):3454-64.

Nishanth G, Deckert M, Wex K, Massoumi R, Schweitzer K, Naumann M, Schlüter D. (2013) CYLD enhances severe listeriosis by impairing IL-6/STAT3-dependent fibrin production. *PLoS Pathog.* 9(6): e1003455. doi:10.1371/journal.ppat.1003455.

Other Publications

Haroon F, Drögemüller K, Händel U, Brunn A, Reinhold D, **Nishanth G**, Mueller W, Trautwein C, Ernst M, Deckert M, Schlüter D .(2011) Gp130-dependent astrocytic survival is critical for the control of autoimmune central nervous system inflammation. *J Immunol.* Jun 1; 186(11):6521-31.

Pick J, Arra Aditya, Hegel K, Lingel H, **Nishanth G**, Fischer K.D, Tedford K, Schlüter D, and Brunner-Weinzierl M. CD152 (CTLA-4) unleashes a Tc17 differentiation program with sustainability. *European Journal of Immunology, under revision.*

Table of Contents

Acknowledgements	II
Publications	III
Table of Contents.....	IV
Abbreviations	VIII
1. Introduction.....	1
1.1 <i>Listeria monocytogenes</i>	2
1.1.1 Pathogenesis of listeriosis	2
1.1.1.1 Immune response to <i>Listeria monocytogenes</i>	3
1.2 <i>Toxoplasma gondii</i>	4
1.2.1 Pathogenesis of toxoplasmosis	4
1.2.1.1 Immune response to <i>Toxoplasma gondii</i>	6
1.3 NF-κB pathway	7
1.3.1 The canonical NF-κB pathway	7
1.3.1.1 The non-canonical NF-κB pathway	7
1.3.1.1.1 The atypical NF-κB pathway	9
1.4 Regulation of T cell response by PKC-θ	9
1.5 Ubiquitination/ Deubiquitination	12
1.6 Regulation of immune response by CYLD.....	14
2. Aims.....	16
2.1 Function of PKC-θ in murine listeriosis	16
2.1.1 Role of PKC-θ in murine toxoplasmosis	16
2.1.1.1 Regulation of murine listeriosis and toxoplasmosis by CYLD	16
3. Materials and methods	17
3.1.Materials	17
3.1.1 Chemicals used for animal experiments	17
3.1.2 Materials for cell culture	17
3.1.3 Materials for molecular biology.....	18
3.1.4 Materials for proteomics	20

3.1.5 Instruments.....	24
3.1.6 Animals	25
3.2 Methods.....	26
3.2.1 Genotyping of the mice strains	26
3.2.2 Bacterial, viral and parasitic infection of mice	26
3.2.3 Blood and organ isolation	27
3.2.4 Isolation of leukocytes from blood, mesenteric lymph node, spleen, liver and brain	27
3.2.5 Flow Cytometry	27
3.2.6 Cytometric bead assay	28
3.2.7 Magnetic-activated cell sorting (MACS) of T cells.....	28
3.2.8 ELISPOT.....	29
3.2.9 Bone marrow-derived dendritic cell (BMDC) and macrophages (BMDM) culture.....	29
3.2.10 Immunization with peptide-coated bone marrow-derived DC	30
3.2.11 Adoptive transfer of T cells	30
3.2.12 Detection of antigen (Ag)-specific CD8 T cells by flow cytometry.....	30
3.2.13 Carboxyfluorescein diacetate succinimidyl ester (CSFE) labeling of cells.....	30
3.2.14 T cell proliferation and activation.....	30
3.2.16 Measurement of apoptosis by flow cytometry.....	31
3.2.16 <i>In vitro</i> infection of DCs with <i>L. monocytogenes</i>	31
3.2.17 <i>In vitro</i> proliferation of T cells.....	31
3.2.18 Immunohistochemistry	32
3.2.19 Reverse transcription-PCR (RT-PCR).....	32
3.2.20 Determination of alanine aminotransferase (ALT) and aspartate aminotransferase (AST)	33
3.2.21 Hepatocyte culture	33
3.2.22 Transfection of hepatocytes	33
3.2.23 Protein isolation and Western blot.....	34
3.2.24 Immunoprecipitation.....	34
3.2.25 ROS assay	35
3.2.26 Affinity purification of anti-IL6 antibody.....	35
3.2.27 IL-6 neutralization	35

3.2.28 Warfarin treatment	35
3.2.29 <i>In vivo</i> small interfering RNA (siRNA) treatment.....	36
3.2.30 Statistics	36
4. Results	37
4.1.1 Function of PKC-θ in murine listeriosis	37
4.1.1.1 PKC-θ is essential for the generation of <i>L. monocytogenes</i> -specific, but not for LCMV-specific CD4 and CD8 T cells.....	37
4.1.1.2 Reduced numbers of MHC class Ia-, MHC class Ib-, and MHC class II-restricted <i>L. monocytogenes</i> -specific T cells in primary and secondary listeriosis of PKC-θ ^{-/-} mice.....	38
4.1.1.3 Impaired control of <i>L. monocytogenes</i> in PKC-θ ^{-/-} mice	39
4.1.1.4 The reduction of <i>L. monocytogene</i> -specific CD8 and CD4 T cells in PKC-θ ^{-/-} mice is organ-dependent	40
4.1.1.5 The role of PKC-θ for the generation of <i>L. monocytogenes</i> -specific T cells and bacterial control is independent of the host genetic background	42
4.1.1.6 Adoptive transfer of WT T cells compensates for PKC-θ-deficiency in listeriosis	43
4.1.1.7 PKC-θ is important for proliferation and survival of <i>L. monocytogenes</i> -specific CD8 T cells, but its function can be partially compensated by neighbouring WT cells.....	45
4.1.1.8 Externally supplemented IL-2, but not inhibition of caspases partially restores proliferation of PKC-θ ^{-/-} T cells <i>in vitro</i>	47
4.1.2 Role of PKC-θ in murine toxoplasmosis	51
4.1.2.1 Infection with <i>T. gondii</i> induces sustained phosphorylation of PKC-θ in CD4 and CD8 T cells	51
4.1.2.2 BALB/c PKCθ ^{-/-} mice succumb to a necrotizing <i>Toxoplasma</i> encephalitis (TE).....	51
4.1.2.3 Reduced numbers of CD4 and CD8 T cells in spleen and brain of <i>T. gondii</i> -infected PKC-θ ^{-/-} mice	52
4.1.2.4 Diminished <i>T. gondii</i> -specific CD4 and CD8 T cell response in PKC-θ ^{-/-} mice	53
4.1.2.5 Reduced cytokine responses in PKC-θ ^{-/-} mice	56
4.1.2.6 Impaired activation of NF-κB, AP1, and ERK in PKC-θ ^{-/-} mice	56
4.1.2.7 Reduced <i>T. gondii</i> -specific IgG production in serum and CSF of PKC-θ ^{-/-} mice.	57
4.1.2.6 WT T cells compensate for PKC-θ-deficiency in toxoplasmosis.....	58
4.2 Regulation of murine listeriosis and toxoplasmosis by CYLD	61
4.2.1 CYLD does not influence the course of <i>Toxoplasma</i> encephalitis	61
4.2.2 CYLD does not influence the course of low dose <i>L. monocytogenes</i> infection.....	62
4.2.3 CYLD prevented survival from severe listeriosis and aggravated liver pathology in listeriosis.....	62
4.2.3.1 CYLD impaired IL-6, IFN-γ and NOX2 mRNA production and recruitment of myeloid cells to the liver.....	64

4.2.3.2 CYLD reduced IL-6, ROS production and killing of <i>L. monocytogenes</i> in macrophages by impairing NF-κB activation.....	66
4.2.3.3 CYLD impaired IL-6-mediated STAT3 activation and fibrin production in hepatocytes by deubiquitination of cytoplasmic STAT3.....	68
4.2.3.3 CYLD reduced activation of p65, JAK2, STAT3, and p38 MAPK as well as fibrin production in livers of <i>L. monocytogenes</i> -infected WT mice	70
4.2.3.4 The protection of <i>Cyld</i> ^{-/-} mice against lethal listeriosis is dependent on IL-6, STAT3 and fibrin.....	72
4.2.3.5 Inhibition of STAT3 reduces fibrin production, survival and pathogen control in <i>L. monocytogenes</i> -infected <i>Cyld</i> ^{-/-} mice.....	73
4.2.3.6 Inhibition of fibrin production abolished protection and increased the hepatic bacterial load of <i>Cyld</i> ^{-/-} mice.	75
4.2.3.7 Inhibition of CYLD partially protected WT mice from lethal listeriosis	76
4.2.3.8 <i>Cyld</i> -deficiency is protective in cerebral listeriosis.....	77
5. Discussion.....	80
References.....	86
Declaration.....	96
Curriculum vitae.....	97

Abbreviations

A

ActA	Actin-assembly-inducing protein A
Ag	Antigen
ALT	Alanine aminotransferase
AP1	Activated protein 1
APC	Antigen-presenting cell
AST	Aspartate aminotransferase
ATP	Adenosine triphosphate

B

BAFF	B-cell activating factor
Bcl-x _L	B-cell lymphoma-extra large
Bcl-	B-cell lymphoma
BHI	Brain heart infusion medium
BMDC	Bone marrow-derived dendritic cell
BMDM	Bone marrow-derived Macrophages
BSA	Bovine serum albumin

C

CBA	Cytometric Bead Assay
CD	Cluster of differentiation
CSFE	Carboxyfluorescein diacetate succinimidyl ester
CFUs	Colony forming units
CNS	Central nervous system
<i>C_T</i>	Threshold cycle
CTL	Cytotoxic T Lymphocyte
CYLD	Cylindromatosis

D

DC	Dendritic cell
DUBs	Deubiquitinating enzymes

E

ERK	Extracellular signal-regulated kinases
-----	--

G

GM-CSF	Granulocyte-macrophage colony-stimulating factor
--------	--

H

HBSS	Hank's Balanced Salt Solution
------	-------------------------------

HDAC	Histone deacetylase
HEPES	(4-(2-Hydroxyethyl)-1-piperazineethanesulfonic acid
HPRT	Hypoxanthine phosphoribosyltransferase

I

IFN-	Interferon
IKK	IκB kinase
IL-	Interleukin
InLA	Internalin A
InLB	Internalin B
i.p.	Intraperitoneal
Itk	IL-2 inducible T-cell tyrosine kinase
i.v.	Intravenous
IκBs	Inhibitors of NF-κB

J

JAMMs	Jab1/Pab1/MPN-domain-containing metallo-enzymes
JNK	c-Jun N-terminal kinase

K

K	Lysine
---	--------

L

<i>L. monocytogenes</i>	<i>Listeria monocytogenes</i>
LCK	Lymphocyte-specific protein tyrosine kinase
LCMV	Lymphocytic choriomeningitis virus
LLO	Listeriolysin O
LMgp	<i>L. monocytogenes</i> expressing the gp ₃₃₋₄₁ -epitope derived from the glycoprotein of LCMV
LMova	Ovalbumin-expressing <i>L. monocytogenes</i>
LPS	Lipopolysaccharide
LTβ	Lymphotoxin-β

M

MACS	Magnetic-activated cell sorting
MAPK	Mitogen-activated protein kinase
M-CSF	Macrophage colony-stimulating factor
MEKK3	MAP/ERK kinase kinase 3
mLN	Mesenteric lymph node
MHV-68	Murine herpes virus-68
MJDs	Machado–Joseph disease protein domain proteases
Mpl	Metalloprotease

MyD88	Myeloid differentiation primary response gene (88)
N	
NFAT	Nuclear factor of activated T-cells
NF-κB	Nuclear factor 'kappa-light-chain-enhancer' of activated B-cells
NIK	NF-κB inducing kinase
NK	Natural killer
NOX2	gp91 ^{phox} nicotine adenine dinucleotide phosphate oxidase
O	
OT-I	MHC class I-restricted, ovalbumin-specific, CD8 T cells
OT-II	MHC class II-restricted, ovalbumin-specific, CD4 T cells
OTUs	Ovarian tumour-related proteases
P	
PAI-1	Plasminogen activator inhibitor-1
PAS	Periodic acid Schiff
PFA	Paraformaldehyde
PMA	Phorbol 12 - myristate 13-acetate
PBS	Phosphate buffered saline
PKC-θ	Protein kinase C-θ
Plc	Phospholipase C
PTK	Protein tyrosine kinase
R	
RIP-1	Receptor-Interacting Protein-1
Rlk	Resting lymphocyte kinase
ROS	Reactive oxygen species
RT-PCR	Reverse transcription-PCR
S	
siRNA	Small interfering RNA
SMAC	Supramolecular activation complex
STAT-	Signal transducer and activator of transcription
T	
<i>T. gondii</i>	<i>Toxoplasma gondii</i>
TAK1	Transforming growth factor β-activated kinase 1
TCR	T cell receptor
TE	<i>Toxoplasma</i> encephalitis
TGF-β	Transforming growth factor beta
Th	T helper
TLR	Toll like receptor

TNF	Tumor necrosis factor
TPL2	Tumor progression locus 2
TRAF2	TNF receptor-associated factor-2

U

Ub	Ubiquitin
UCHs	Ubiquitin carboxy-terminal hydrolases
USPs	Ubiquitin-specific proteases

W

WB	Western blot
WT	Wildtype

7

7-AAD	7-amino actinomycin D
-------	-----------------------

1. Introduction

The severity and outcome of infectious diseases are strongly regulated by the underlying pathogen and the host immune response to the invading pathogens. In order to effectively control an infectious disease, activation of various cells of the immune system is important. In parallel, multiple pathways exist to control the immune response in order to prevent an immunopathology induced by the hyperactivation of the immune system. Both, the activation and suppression of immune cells is critically regulated by signal transduction molecules expressed by cells of the immune system.

NF-κB (nuclear factor 'kappa-light-chain-enhancer' of activated B-cells), is a key signaling complex responsible for the activation of many genes including immunologically important ones (Lawrence, 2009; Baker et al., 2011; Hayden and Ghosh, 2011). Therefore, the regulation of NF-κB by either inducing or inhibiting signaling pathways holds a centre stage in the regulation of immune responses. Two signaling molecules which regulate NF-κB activation in immune cells are protein kinase C (PKC)-θ and cylindromatosis (CYLD). PKC-θ is a serine-threonine kinase, which is important for the activation of NF-κB in T cells but not in other cells of the immune system (Hayashi and Altman, 2007; Marsland and Kopf, 2008), whereas the deubiquitinase CYLD inhibits NF-κB activity in all cells of the immune system (Sun, 2010; Urbanik et al., 2011; Harhaj and Dixit, 2012). In T cells, CYLD binds directly to PKC-θ and, thereby, inhibits NF-κB and Nuclear factor of activated T-cells (NFAT) activity (Thuille et al., 2013).

The impact of individual signal transduction molecule on the course of different infectious diseases is dependent on the underlying pathogen. Therefore, a functional analysis of signal transduction molecules employing different infectious disease models is of great value to understand the role of signal transduction molecules in host defense. Two important human diseases, which are also widely used in experimental models to study the function of the immune system in infectious diseases, are murine listeriosis and toxoplasmosis.

1.1 *Listeria monocytogenes*

Importantly *L. monocytogenes* is a facultative intracellular bacterium which can infect numerous host cells including hepatocytes and macrophages (Lorber, 1997). *L. monocytogenes* does not cause illness in the general population but may cause life threatening infections in the elderly (>60 years) immunosuppressed persons, transplant patients, patients with impaired cell-mediated immunity and fetuses (Hof et al., 1997). The clinical syndromes associated with listeriosis are neonatal infections, infections of the central nervous system and gastroenteritis (Hof et al., 1997). Apart from its clinical relevance, it is a powerful model to study the role of cell-mediated immunity in resistance to facultative intracellular pathogens.

1.1.1 Pathogenesis of listeriosis

L. monocytogenes infection occurs through the consumption of contaminated food including milk, cheese, vegetables, and meat products. The natural route of infection is via the gastrointestinal tract. *L. monocytogenes* infects intestinal epithelial cells by binding of the bacterial surface proteins internalin A (InlA) and internalin B (InlB), to receptors on the host cell (Braun and Cossart, 2000). Internalin A promotes internalization through E-cadherin, while Internalin B binds to the c-Met receptor tyrosine kinase and mediates internalization. Thereafter, the bacterium traverses the intestine and infects organs such as liver and spleen, where they are taken up by the macrophages (Pamer, 2004). *L. monocytogenes* escapes the host phagosome by secreting listeriolysin O (LLO) (Fig. 1) and enters the cytoplasm (Grenningloh et al., 1997; Hamon et al., 2006). In the cytoplasm, *L. monocytogenes* expresses the actin-assembly-inducing protein A (ActA), which nucleates actin and causes actin polymerization. This propels *Listeria* through the cytoplasm. Importantly, this enables *Listeria* to reach the host cell membrane and to infect neighbouring cells without contact to the extracellular milieu (Pamer, 2004). Here the bacterium is enclosed in a double membrane vacuole called the secondary vacuole. *L. monocytogenes* escapes the secondary vacuole by secreting phospholipase C (PlcA and PlcB), metalloprotease (Mpl) and LLO (Pamer, 2004).

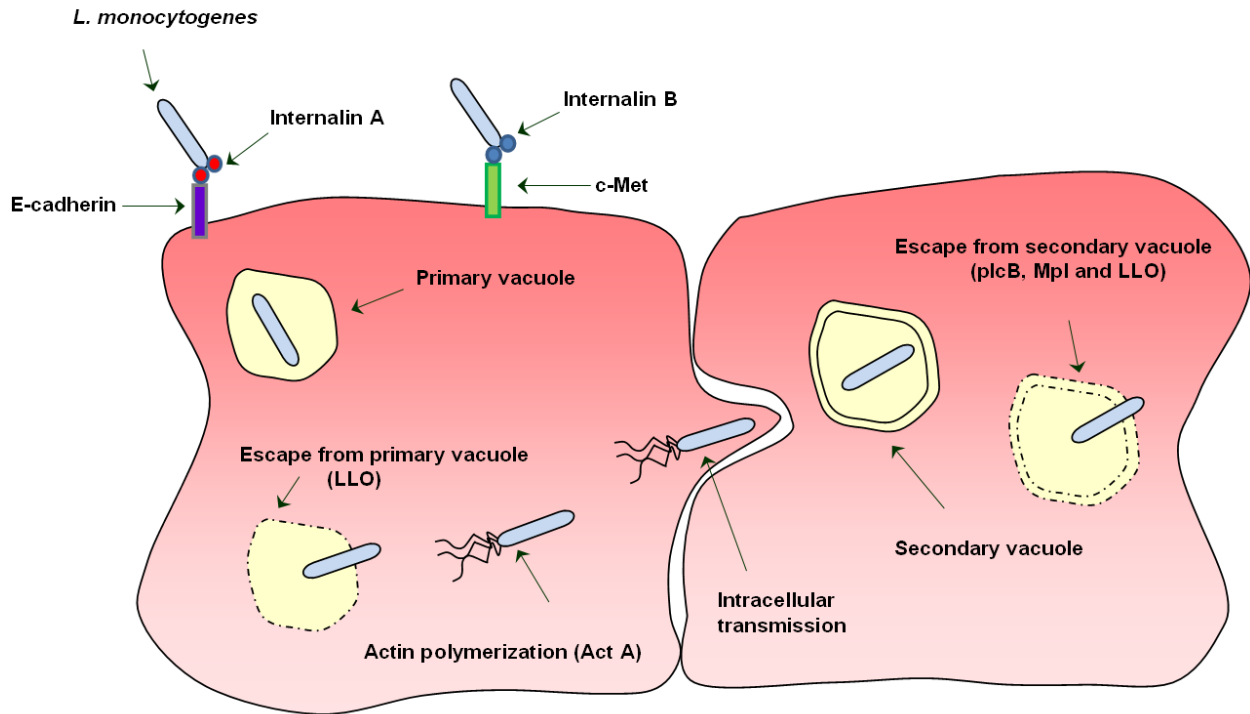


Figure 1. Pathogenesis of *Listeria monocytogenes*.

L. monocytogenes internalization is mediated via the cell surface proteins internalin A and B. Upon internalization, the bacterium escapes the phagocytic vacuole by secreting listeriolysin O. In the cytoplasm *Listeria* causes polymerization of the cellular actin via expression of the ActA gene, which propels the bacterium into the neighbouring cells. Here the bacterium is enclosed in a secondary vacuole. *L. monocytogenes* escapes the secondary vacuole by secreting phospholipases, metalloprotease, and listeriolysin O (modified from Pamer, 2004).

1.1.1.1 Immune response to *Listeria monocytogenes*

Both innate and adaptive immune responses play an important role in conferring protection against *L. monocytogenes*. For an effective control of *Listeria*, the production of various cytokines and immune mediators including interferon (IFN γ), Tumor necrosis factor (TNF), interleukin (IL)-2, IL-6, IL-17 and the gp91^{phox} nicotine adenine dinucleotide phosphate oxidase (NOX2)-dependent production of reactive oxygen species (ROS) are essential (Buchmeier and Schreiber, 1985; Pfeffer et al., 1993; Havell, 1989; Kaech and Ahmed, 2001; Dalrymple et al., 1995; Xu, 2010; Shiloh et al., 1999; Dinauer et al., 1997). While IL-4 plays a detrimental role in listeriosis (Kaufmann et al., 1997), IFN- γ is necessary for survival of acute systemic murine listeriosis. IFN- γ activates macrophages, which kill *Listeria* in a NOX2-dependent mechanism (Harty and Bevan, 1995; Shiloh et al., 1999). Kupffer cells, i.e. liver resident macrophages of liver produce IL-6, which induces the activation of Signal transducer and activator of transcription 3 (STAT3) in hepatocytes and protects by inducing neutrophilia (Gregory et al.,

1998). In addition to pro-inflammatory cytokines, immunosuppressive cytokines, in particular IL-10, are important in preventing lethal immunopathology, especially in cerebral listeriosis (Deckert et al., 2001). In addition to immune responses, fibrin plays a protective role in listeriosis by limiting bacterial spread, suppressing haemorrhage, and pathology (Mullarky et al., 2005; Lim et al., 2007b). The molecular mechanisms which regulate the production of fibrin during infectious diseases are only incompletely understood (Lim et al., 2007b).

The murine model of listeriosis has been widely used to study the host-pathogen interaction. In particular, murine listeriosis has been proven as a powerful model to decipher immune reactions contributing to the control of *L. monocytogenes*.

1.2 *Toxoplasma gondii*

Toxoplasma gondii (*T. gondii*) is an obligate intracellular protozoan parasite with a broad host range. The specific hosts of *T. gondii* are felids, while humans and other warm blooded animals serve as intermediate hosts. Although it infects one third of the world's population (Montoya and Liesenfeld, 2004), it is an uncommon cause of disease. In healthy individuals, toxoplasmosis may show mild flu-like symptoms, such as fever, muscle pain, and lymphnode swelling. In most cases *T. gondii* infection is clinically asymptomatic. Nevertheless, the parasite partially escapes elimination by the immune system and persists in the central nervous system (CNS) of its host (Luft and Remington, 1992). In contrast to immunocompetent persons, immunocompromised individuals, patients receiving immunosuppressive drugs for organ transplant, infected pregnant women, congenitally infected fetuses and newborns may suffer from a life-threatening toxoplasmosis due to the inability to prevent parasite-induced tissue necrosis (Ambroise-Thomas and Pelloux, 1993; Luft and Remington, 1992; Luft et al., 1993)

1.2.1 Pathogenesis of toxoplasmosis

The life cycle of *T. gondii* can be separated into a sexual and an asexual cycle. The sexual replication of *T. gondii* takes place in the definitive host, i.e. cat and other felidae, whereas asexual reproduction takes place in numerous warm blooded intermediate hosts, including humans. During its life cycle, *T. gondii* exists in different forms: rapidly multiplying tachyzoites, oocysts (containing sporozoites), tissue cysts (containing slow multiplying bradyzoites) and gametocytes (male and female gametes in the intestine of cats) (Dubey, 1998). After ingestion of *T. gondii*, the parasite penetrates the intestinal epithelial cells of the cat and undergoes

gametogony. An oocyst is formed around the fertilized gamete. The oocyst, which is still unsporulated, is discharged into the intestinal lumen and is shed in the feces of the cat (Dubey and Frenkel, 1972; Dubey, 1998) (Fig. 2). The oocyst undergoes sporulation to form the infective sporocyst. Each sporulated oocyst contains two sporocysts, each of which contains four sporozoites (Dubey, 1998). Upon consumption of food contaminated with sporulated oocyst, the ingested cysts are digested by the acidic conditions of the stomach leading to release of bradyzoites. The bradyzoites enter the intestine where they replicate asexually into tachyzoites (Bohne et al., 1993; Soete et al., 1993). Continuous replication leads to the rupture of the infected cell and the tachyzoites then disseminate to various tissues through the blood and the lymphatic system. Once the tachyzoites infect the brain and muscle cells, they undergo stage conversion to slow multiplying bradyzoites which ultimately reside in the form of tissue cysts (Dubey, 1977; Dubey, 1980; Dubey, 1985). The ingestion of meat contaminated with tissue cyst by the cat starts a new cycle of infection.

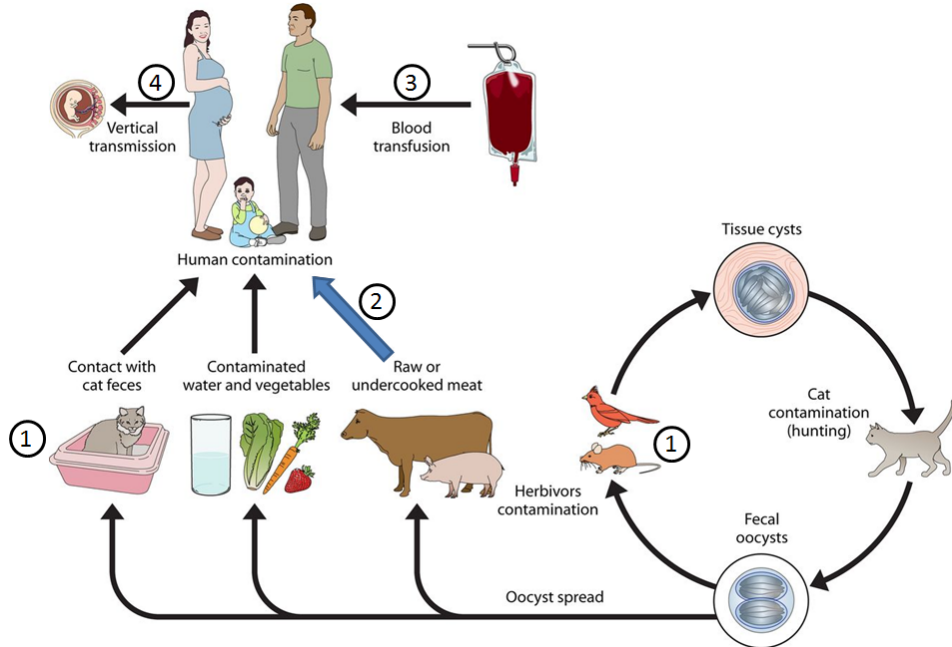


Figure 2. Life cycle of *T. gondii*.

The life cycle of *T. gondii* is divided into a sexual and an asexual part. The sexual cycle occurs in the intestine of the definitive host, the cat which sheds the oocysts in the feces after consumption of prey (mice, birds, etc) (1). These oocysts can infect humans and other warm-blooded animals triggering the asexual life cycle (1). In addition, consumption of meat contaminated with tissue cysts can cause human infections. Humans can also be infected by blood products containing viable *T. gondii* tachyzoites (3). Clinically important is the vertical transmission of *T. gondii* from primarily infected pregnant women to fetuses (Adapted from Esch and Petersen, 2013).

1.2.1.1 Immune response to *Toxoplasma gondii*

IFN- γ plays an important role in both acute and chronic toxoplasmosis. Control of *T. gondii* is mainly dependent on IFN- γ -producing T cells and NK cells (Gazzinelli et al., 1992; Suzuki et al., 1988; Hunter et al., 1994). IFN- γ enhances MHC class II expression of macrophages and fosters dendritic cell (DC) response, which leads to a strong pathogen-specific T cell response (Guan et al., 2007). In addition, IL-4, antibody production by B cells contribute to the control of *T. gondii* in the CNS (Suzuki et al., 1996).

T cells are indispensable for the control of intracellular toxoplasms. The efficiency of the T cell response is determined by several T cell-intrinsic signaling molecules including Tumor progression locus 2 (TPL2), Transforming growth factor beta (TGF- β), STAT4, STAT6, myeloid differentiation primary response gene (88) (MyD88), Tec kinases (IL-2 inducible T-cell tyrosine kinase (Itk) and resting lymphocyte kinase (Rlk)), and NF- κ B (Caamano et al., 1999; Caamano et al., 2000; Cai et al., 2000; Jin et al., 2009; LaRosa et al., 2008; Lighvani et al., 2001; Mason et al., 2004; Schaeffer et al., 1999; Watford et al., 2008). Several studies have shown that response in toxoplasmosis is critically regulated by various NF- κ B proteins: RelB is important for the IFN- γ -production of T cells (Caamano et al., 1999). NF- κ B2 inhibits T cell apoptosis (Caamano et al., 2000), and c-Rel is crucial for T cell activation, proliferation and IFN- γ production (Mason et al., 2004). Nonetheless, the signaling pathways leading to the activation of NF- κ B in *Toxoplasma*-specific T cells are incompletely understood.

Both, the bacterium *L. monocytogenes* and the parasite *T. gondii* are intracellular pathogens. Immunity to both pathogens is mediated by innate immune responses exerted by macrophages, DC, granulocytes and Natural killer (NK) cells as well as an activation of pathogen-specific T cells (Chang et al., 2007; Plitas et al., 2008). Whereas the immune system is able to eradicate *Listeria* within 2 to 3 weeks of infection, *T. gondii* partially escapes the anti-parasitic immune response and persists in the central nervous system of its host. The alteration in signal transduction molecules in both diseases is only partially explored and, therefore, we were interested in the functional role of NF- κ B regulators PKC- θ and CYLD in these prototypes of intracellular infections.

1.3 NF-κB pathway

The NF-κB family of transcription factors regulates a number of cellular processes including development, cell growth, apoptosis and also controls the expression of immunologically important genes. The NF-κB family consists of five members called RelA (p65), RelB, c-Rel, NF-κB1 (p50/p105), and NF-κB2 (p52/p100). RelA, RelB, and c-Rel are associated with inhibitory proteins termed inhibitors of NF-κB (IκBs), while NF-κB1 and NF-κB2 are large precursors, p105 (105kDa) and p100 (100kDa), which are posttranslationally processed to the DNA-binding subunits p50 and p52, respectively (Gilmore, 2006) (Fig. 3). The NF-κB family members have a highly conserved DNA-binding/dimerization domain called the Rel homology domain. In addition RelA, RelB, c-Rel, have a transactivation domain which activates transcription (Ghosh, 2002) while p50 and p52 lack the transactivation domain, they promote gene transcription by forming heterodimers with RelA, RelB, or c-Rel or other co-activators like B-cell lymphoma 3-encoded protein (Bcl-3) (Massoumi et al., 2006). The NF-κB signaling occurs either via degradation of IκB proteins (canonical pathway) or via the processing of precursors p105 and p100.

1.3.1 The canonical NF-κB pathway

The canonical NF-κB pathway is the most predominant of the two NF-κB signaling pathways. NF-κB is present in an inactive form in the cytoplasm bound to inhibitory IκB kinase proteins (IKK α , IKK β , IKK γ) (Hayden, 2004) (Fig. 3). Upon stimulation with pro-inflammatory agents such as TNF, lipopolysaccharide (LPS) or IL-1 β signals mediated by MAP/ERK kinase kinase 3 (MEKK3) lead to the activation of the IKK complex. The activated IKK β phosphorylates IκB α . The phosphorylated IκB α undergoes subsequent ubiquitination and degradation by the 26S proteasome. The liberated RelA-p50 complex translocates to the nucleus, binds to the regulatory regions on the DNA and initiates transcription of target genes that encode for proliferation, survival and immunoregulatory functions (Gilmore, 2006).

1.3.1.1 The non-canonical NF-κB pathway

The non-canonical NF-κB pathway is very important in B cells but is also present in other cell types. The NF-κB dimer is held in an inactive state by the extended C-terminal domain of the precursor p100. In response to B-cell activating factor (BAFF), lymphotoxin-β (LTβ) and CD40 stimulation, signals mediated by the NF-κB inducing kinase (NIK) leads to the phosphorylation

of IKK α catalytic subunit (Mahoney, 2008; Zarnegar, 2008) (Fig. 3). The IKK α homodimer phosphorylates NF- κ B2/p100 and the C-terminal inhibitory domain of the phosphorylated p100 is proteolytically cleaved to release the p52-RelB complex. The transcriptionally active p52-RelB complex translocates to the nucleus and initiates transcription of target genes (Zarnegar, 2008).

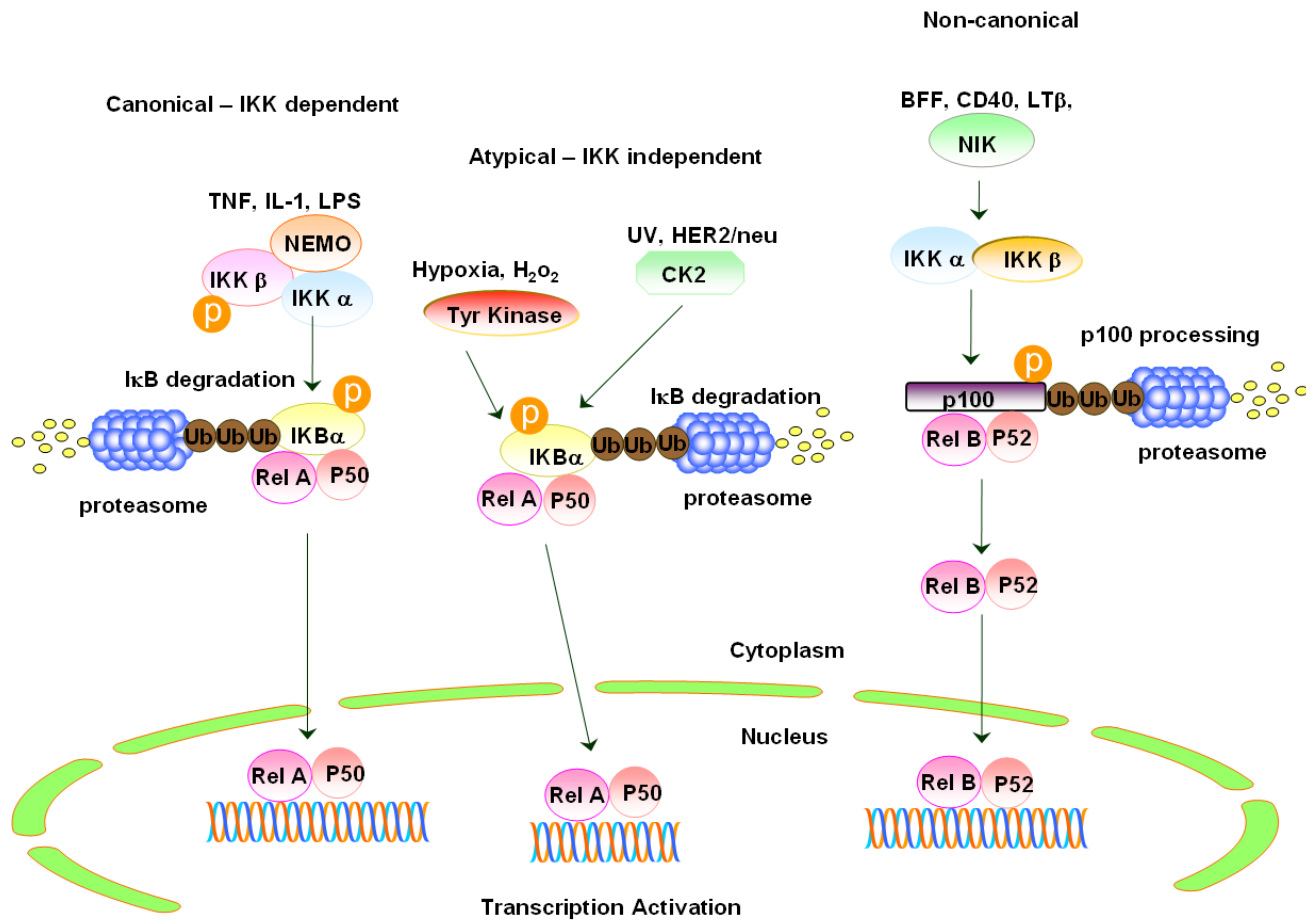


Figure 3. The NF- κ B pathway

The canonical NF- κ B pathway induced by TNF, IL-1 and LPS is dependent on activation of IKK. Activation of IKK results in the phosphorylation of I κ B α leading to its ubiquitination and subsequent degradation by the 26S proteasome. This causes release of the RelA p50 complex, which translocates to the nucleus and initiates transcription. The atypical pathways of NF- κ B activation is IKK-independent. In this pathway Casein kinase-II (CK2) and other tyrosine-kinases phosphorylate I κ B α thereby initiating downstream NF- κ B activation. The non-canonical pathway results in the activation of IKK α by the NF- κ B-inducing kinase (NIK), followed by phosphorylation of the NF- κ B subunit p100 by IKK α . This results in proteasome-mediated processing of p100 to p52. p52 forms heterodimer with RelB, translocates to the nucleus and initiates transcription (modified from Perkins, 2007)

1.3.1.1 The atypical NF-κB pathway

In addition to the canonical and the non-canonical pathways, the atypical NF-κB pathway regulates immune functions (Beinke, 2004). The activation of the atypical NF-κB pathway is IKK independent. The IKK independent activation of NF-κB is mediated via protein tyrosine kinases (PTK) in response to hypoxia or H₂O₂ stimulation or via Casein kinase-II (CK2) in response to UV or expression of oncogene Her-2/neu. The PTK and CK2 in turn phosphorylate IκBα leading to proteasomal degradation and subsequent nuclear translocation of RelA-p50 complex (Beinke, 2004; Sun, 2008b).

1.4 Regulation of T cell response by PKC-θ

PKC-θ is a serine/threonine kinase, which is selectively expressed in T cells, muscle cells, and platelets, and plays an important role for the activation of T cells. It is widely accepted that PKC-θ is the only member of the PKC family that takes the ‘center stage’ in the T cell supramolecular activation complex (SMAC). SMAC is a region of the membrane and cytoplasmic polarization formed at the contact site between a T cell and an antigen-presenting cell (APC) during recognition of an antigen (Berg-Brown et al., 2004). Upon stimulation of the T cell receptor (TCR), PKC-θ translocates to the immunological synapse, where it is phosphorylated by lymphocyte-specific protein tyrosine kinase (LCK), and subsequently leads to the activation of the transcription factors NF-κB, NFAT, and activated protein 1 (AP1) (Berg-Brown et al., 2004) (Fig. 4).

PKC-θ plays a role in several pathways involved in T cell activation and survival. Recent studies have shown that PKC-θ plays a key role in the activation of the NF-κB signaling pathway in mature T cells. Activation of T cells stimulates the canonical NF-κB pathway and PKC-θ is essential for the TCR/CD28-mediated activation of NF-κB. TCR/CD28 stimulation induces the degradation of IκBα, IκBβ, and IκBε, and PKC-θ is required for IκBα and IκBε but not IκBβ degradation. The critical role of NF-κB in inducing transcription of the IL-2 gene implicates PKC-θ as an essential factor for production of IL-2, a major T cell growth factor. It has also been discussed that AP1 contributes to the production of IL-2 in T cells and that PKC-θ plays a role in the activation of AP1. The transcription factor AP1 is composed of a dimer of Jun and/or Fos proteins and is important in the transcriptional activation of many genes. The AP1 activating capacity of PKC-θ is dependent on intact Ras function, but the mechanism that links PKC-θ to

Ras is unknown. Genetic ablation of PKC-θ does not impair c-Jun N-terminal kinase (JNK) activation, which suggests that PKC-θ regulates AP-1 activity independently of the JNK pathway, possibly at the level of c-fos or c-jun transcription (Arendt et al., 2002). (Li et al., 2004) showed that SPAK, a mitogen-activated protein kinase (MAPK), acts as a PKC-θ interacting kinase. SPAK synergized with constitutively active PKC-θ to activate AP-1, but not NF-κB. However, so far, it has not been confirmed by other groups that SPAK is in fact a PKC-θ interacting kinase.

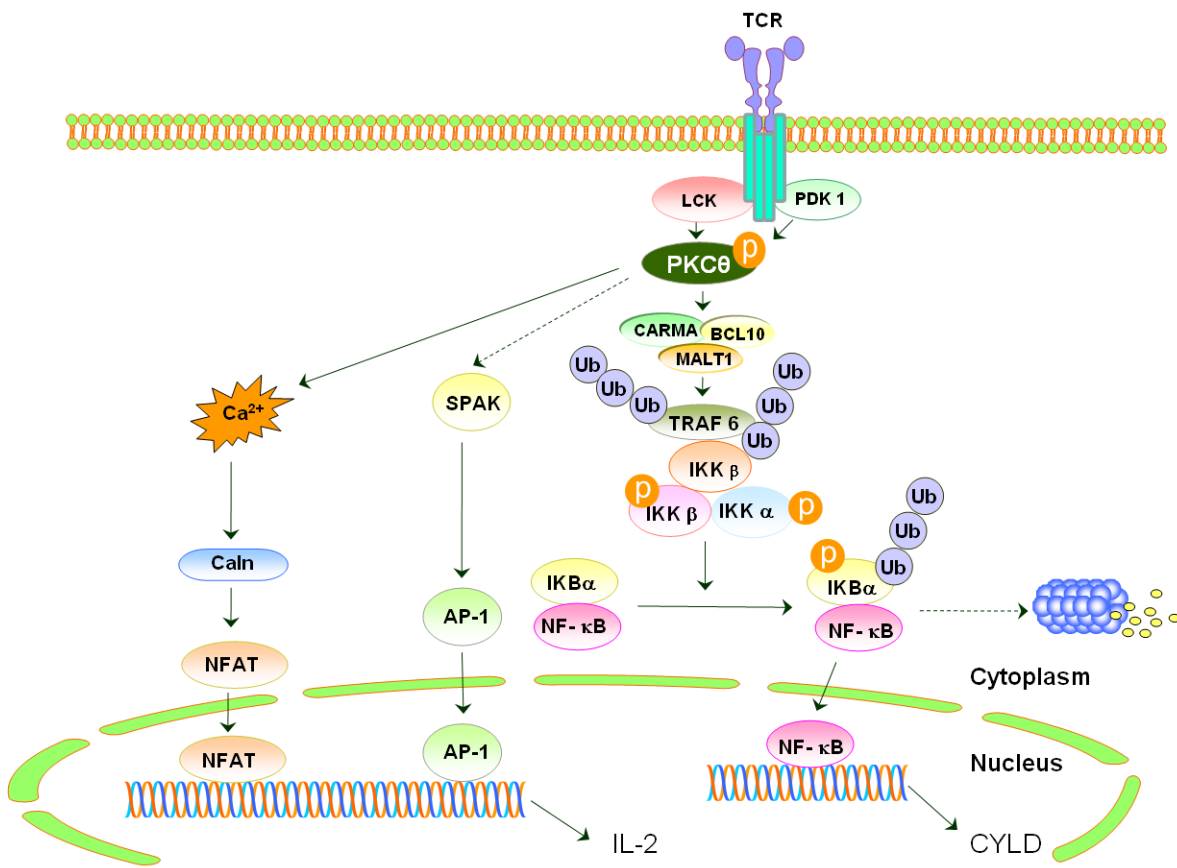


Figure 4. Regulation of T cell signaling by PKC-θ

Stimulation of the TCR initiates a cascade of PKC-θ-mediated downstream signaling events leading to the activation of transcription factors NF-κB (via the CARMA1, BCL10, MALT1 complex), AP-1 (via SPAK), and NF-AT (via Ca^{2+} /calcineurin) (modified from Isakov, 2012)

It is widely accepted that elevated intracellular calcium levels activate calcineurin, which subsequently dephosphorylates NFAT, resulting in nuclear translocation. Once in the nucleus, NFAT presumably binds DNA in a sequence-specific fashion resulting in altered transcription of various genes. In $\text{PKC-}\theta^{-/-}$ mice, peripheral mature T cells, displayed significantly decreased

TCR-induced Ca^{2+} influx and activation of NFAT. Reporter studies showed that knockdown of endogenous PKC-θ expression in Jurkat T cells significantly inhibited TCR-induced activation of NFAT. TCR crosslinking of PKC-θ^{-/-} T cells resulted in significantly decreased intracellular Ca^{2+} levels as compared to wildtype T cells suggesting a positive role for PKC-θ in TCR-mediated Ca^{2+} mobilization. The activation of NFAT via calcineurin was intact in PKC-θ^{-/-} Jurkat cells showing that the defective NFAT activation in PKC-θ^{-/-} T cells relies completely on the defective increase of Ca^{2+} .

There is good evidence that PKC-θ contributes to the inhibition of apoptosis of activated T cells. This effect is largely mediated by the PKC-θ mediated activation of NF-κB and the NF-κB-dependent activation of anti-apoptotic molecules. Barouch-Bentov et al (2005) showed that PKC-θ plays also an important role in the inhibition of apoptosis of activated T cells. Antigen stimulated PKC-θ^{-/-} T cells undergo accelerated apoptosis associated with deregulated expression of B-cell lymphoma 2 (Bcl-2) family proteins and display reduced activation of extracellular signal-regulated kinases (ERK) and JNK. The poor survival of PKC-θ deficient T cells was associated with reduced expression of Bcl-2 and B-cell lymphoma-extra large (Bcl-xL) diminished cytotoxic T lymphocyte (CTL) activity, and reduced IFN-γ expression, which were partially or fully restored by co-culture with wildtype T cells or by addition of exogenous IL-2. Thus, the function of PKC-θ can be compensated for by other signaling molecules.

Most of the data discussed so far on the role of PKC-θ in T cells were derived from *in vitro* studies, and, therefore, it was important to determine whether PKC-θ plays in fact an important role for the activation of T cells *in vivo*. Unequivocally, all experimental studies in murine T cell-mediated autoimmune diseases revealed that PKC-θ is essential for the induction of autoimmune diseases. However, the functional importance of PKC-θ for the activation and survival of pathogen-specific T cells in infectious diseases is much more complex and strongly dependent on the underlying pathogen. It has been shown by (Marsland et al., 2004) that PKC-θ plays a critical role in the development of T helper (Th) 2 cell but not Th1 cell responses in murine leishmaniasis. In addition, PKC-θ was dispensable for the development of virus-specific cluster of differentiation (CD)4 and CD8 T cells in various viral infections including vaccinia virus, lymphocytic choriomeningitis virus (LCMV), and murine herpes virus-68 (MHV)-68 infection (Marsland et al., 2005; Giannoni et al., 2005). Further studies by (Marsland et al., 2005) indicate that the activation of DC is very strong in viral infections and these highly activated DC

can compensate for a PKC-θ deficiency in T cells by activating alternative T cell signaling pathways. In fact, additional *in vitro* experiments showed that stimulation of PKC-θ^{-/-} T cells with TNF and IL-1 results in a normal NF-κB activation, proliferation and IL-2 production of T cells (Marsland et al., 2005). Furthermore, stimulation of DC via Toll like receptor (TLR) 9, which is also activated by viruses, compensates for PKC-θ-deficiency in T cells and induces activation and proliferation of virus-specific T cells *in vitro*. However, it remains unclear whether activation of DC is strong enough in every infectious disease to compensate for PKC-θ deficiency in T cells.

1.5 Ubiquitination/ Deubiquitination

Ubiquitination and deubiquitination are very important post-translational modifications, which have a profound effect on cell biology. For example, the ubiquitination of IκBα and its subsequent proteasomal degradation are crucial in the canonical NF-κB pathway (Fig. 3). Ubiquitins (Ub) are small (76 amino acid) regulatory proteins which are covalently attached to the substrate molecules by a process called ubiquitination. Ubiquitination is a three step enzymatic process catalysed by three different enzymes namely Ub-activating (E1), Ub-conjugating (E2) and Ub-ligating (E3) enzymes (Fig. 5) (Hershko, 1998). The first step involves the activation of ubiquitin by the activating enzyme E1. This reaction is adenosine triphosphate (ATP) dependent. In the second step the activated ubiquitin is transferred to the conjugating enzyme E2 by forming an E2-Ub thioester bond. In the final step the ubiquitin ligating enzyme E3 attaches ubiquitin to a substrate protein through an isopeptide bond between the carboxyl terminus of ubiquitin and the ε-amino group of a lysine (K) residue in the target protein.

The fate of the substrate molecule depends upon the type of ubiquitin linkage. The ubiquitin molecules contains 7 lysine residues (K6, K11, K27, K29, K33, K48 and K63), therefore the ubiquitin modification of the substrate proteins are diverse (Xu, 2009). The most well studied ubiquitin modifications are the K48 and K63-linked ubiquitination (Hicke, 2003). If the ubiquitin chains on the substrate protein are linked by K48, the protein is targeted for degradation by the 26S proteasome (Hershko, 1998; Hochstrasser, 1995), while K63-linked polyubiquitin chains regulate non-degradative functions such as protein trafficking, protein–protein interactions, DNA repair and regulation of signal-transduction (Adhikari et al., 2007; Chen, 2005; Hershko, 1998).

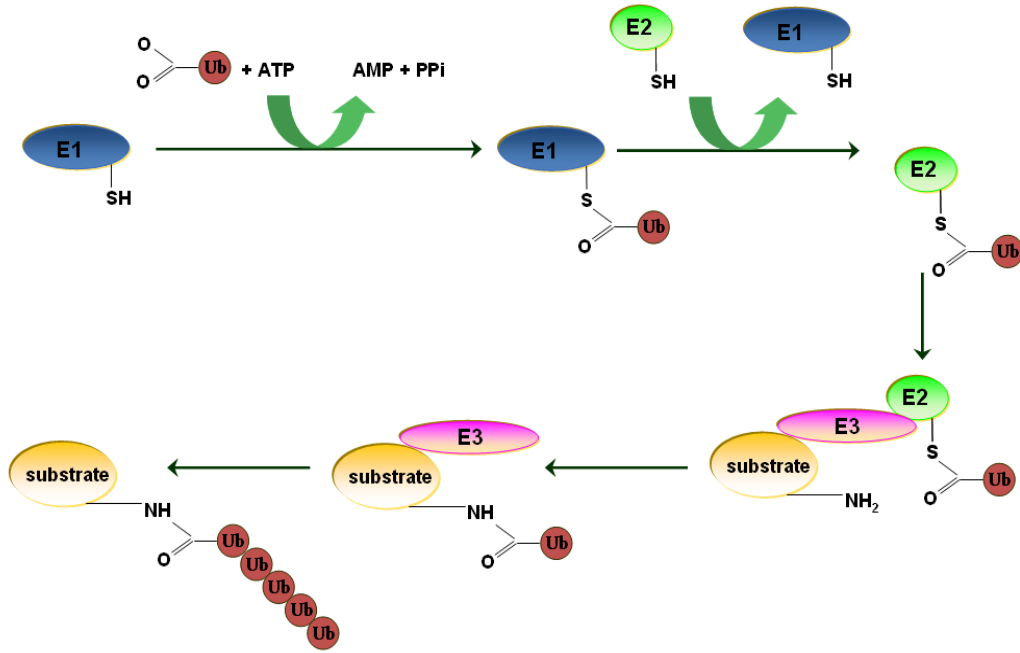


Figure 5. Ubiquitination process

The ubiquitination process involves three enzymes, which catalyze three different reactions; ubiquitin-activating enzymes E1 (which activates ubiquitin), ubiquitin-conjugating enzymes E2 (which transfer ubiquitin to the E3 enzyme) and ubiquitin-ligases which ligates the ubiquitin molecules to the substrate protein (modified from Rieser et al., 2013).

Ubiquitination is a reversible process and ubiquitin molecules can be removed from substrate proteins by deubiquitinating enzymes (DUBs). DUBs are proteases that hydrolyze ubiquitin chains from the substrate proteins, by a process known as deubiquitination, thereby regulating ubiquitin-mediated signaling pathways.

DUBs are classified into five families based on their catalytic domains as the ubiquitin carboxy-terminal hydrolases (UCHs), the ubiquitin-specific proteases (USPs), the ovarian tumour-related proteases (OTUs), the Machado–Joseph disease protein domain proteases (MJDs), and the Jab1/Pab1/MPN-domain-containing metallo-enzymes (JAMMs) (Nijman, 2005; Sun, 2008a). The UCH family of DUBs cleave short ubiquitinated peptides, which play an important role in the recycling of free ubiquitin. The UCH family member UCH-L1 is one of the most abundant proteins in the mammalian nervous system, and is associated with the development of neurodegenerative diseases (Gong, 2007; Sun, 2008a). The USP is the largest family of DUBs containing two conserved cysteine and histidine motifs in their domain (Gong, 2007). CYLD, a USP family member has been widely studied in the regulation of immune response. OTUs are the second largest of the DUB families (Gong, 2007; Makarova, 2000).

Several OTU-family members, such as A20, Cezanne, DUBA and otubain-1, are known to regulate the immune responses. Very little is known about the MJD and JAMM families of DUBs.

1.6 Regulation of immune response by CYLD

CYLD is a deubiquitinating enzyme which plays a pivotal role in immune response and inhibition of tumor cell development. Humans with functional inactive CYLD develop benign cutaneous tumors of the skin appendage. (Massoumi et al., 2006) showed that CYLD inhibits tumor cell proliferation by blocking Bcl-3-dependent NF- κ B signaling. Bcl-3, a NF- κ B co-activator, is ubiquitinated at K63, which serves as a recognition signal for its entry into the nucleus. Once in the nucleus, Bcl-3 activates cell cycle genes including cyclin D1 and induces cell proliferation. CYLD deubiquitinates Bcl-3, prevents its nuclear translocation into the nucleus, and, thereby, inhibits the proliferation of the cell.

Several studies have shown that CYLD targets multiple signaling molecules. In macrophages, CYLD has a high specificity in cleaving K63-linked polyubiquitin chains and thereby terminates activity of several molecules including transforming growth factor β -activated kinase 1 (TAK1), TNF receptor-associated factor (TRAF) 2, TRAF6, receptor-interacting protein-1 (RIP-1), NF- κ B essential modulator, c-Jun amino terminal kinase, retinoic acid-inducible gene-I, B cell Bcl-3 and p38MAPK (Harhaj and Dixit, 2012). Consequently, CYLD inhibits the activation of the transcription factor NF- κ B (Fig. 6). (Reiley et al., 2006) suspected CYLD plays a role in T cell development. However, several other studies failed to show an effect of CYLD on T cell development. The same authors published that CYLD positively regulates LCK, which is essential for proximal TCR cell signaling and thymocyte development, and that CYLD inhibits constitutive action of TAK1 and its downstream signaling molecules (Reiley et al., 2007; Zhang et al., 2006). In contrast, four other CYLD^{-/-} mice developed independently by other researchers did not show any T cell abnormality (Lim et al., 2007b; Massoumi et al., 2006; Zhang et al., 2006). Moreover, CYLD is a crucial B-cell regulator. Cyld deficiency results in activation of the NF- κ B pathway in B cells, which is associated with increased expression of several NF- κ B target genes, including those encoding B-cell activation markers (CD21, CD23, CD80 and CD86) and NF- κ B members (NF- κ B2 and RelB) (Jin et al., 2007).

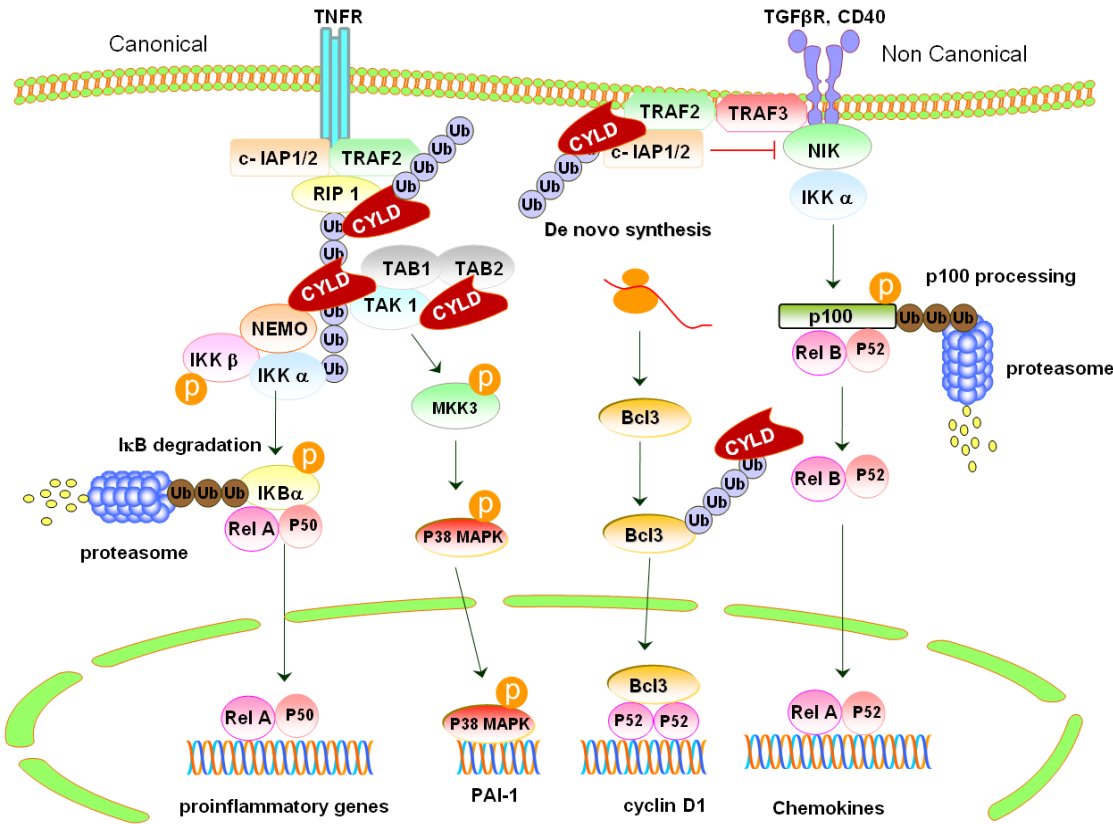


Figure 6. Regulation of NF- κ B and MAPK by CYLD

CYLD negatively regulates the canonical NF- κ B pathway by removing K63-linked ubiquitin molecules from RIP1, TAK1 and NEMO. CYLD also inhibits the MAPK pathway by deubiquitinating TAK1. In addition, CYLD indirectly inhibits the non-canonical NF- κ B pathway, since the inducible expression of non-canonical NF- κ B members, RelB and NF- κ B2 p100 and the co-factor Bcl3 depends on the canonical NF- κ B activation. (modified from Sun, 2010).

However, the precise target of CYLD leading to NF- κ B activation in B cells is unknown. (Jin et al., 2007) suggested that CYLD regulates a signaling molecule upstream of IKK, as IKK is constitutively activated in CYLD-deficient B cells. *Cyld*^{-/-} B cells have abnormalities in both maturation and homeostasis, characterized by the hyperproduction of marginal-zone B cells and B cell hyperplasia in peripheral lymphoid organs (Kayagaki et al., 2002; Keats et al., 2007).

Very few studies addressed the role of CYLD in infections. *Cyld*^{-/-} mice infected with *Haemophilus influenza* and *Escherichia coli* developed hyperinflammation due to a strong activation of the NF- κ B signaling pathway (Lim et al., 2007a; Lim et al., 2008). Surprisingly CYLD-deficiency protected mice from pneumolysin-induced acute lung injury and lethality (Lim et al., 2007b). CYLD was highly induced by pneumolysin of *Streptococcus pneumoniae*, and it inhibited MEKK3-p38 kinase-dependent expression of plasminogen activator inhibitor-1 (PAI-1) in the lung, thereby potentiating acute lung injury and mortality.

2. Aims

The signaling molecules PKC-θ and CYLD regulate diverse biological functions of cells of the immune system and have been reported to be either protective or deleterious in infectious diseases. To gain more insight into the role of PKC-θ and CYLD in infectious diseases, we studied the role of these signaling molecules in murine listeriosis and toxoplasmosis.

2.1 Function of PKC-θ in murine listeriosis

To study the impact of PKC-θ on murine listeriosis, we first determined the effect of PKC-θ deficiency on the control of *Listeria*. In the immune system, PKC-θ is expressed only in T cells. Therefore, we studied the influence of PKC-θ on the control of *L. monocytogenes* and number, frequencies, and kinetics of *Listeria*-specific T cells. Further, we clarified the impact of PKC-θ on the proliferation and survival of *Listeria*-specific T cells. Finally, we identified the factors which compensate for PKC-θ deficiency in T cells during listeriosis.

2.1.1 Role of PKC-θ in murine toxoplasmosis

To investigate the importance of PKC-θ in murine toxoplasmosis, we examined the influence of PKC-θ on the survival and parasite control in *T. gondii* infected mice. In addition, we investigated the effect of PKC-θ on the induction of *T. gondii*-specific CD4 and CD8 T cell response and enumerated the frequency of these *T. gondii*-specific T cells in various organs. Furthermore, we analyzed the influence of PKC-θ on signaling molecules in T cells of *T. gondii* infected mice.

2.1.1.1 Regulation of murine listeriosis and toxoplasmosis by CYLD

To examine the influence of CYLD on murine listeriosis, we studied whether CYLD induces a hyperactivation of the immune system, which may cause death of *Listeria*-infected mice or result in an improved pathogen control. Since CYLD negatively regulates immune responses, we examined whether CYLD deficiency influences cytokine production during listeriosis. Furthermore, whether CYLD induces tissue protective factors including PAI-1 and fibrin. Finally, we determined how CYLD regulates different signaling molecules during listeriosis. In additional experiments ,we evaluated the effect of CYLD on toxoplasmosis.

3.Materials and methods

3.1.Materials

3.1.1 Chemicals used for animal experiments

Isoflurane (forene ®)	Abbott, Wiesbaden, Germany
Embedding medium	Sakura Finetek Europe BV, Zoeterwoude Netherlands (TissueOCTTM Tek ® compound)
2 - methylbutane	Roth, Karlsruhe, Germany
4% paraformaldehyde (PFA)	Roth, Karlsruhe, Germany

3.1.2 Materials for cell culture

All cell culture work was carried out under a laminar flow hood. The sterile cell culture media were prewarmed in a water bath at 37 °C before use. Cells were cultured in an incubator at 37 °C, 5% CO₂ and 60% of water vapor. The cell culture plastic materials were purchased from Greiner Bio-One (Frickenhausen, Germany) and Roth (Karlsruhe, Germany).

Hank's	PAA Laboratories, Pasching, Austria
Hybridoma culture medium	DMEM (PAA Laboratories GmbH, Pasching, Austria), 10% fetal calf serum (FCS, PAA Laboratories GmbH, Pasching, Austria), 100 U Penicillin / streptomycin (PAA Laboratories GmbH, Pasching, Austria)
BMDC and BMM	RPMI 1640 (PAA Laboratories GmbH, Pasching, Austria), 20% fetal calf serum (FCS, PAA Laboratories GmbH, Pasching, Austria), 100 U Penicillin / streptomycin (PAA Laboratories GmbH, Pasching, Austria, 2 mM L-alanine-L-glutamine,GM-CSF (for BMDC), M-CSF (for BMDM) 20ng/ml.
PBS	PAA Laboratories GmbH, Pasching, Austria
Trypsin	PAA Laboratories GmbH, Pasching, Austria
Trypan blue	Sigma-Aldrich, Steinheim, Germany

3.1.3 Materials for molecular biology

Ethanol (70%, 98%)	Pharmacy of the University Hospital Magdeburg
EasyDNA kit	Invitrogen, Karlsruhe, Germany
DNeasy Blood and Tissue Kit	Qiagen, Hilden, Germany
Primers	Eurofins MWG Operon, Ebersberg, Germany
PCR Buffer, 10x	Qiagen, Hilden, Germany
HotStar Taq	Qiagen, Hilden, Germany
β-mercaptoethanol	Roth, Karlsruhe, Germany
RNeasy Mini Kit	Qiagen, Hilden, Germany
Oligo-dT	Invitrogen, Karlsruhe, Germany
dNTP	Invitrogen, Karlsruhe, Germany
5x First Strand Buffer	Invitrogen, Karlsruhe, Germany
DTT	Invitrogen, Karlsruhe, Germany
Superscript II Reverse Transcriptase	Invitrogen, Karlsruhe, Germany
Sterile distilled water	Berlin Chemie AG, Berlin, Germany
TaqMan Universal PCR master mix	Applied Biosystems, Darmstadt, Germany
TaqMan Gene Expression Assays	were obtained from Applied Biosystems, Darmstadt, Germany

Table 1 Genotyping primers

Mice strain	primer sequence (5' → 3')	amplicon size
PKC-θ mice		
Sense	5'-TAAGAGTAATCTTCCAGAGC-3'	400bp
Antisense	5'-TTGGTTCTCTGAACCTCTGC-3'	564bp
Neomycin resistance	5'-ACTGCATCTGCGTGTTCGAA-3'	
	WT mice amplicon size = 400bp, PKC $\theta^{-/-}$ mice, amplicon size = 564bp	
OT-I mice		
OIMR0015	5'-CAA ATG TTG CTT GTC TGG TG-3'	200bp
OIMR0016	5'-GTC AGT CGA GTG CAC AGT TT-3'	
OIMR 0675	5'-AAG GTG GAG AGA GAC AAA GGA TTC -3' 300bp	
OIMR 0676	5'- TTG AGA GCT GTC TCC -3'	
OT-I transgenic mice are positive for both 400bp and 300bp amplicons		
OT-II mice		
OIMR1825	5'-GCT GCT GCA CAG ACC TAC T-3'	500bp
OIMR1826	5'-CAG CTC ACC TAA CAC GAG GA-3'	
OIMR1880	5'-AAA GGG AGA AAA AGC TCT CC-3'	160bp
OIMR1881	5'-ACA CAG CAG GTT CTG GGT TC-3'	
OT-II transgenic mice are positive for both 500bp and 160bp amplicons		

Cyld^{-/-} mice

Cyld sense	5'-ACAAACATGGATGCCAGGTTG-3'	850bp
Cyld Antisense	5'-CCGCTAATAAAGGTCTCTG-3'	
LACZ sense	5'-GACACCAGACCAACTGGTAATGGTAGCGAC-3'	1000bp
LACZ Antisense	5'-GCATCGAGCTGGTAATAAGCGTTGGCAAT-3'	

WT mice, amplicon size = 850bp, Cyld^{-/-} mice, amplicon size = 1000bp

3.1.4 Materials for proteomics

RIPA buffer	50 mM Tris / HCl pH 7.5, 100 mM NaCl (Roth, Karlsruhe, Germany), 5 mM EDTA, 10 mM, H ₂ PO ₄ (both Merck, 1% Triton X-100, 0.25% deoxycholic acid, Protease inhibitor cocktail, 20 mM sodium fluoride, 0.2 mM phenyl methyl sulfonyl fluoride, 1mM Sodium molybdate, 20 mM glycerol-2-phosphate, 1 mM sodium phosphate buffer (all Sigma-Aldrich, Steinheim, Germany), 10% glycerol (Calbiochem, Darmstadt, Germany), 1Tbl./10ml. PhosStop (Roche, Mannheim, Germany)
BSA	Sigma-Aldrich, Steinheim, Germany
Bradford reagent	Bio-Rad, Munich, Germany
5x SDS buffer	Fermentas, St. Leon-Rot, Germany
SDS-polyacrylamide stacking gel	Distilled water, 5% acrylamide 30% (AppliChem, Darmstadt, Germany), 0.17 M Tris pH 7.4, 0.1% Sodium dodecyl sulfate (both Roth, Karlsruhe, Germany), 0.1% ammonium persulfate, 0.1% TEMED (both Sigma-Aldrich, Steinheim, Germany)

SDS-polyacrylamide separating gel	Distilled water, 6 to 10% acrylamide 30% (Applichem, Darmstadt, Germany), 0.4 M Tris pH 8.8, 0.1% Sodium dodecyl sulfate (both Roth, Karlsruhe, Germany), 0.1% ammonium persulfate, 0.1% TEMED (both Sigma-Aldrich, Steinheim, Germany)
Gel running buffer pH 8.3	25 mM Tris, 0.1% sodium dodecyl sulfate (both Roth, Karlsruhe, Germany), 250 mM glycine (Sigma Aldrich, Steinheim, Germany)
Transfer buffer pH 8.4	25 mM Tris, 0.1% sodium dodecyl sulfate (both Roth, Karlsruhe, Germany), 500 mM glycine (Sigma-Aldrich, Steinheim, Germany), 20% Methanol (J.T. Baker, Deventer, Netherlands)
Polyvinylidene fluoride (PVDF) Membrane Immobilon P	Millipore, Schwalbach, Germany
Filter paper	Roth, Karlsruhe, Germany
TBS-Tween 20, pH 7.4	20 mM Tris, 140 mM NaCl (both Roth, Karlsruhe, Germany), 0.1% (v / v) Tween 20 (Sigma -Aldrich, Steinheim, Germany)
Protein marker	Fermentas, St. Leon-Rot, Germany
Blotting grade milk powder	Roth, Karlsruhe, Germany

Table 3. Antibodies for Western blotting and Immunoprecipitation (IP)

Primary antibody	Blocking solution	Antibody dilution
All antibodies were obtained from (Cell Signaling Technology Danvers, MA, USA) unless stated otherwise.		
Anti-GAPDH (# 5174)	1% BSA 1% milk powder	1:1000
Anti-IκBα (# 9242)	5% BSA	1:1000
Anti-phospho-Jak2 (# sc-101718) (Santa Cruz biotechnology, Heidelberg,Germany)	5% BSA	1:500

Anti-phospho-p65 (# 3033)	5% BSA	1:1000
Anti-p65 (# 4764)	5% BSA	1:1000
Anti-phospho-STAT3 (# 9131)	1% BSA 1% milk powder	1:1000
Anti-STAT3 (# 9139)	1% BSA 1% milk powder	1:1000
Anti-phospho-p38 MAPK (# 9211)	1% BSA 1% milk powder	1:1000
Anti-p38 MAPK (# 9212)	1% BSA 1% milk powder	1:1000
Anti-PAI-1(# sc-5297) (Santa Cruz biotechnology, Heidelberg,Germany)	5% BSA	1:200
Anti-Jak2 (# 3230)	1% BSA 1% milk powder	1:1000
Anti-ubiquitin K63 (# 3936)	5% BSA 1% milk powder	1:1000
Anti-tubulin (# 2148)	5% BSA	1:1000
Anti-HDAC (# 5356)	1% BSA 1% milk powder	1:1000
Anti-phospho-I κ B α (# 9246)	5% BSA	1:1000
Anti-HA (# 2367)	5% milk powder	1:1000
Anti-DDK (# TA50011-100) (ORIGENE Rockville, MD)	5% BSA	1:1000
Anti- β -chain fibrin antibody (# 350) (American Diagnostica, Stamford, CT)	5% BSA	1:500

Secondary antibodies for Western Blotting

Polyclonal Swine Anti-Rabbit Immunoglobulins/HRP (# P 0399) Dako , Glostrup, Denmark
 Polyclonal Rabbit Anti-Mouse Immunoglobulins/HRP (# P 0260) Dako , Glostrup, Denmark

Table 4. Antibodies for flow cytometric analysis

Antibody	Clone
PE -anti-mouse Vα2 T-cell receptor mAb (mouse)	B20.1)
PECy5-anti-mouse CD8α mAb (rat)	(53-6.7)
PECy5-anti-mouse CD4 mAb (rat)	(RM 4-5)
FITC-anti-mouse CD11c mAb (hamster)	(V418)
FITC- anti-mouse F4/80 mAb (rat)	(BM8)
PE-anti-mouse NK1.1 mAb (rat)	(PK136)
FITC-anti-mouse Ly6G (rat)	(RB6-8C5)
FITC-anti-mouse Ly6C (rat)	(AL-21)
PE -anti-mouse CD44 (rat)	(IM7)
PE -anti-mouse CD69 (rat)	(H1.2F3)
FITC- anti-mouse B220 mAb (rat)	(RA3-6B2)
FITC -anti-mouse CD62L (rat)	(MEL-14)
PECy5-anti-mouse CD45 mAb (rat)	(30-F11)
PE - anti-mouse MHC ClassII (rat)	(M5/114.15.2)
PE -mouse-IgG isotype control	(G155-178)
PE -rat-IgG isotype control	(A95-1)
PECy5 - rat-IgG isotype control	(A95-1)
FITC -hamster-IgG isotype control	(HTK888)
FITC -rat-IgG isotype control	(A95-1)
PE -anti-mouse Annexin V	
7 AAD	
(All antibodies obtained from BD Biosciences,Heidelberg,Germany and used at a concentration of 1µg/ 1x10 ⁶ cells)	

Peptides

MHC class Ia SIINFEKL (OVA ₂₅₇₋₂₆₄)	JPT, Berlin, Germany
KAVYNFATM (LCMVgp ₃₃₋₄₁)	JPT, Berlin, Germany
MHC class I b fMIGWII tetramers	JPT, Berlin, Germany
Gra6-HPGSVNEFDF (HF10)	JPT, Berlin, Germany

Fusion protein

DimerX H-2L ^d	BD Biosciences, Heidelberg, Germany
--------------------------	-------------------------------------

Kits

Active Caspase-3 PE Mab Apoptosis kit	BD Biosciences, Heidelberg, Germany
NE-PER Nuclear and Cytoplasmic Extraction Reagents	Thermo scientific, MA, USA
CD4/ CD8/Pan T cell isolation kits, mouse	Miltenyi Biotec, Bergisch Gladbach, Germany
Pierce ECL Plus Western Blotting substrate	Thermo scientific, MA, USA
Mouse Th1/Th2/Th17 Cytokine	BD Biosciences, Heidelberg, Germany
Total ROS Detection Kit	ENZO Life Sciences, Farmingdale, USA

3.1.5 Instruments

Pipette	Eppendorf, Hamburg, Germany
Power PAC 200	Bio-Rad, California, USA
Semi Dry blotter	Peq lab, Erlangen, Germany
Centrifuge 5415R	Eppendorf, Hamburg, Germany
Incubator	Heraeus, Hanau, Germany
FACS Canto II	BD Biosciences, Heidelberg, Germany
PCR machine	Peq lab, Erlangen, Germany
Pipette boy	Eppendorf, Hamburg, Germany
Thermomixer compact	Eppendorf, Hamburg, Germany
Documentation station	Herolab GmbH, Wiesloch, Germany
Bio-Rad Mini protein system	Bio-Rad, California, USA
Neubauer counting chamber	Lauda-Königshofen, Germany
Coverslip (for Neubauer counting chamber)	Roth, Karlsruhe, Germany
Chemo Cam Luminescent Image Analysis system	INTAS, Göttingen, Germany

3.1.6 Animals

Age and sex matched C57BL/6 and BALB/c wildtype (WT) mice, obtained from Harlan (Borchen, Germany), as well as C57BL/6 PKC- $\theta^{-/-}$, BALB/c PKC- $\theta^{-/-}$ mice (Sun et al., 2000) were used. TCR transgenic mice, with MHC class I-restricted, ovalbumin-specific, CD8 T cells (OT-I) (Hogquist et al., 1994) and MHC class II-restricted, ovalbumin-specific, CD4 T cells (OT-II) (Barnden et al., 1998) respectively, mice were crossed with C57BL/6 PKC- $\theta^{-/-}$ mice in our animal facility. C57BL/6 Cyld $^{-/-}$ mice were obtained from Dr. Ramin Massoumi Department of Laboratory Medicine, Lund university, Malmö, Sweden (Massoumi et al., 2006). All animals were kept under conventional conditions in an isolation facility throughout the experiments. Experiments were approved and supervised by local governmental institutions. All animal experiments were in compliance with the German animal protection law in a protocol approved by the Landesverwaltungsamt Sachsen-Anhalt (file number: 203.h-42502-2-901, University of Magdeburg).

3.2 Methods

3.2.1 Genotyping of the mice strains

For genotyping of mice, a tissue sample of the tail tip was removed and transferred to a 2 ml Eppendorf tube. Genomic DNA from mouse tail was isolated using easyDNA kit (Invitrogen, Karlsruhe, Germany) according to the manufacturers, protocol. PCR was performed using primers indicated in Table 1.

3.2.2 Bacterial, viral and parasitic infection of mice

WT *L. monocytogenes* (EGD strain), recombinant ovalbumin-expressing *L. monocytogenes* (LMova) and recombinant *L. monocytogenes* expressing the gp₃₃₋₄₁-epitope derived from the glycoprotein of LCMV (LMgp, strain XFL703) (Foulds et al., 2002) were grown in tryptose soy broth and aliquots of log-phase cultures were stored at -80°C. For each experiment, the respective strain of *L. monocytogenes* was thawed and diluted appropriately in sterile pyrogen-free phosphate buffered saline (PBS) (pH 7.4) and intraperitoneal (i.p.) or intravenously (i.v.) applied at the indicated concentration. Mice were i.p. infected with 1x10⁴ WT *L. monocytogenes*, 5x10⁴ LMgp33 or 5x10⁴ LMova for primary and 1x10⁶ WT *L. monocytogenes* or 5x10⁶ LMova for secondary infection. For i.v. infection, fresh log-phase cultures were prepared from frozen stocks and 5x10⁵ *L. monocytogenes* diluted in 200 µl sterile pyrogen-free PBS (pH 7.4) were injected. For each experiment, the bacterial dose used for infection was controlled by plating an inoculum on tryptose soy agar and counting colonies after incubation at 37°C for 24 h.

To determine CFUs in spleens and livers of *L. monocytogenes*-infected mice, organs were dissected and homogenised with sterile tissue grinders. Ten-fold serial dilutions of the homogenates were plated on tryptose-soy agar. Bacterial colonies were counted microscopically after incubation at 37°C for 24h.

Lymphocytic choriomeningitis (LCM) virus (strain WE) was generated and titrated on L929 cells as plaque forming units and mice were i.v. infected with 1x10⁵ PFU (Utermöhlen et al., 1996). *T. gondii* cysts of the DX strain (type II strain) (Fischer et al., 2000) were harvested from the brains of chronically infected NMRI mice. Parasites were adjusted to a concentration of 10 cysts/ml in 0.1 M PBS, and 500 µl were administered orally by gavage to the experimental animals.

3.2.3 Blood and organ isolation

Animals were anesthetized with isoflurane (Baxter, Deerfield, IL). Blood was obtained by puncture of the heart with a 25 gauge needle attached to a 1 ml syringe. Isolated blood was mixed with heparin/PBS to prevent clotting of the blood. Before isolation of organs mice were intracardially perfused with 0.9% NaCl to remove contaminating intravascular leukocytes.

For histology, the mice were perfused and the organs were isolated. The organs were either snap frozen in embedding medium at -80 ° C in the presence of 2-methylbutane and stored at -80 ° C or the isolated organs were perfused and fixed in 4% paraformaldehyde (PFA) for 24 h and then stored at 4 ° C in PBS before paraffin embedding.

3.2.4 Isolation of leukocytes from blood, mesenteric lymph node, spleen, liver and brain

Splenic and mesenteric lymph node (mLN) leukocytes were obtained by passing these lymphatic organs through a 70 µm cell strainer, while 100 µm cell strainers were used to obtain the leukocytes from liver and brain (BD Biosciences, Heidelberg, Germany). Erythrocytes in blood, spleen, and mLN were lysed by incubating the cells in lysis buffer (155 mM NH₄Cl, 12 mM, NaHCO₃, and 0.1 mM EDTA) 4 ° C for 10 min. The cells were washed with Hank's Balanced Salt Solution (HBSS) + 3% FCS at 1200 rpm for 6 min. The cell pellet was resuspended in PBS and the number of cells was determined.

The leukocytes from liver and brain were separated by Percoll gradient centrifugation (GE Healthcare, Freiburg, Germany). The cell pellet was resuspended in 10 ml Percoll at a density of 1.098 g. A density gradient was created by overlaying Percoll densities of 1.07 g, 1.05 g, 1.03 g, and 1.00 g. The cells were then centrifuged at 1200x g for 20 min with rapid start-up, but without rotor brakes. The upper layers of densities 1.00 g and 1.03 g, were carefully removed and discarded. The densities between 1.05 g and 1.07 g and 1.098 g of Percoll gradient, where all the leukocytes accumulated, were transferred to a fresh Falcon tube and washed with cell culture medium. Finally, the cell pellet was resuspended in cell culture medium and the number of cells was determined.

3.2.5 Flow Cytometry

For staining of extracellular proteins, the cells were transferred to a FACS tube and washed in 3 ml of cold PBS at 1200 rpm for 6 min. 1 µg CD16/32 antibody per 10⁶ cells diluted in 50 µl PBS was added and incubated in the dark at 4 °C for 10 min, to block non-specific binding sites.

Subsequently, the cells were incubated with the specific antibodies as indicated in Table 4 for 30 min at 4 °C in the dark. Finally, the cells were washed in 3 ml of cold PBS. The cell pellet was resuspended in 250 µl cold PBS and measured within 4 h. For detection of intracellular proteins, 1 µl / ml GolgiPlug was added to the cell suspension, to block intracellular protein transport and to enrich protein concentration in the Golgi complex. To increase cytokine production, the cells were stimulated with phorbol 12-myristate 13-acetate (PMA) and Ionomycin at concentration of 5 µl / ml each and incubated at 37 °C for 4 h. After 2 washes with PBS, the cells were incubated with anti-FcR (CD16/32) to block nonspecific binding for 10 min. Thereafter, extracellular proteins were stained by the addition of specific antibodies for 20-minute incubation at 4 °C. After washing twice with PBS, intracellular proteins were stained. First, the cells were fixed in 250µl of Cytofix / Cytoperm at 4 °C for 20 minutes and permeabilized with 1 ml PermWash at 1:10 dilution. The cells were then incubated with the specific antibodies diluted in Perm Wash and incubated at 4 °C for 30 min. After 2 washes with PermWash , the cells were pelleted , resuspended in cold PBS and stored in the dark at 4 °C until analysis. The flow cytometric measurements were performed with a FACSCanto II (BD Biosciences) and the analysis was performed with the FACSDiva 6 software (BD Biosciences).

3.2.6 Cytometric bead assay

Cytokine levels in serum were analyzed by flow cytometry using the Cytometric Bead Assay (CBA) from BD Biosciences (Heidelberg, Germany) using the manufacturer's protocol and FCAP Array™ (version 3, BD Biosciences) software.

3.2.7 Magnetic-activated cell sorting (MACS) of T cells

CD4, CD8 and Pan T cells were isolated using MACS isolation kits (Miltenyi). Splenocytes were centrifuged at 300 g for 10 min. The cell pellet was resuspendend in 40 µl of MACS buffer (0.5% bovine serum albumin (BSA), and 2 mM EDTA in (PBS) pH7.2) per 10^7 cells. 10 µl of the respective biotin-antibody cocktail was added per 10^7 cells, mixed and incubated for 10 min at 4 °C. After incubation, 30 µl of MACS buffer and 20 µl of anti-biotin MicroBeads per 10^7 total cells were added, mixed well and incubated at 4 °C for 15 min. The cells were then washed by adding 1–2 ml of MACS buffer per 10^7 cells and centrifuged at 300 g for 10 min. The pellet was resuspended in 500 µl MACS buffer up to 10^7 cells. LS columns were placed in the magnetic field of the MACS separator. The column was prepared by rinsing with 3ml of MACS buffer.

The cell suspension was applied onto the column, the column was washed with 3×3 ml MACS buffer and the flow through was collected which contained unlabeled T cells. The elute was centrifuged at 300 g for 10 minutes. The pellet containing the enriched T cells were resuspended in 500 µl of MACS buffer. The purity of CD4⁺ and CD8⁺ T cells was 90-95% as determined by FACS staining.

3.2.8 ELISPOT

The number of antigen-specific CD4 and CD8 T cells was determined by an IFN-γ specific ELISPOT. Triplicates of isolated splenic leukocytes (2×10^5 , 2×10^4 , 2×10^3 cells/well) from infected mice on C57BL/6 background were added to rat anti-mouse IFN-γ (Biosource, Camarilla, CA) coated ELISPOT plates and co-incubated with spleen cells from non-infected WT C57BL/6 mice (2×10^5 /well), which were pre-loaded with LLO₁₉₀₋₂₀₁ (10^{-6} M), the LCMV-derived epitope gp₆₁₋₈₀-(10^{-6} M), OVA₂₅₇₋₂₆₄ (10^{-8} M), and gp₃₃₋₄₁ (10^{-8} M) peptide, respectively. Isolated splenic and hepatic leukocytes from infected BALB/c were co-incubated with spleen cells from non-infected BALB/c WT mice (2×10^5 /well), loaded with LLO₁₈₉₋₂₀₀ (10^{-6} M) or LLO₉₁₋₉₉-(10^{-8} M) peptide. Controls included co-incubation of isolated leukocytes with spleen cells without peptide loading and incubation of leukocytes from non-infected mice with peptide loaded spleen cells. All ELISPOT plates were incubated overnight and developed with biotin-labeled rat anti-mouse IFN-γ (BD Pharmingen, San Diego, USA), peroxidase-conjugated streptavidin and amino-ethylcarbazole dye solution (Sigma-Aldrich, Munich, Germany). The spots were counted microscopically and the number of Ag-specific cells per organ was calculated from the number of spots of triplicate wells and the number of leukocytes per organ.

3.2.9 Bone marrow-derived dendritic cell (BMDC) and macrophages (BMDM) culture

Femur and tibia were aseptically removed from mice, the bone ends were cut, and the bone marrow cavity was flushed with HBSS. The resulting cell suspension was washed twice and cultured in petri dishes with DMEM supplemented with 10% FCS, 50 U/ml penicillin/streptomycin, 1% non-essential amino acids, 1% glutamine, 20 ng/ml granulocyte-macrophage colony-stimulating factor GM-CSF (for BMDC), 20ng/ml macrophage colony-stimulating factor (M-CSF) (for BMDM), and 50 µM 2-mercaptoethanol for 3 days. Medium was changed every 3 days and non-adherent cells were removed by washing the dishes. After 6 days, adherent BMDMs were harvested and used for experiments.

3.2.10 Immunization with peptide-coated bone marrow-derived DC

BMDCs were matured with lipopolysaccharide (LPS) (500 ng/ml) for 48 h. After 48 h ovalbumin (OVA₂₅₇₋₂₆₄) (10^{-5} M) and listeriolysin (LLO₁₉₀₋₂₀₁) (10^{-4} M) peptides, respectively were added to cultures 4 h before harvest. Based on the percentage of CD11c⁺ cells as determined by flow cytometry, 2.5×10^5 mature BMDCs were injected i.v. per mouse. Control mice were treated with non-peptide loaded BMDCs.

3.2.11 Adoptive transfer of T cells

Polyclonal T cells were isolated from the spleen of non-infected C57BL/6 WT or PKC-θ^{-/-} mice by MACS using a pan T cell isolation kit (Miltenyi) as described earlier. 2×10^7 T cells were injected i.v. into C57BL/6 PKC-θ^{-/-} mice 24 h prior to infection with WT *L. monocytogenes*. CD8 and CD4 T cells were isolated from spleens of non-infected WT and PKC-θ^{-/-} OT-I and OT-II mice using CD8 and CD4 T cell isolation kits (Miltenyi) respectively as described earlier. 5×10^6 purified OT-I or OT-II T cells were injected i.v. into recipient mice 24 h prior to infection.

3.2.12 Detection of antigen (Ag)-specific CD8 T cells by flow cytometry

Splenic Ag-specific CD8 T cells were detected by staining with PE-conjugated MHC class Ia SIINFEKL (OVA₂₅₇₋₂₆₄) and PE-conjugated KAVYNFATM (LCMVgp₃₃₋₄₁) pentamers (both from ProImmune, Oxford, UK) and PE-conjugated MHC class Ib fMIGWII tetramers (Pamer, 2004), respectively in combination with anti-CD8-FITC (clone 53-6.7). Control staining was performed with isotype-matched control antibodies.

3.2.13 Carboxyfluorescein diacetate succinimidyl ester (CFSE) labeling of cells

The cells to be labeled were counted and resuspended in prewarmed PBS with 0.1% BSA at a final concentration of 1×10^6 cells/ml. 2 µl of 5 mM stock CFSE solution per ml of cells was added for a final working concentration of 10 µM. The cells were then incubated at 37°C for 10 min. The staining was quenched by adding 5 volumes of ice-cold culture medium to the cells and incubating for 5 min on ice. The cells were then pelleted and resuspended in fresh culture medium.

3.2.14 T cell proliferation and activation

CD8 T cells from OT-I WT and OT-I PKC-θ^{-/-} or CD4 T cells from OT-II WT and OT-II PKC-θ^{-/-} T cells were purified using CD4⁺ and CD8⁺ isolation kits (Miltenyi), respectively. Purified cells

were washed in cold PBS, resuspended at 5×10^6 cells/ml and labeled with CFSE (Invitrogen, Oregon, USA) at a final concentration of 0.5 μ M at RT for 10 min. The reaction was terminated with PBS containing 5% FCS. 5×10^6 CFSE-labeled T cells of the mouse strains were injected into the lateral tail vein of recipient mice 1 day prior to infection with LMova. Proliferation and activation of CFSE-labeled cells were characterized by staining with anti-CD8- PECy5 (clone 53-6.7) or anti-CD4-PECy5 (clone RM4-5), in combination with anti-V α 2-PE (clone B20.1), anti-CD44-PE (clone IM7), and anti-CD69-PE (clone H1.2F3), respectively, followed by flow cytometry.

3.2.16 Measurement of apoptosis by flow cytometry

Apoptosis was analyzed by quantifying phosphatidylserine residues exposed on the external cell membrane. In brief, cells were resuspended in annexin binding buffer (10mM (4-(2-hydroxyethyl)-1-piperazineethanesulfonic acid (HEPES)/NaOH, pH 7,4; 140 mM NaCl; 2,5 mM CaCl₂) and stained with Annexin V-PE and 7-amino actinomycin D (7-AAD) for 15 min. at RT, in combination with anti-CD8-APC or anti-CD4-APC. Stained cells were analyzed by flow cytometry within one hour. Active caspase-3 was detected by flow cytometry using the Active Caspase-3 PE Mab Apoptosis kit (BD Bioscience), in combination with anti-CD8-APC.

3.2.16 *In vitro* infection of DCs with *L. monocytogenes*

LMova was grown in brain heart infusion medium (BHI medium), washed in antibiotic-free RPMI and added to BMDCs at a multiplicity of infection of 1:100 in RPMI1640 medium with 10%FCS 50 μ M 2-mercaptoethanol without antibiotics. After 1 h of infection, 50 μ g/ml gentamicin was added to kill extracellular bacteria for additional 3 h . Thereafter, infected BMDCs were washed in PBS, resuspended in RPMI supplemented with 10 μ g/ml gentamicin and co-cultured with T cells.

3.2.17 *In vitro* proliferation of T cells

Non-infected and LMova-infected BMDCs were added to 96-well round bottom plates at 1- 2×10^4 per well. MACS-purified primary, CFSE-labeled OT-I WT and OT-I PKC- $\theta^{-/-}$ T cells (2×10^5 cells/well), respectively, were added to WT BMDCs and cultured in 200 μ l RPMI 1640 medium with 10% FCS, 50 μ M 2-mercaptoethanol, 50 U/ml penicillin/streptomycin and 10 μ g/ml gentamicin. In some experiments, BMDCs-T cell cultures were supplemented with

murine recombinant rIL-2 (15 ng/ml; Peprotech, NJ, USA), 40 µM Z-VAD-FMK (pan-caspase) inhibitor (Bachem AG, Bubendorf, Switzerland), and 100 µM caspase-3 inhibitor VII (Calbiochem, San Diego, USA), respectively. After 48 h, CFSE profiles of T cells were analyzed by flow cytometry.

3.2.18 Immunohistochemistry

Immunohistochemistry was performed in collaboration with Prof. Dr. Martina Deckert (Department of Neuropathology, University Hospital Cologne, Germany). For immunohistochemistry on frozen sections, mice were perfused intracardially with 0.9% NaCl in methoxyflurane anaesthesia. For histology on paraffin sections, anesthetized mice were perfused with 4% paraformaldehyde in PBS, liver was removed and fixed with 4% paraformaldehyde for 24 h. Paraffin sections (4 µm) were used for periodic acid Schiff (PAS) staining. Immunostaining of *L. monocytogenes* and *T. gondii* was performed with rabbit anti-*L. monocytogenes* (BD Biosciences) and rabbit anti-*T. gondii* polyclonal antibody (Ab) (DCS, Hamburg, Germany), respectively followed by peroxidase-labeled goat anti-rabbit immunoglobulin G F(ab')₂ fragments (Jackson-Dianova, Hamburg, Germany). Peroxidase reaction products were visualized by 3,3'-diaminobenzidine tetrahydrochloride (Sigma, Deisenhofen, Germany), and H₂O₂ was used as the co-substrate. Images were acquired with a Zeiss Axiophot using Zeiss Axioplan objective lenses, a Zeiss Axicam camera and Zeiss Axiovision software (all from Zeiss, Oberkochen, Germany).

3.2.19 Reverse transcription-PCR (RT-PCR)

Isolation of mRNA from the livers and spleens of uninfected and infected mice was performed with an RNAeasy kit (Qiagen, Hilden, Germany). The SuperScript reverse transcriptase kit with oligo(dT) primers (Invitrogen) was used to transcribe mRNA into cDNA as described by the manufacturer. Quantitative RT-PCR for Cyld, IL-6, IFN-γ, TNF, iNOS, IGTP, NOX2, and hypoxanthine phosphoribosyltransferase (HPRT) was performed with cDNA using individual Taqman® gene expression assay (Applied Biosystems, Darmstadt, Germany). Amplification was performed with a GeneAmp 5700 sequence detection system (Applied Biosystems). Quantitation was performed with the sequence detector software SDS (version 2.1; Applied Biosystems), according to the $\Delta\Delta C_T$ threshold cycle (C_T) method with HPRT as the housekeeping gene. Data are expressed as the increase in the level of mRNA expression in infected mice over uninfected

controls of the respective mouse strains (Livak and Schmittgen, 2001). All primers and probes were obtained from Applied Biosystems.

3.2.20 Determination of alanine aminotransferase (ALT) and aspartate aminotransferase (AST)

Liver enzymes (ALT, AST) were measured in collaboration with Dr. Katrin Borucki (Institute of Clinical Chemistry, University of Magdeburg) according to recommendation of the International Federation of Clinical Chemistry using commercial tests (Roche Diagnostics, Mannheim, Germany; on the Modular platform) with pyridoxal phosphate activation at 37°C and measurement on the Cobas Modular platform (Roche, Mannheim, Germany).

3.2.21 Hepatocyte culture

Mouse liver was perfused with HEPES buffer followed by collagenase solution (Sigma). Isolated hepatocytes were washed with PBS. 1×10^6 cells were plated on 6 cm dishes in DMEM containing 10% FCS, 10% non essential amino acids, 1% L-glutamine and a combination of penicillin and streptomycin. The medium was changed after 4 h. The cells were then cultured in DMEM containing 10% FCS, 10% non essential amino acids, 1% L-glutamine and a combination of penicillin and streptomycin. The cells were stimulated with 200 ng/ml recombinant IL-6 (PeproTech GmbH, Hamburg, Germany). Cells were harvested at the indicated time points, and proteins were isolated for Western blot (WB).

3.2.22 Transfection of hepatocytes

Cultivated hepatocytes (5×10^6 cells per experimental group) were transiently transfected with HA-tagged ubiquitin in which all lysines were mutated to arginines (HA-ubiquitin-KO, plasmid 17603), ubiquitin with only K63 and mutation of all other lysines to arginines (HA-ubiquitin K63, plasmid 17606) ubiquitin with all lysines present (HA-ubiquitin-WT, plasmid 17608; all from Addgene, Cambridge MA), HA-CYLD WT, HA-CYLD C/S (catalytically inactive CYLD) (Massoumi, 2009), and MYC-DDK STAT3 (Origene, Rockville, MD) plasmids as indicated using the Lipofectamine 2000 reagent (Invitrogen, San Diego, CA) according to the manufacturer's instructions for 48 h. Transfected hepatocytes were stimulated with IL-6 (200 ng/ml, PeproTech) for 1 h.

3.2.23 Protein isolation and Western blot

MACS isolated T cells, cultivated hepatocytes and liver tissue were lysed in cold RIPA buffer at 4 °C for 15 min. The suspension was centrifuged for 10 min at 14,000 rpm. The supernatant was transferred into a fresh tube. The protein content of the supernatant was determined photometrically using the Bradford reagent (Bradford, 1976) as described by the manufacturer. Equal amounts of proteins were separated on 10% SDS-polyacrylamide gels, transferred to polyvinylidene fluoride membranes followed by incubation with antibodies indicated in Table 3 (Laemmli, 1970). Cytoplasmic and nuclear proteins were isolated with a commercial kit (NE-Per Nuclear and Cytoplasmic Extraction Kit; Thermo Scientific,). The purity and amount of cytoplasmic and nuclear proteins was controlled by staining for tubulin and histone deacetylase (HDAC) (both antibodies from Cell Signaling), respectively. Blots were developed using an ECL Plus kit (GE Healthcare, Freiburg, Germany). For quantitation of protein intensities by densitometry, WB images were captured using the Intas Chemo Cam Luminescent Image Analysis system (INTAS Science Imaging Instruments,) and analyzed with the LabImage 1D software (Kapelan Bio-Imaging Solutions, Leipzig, Germany).

3.2.24 Immunoprecipitation

Unstimulated and IL-6 (200 ng/ml)-stimulated mouse hepatocytes were lysed on ice as described before. In a pre-clearing phase, Sepharose G beads (GE Healthcare Europe GmbH, Munich, Germany) were incubated for 30 min with cell lysates under continuous shaking at 4°C. The beads were removed by centrifugation at 10,000 rpm for 5 sec and equal amounts of lysates were incubated with anti-STAT3, anti-CYLD, anti-HA and anti-DDK antibodies, respectively, at 4°C overnight. The immune complex was captured by incubating with Sepharose G beads overnight at 4°C. The beads were then washed 3 times with PBS by centrifugation at 10,000 rpm for 5 sec. The pellet containing Sepharose G immune complexes was suspended in buffer 2 (SDS, 1 M pH 6,8 Tris, glycerol; 2-mercaptoethanol) and boiled at 100°C for 5 min. After centrifugation at 10,000 rpm for 5 sec, the supernatant was used to detect STAT3, CYLD, HA, DDK, K63 ubiquitin, tubulin, HDAC and GAPDH.

3.2.25 ROS assay

ROS was determined in supernatant of cultivated *L. monocytogenes*-infected macrophage using a total ROS detection kit for flow cytometry according to the manufacturer's protocol (ENZO Life Sciences, Farmingdale, USA).

3.2.26 Affinity purification of anti-IL6 antibody

Anti-IL-6 hybridoma cell line (clone MP520F3) obtained from ATCC (Manassas, Virginia) were cultured in 150 cm² culture flasks in RPMI medium supplemented with 10% FCS and a combination of penicillin and streptomycin. When the culture reached confluence, the supernatant from the cell culture containing the anti-IL6 antibody was harvested and subjected to affinity chromatography using AKTAprime chromatographic system (GE, Freiburg, Germany). HiTrap Protein G HP column (GE, Freiburg, Germany) was precleaned with 5 ml of elution buffer (0.1 M glycine-HCl, pH 2.7) and then equilibrated with 5 ml of binding buffer (0.02 M sodium phosphate, pH 7.0). The supernatant from the anti-IL6 hybridoma cell culture were loaded onto the column and the flow rate was maintained at 0.2 ml/min as the sample was applied. The column was then washed with 10 ml binding buffer at a flow rate of 1 ml/min. The antibodies were then eluted into 10 (1 ml) fractions into tubes containing 80 µl of the neutralization buffer (1 M Tris-HCl, pH 9.0) at a flow rate of 1 ml/min. The eluted samples were pooled and the protein concentration was determined.

3.2.27 IL-6 neutralization

In IL-6 neutralization experiments, mice were treated with 0.5 mg neutralizing anti-IL-6 antibody i.p (clone MP5-20F3, rat IgG1; ATCC) or isotype mAb (anti-rat IgG1; Sigma), respectively. Antibodies were applied 24 h prior to *L.monocytogenes* infection.

3.2.28 Warfarin treatment

Warfarin (3-(α -acetonylbenzyl)-4-hydroxycoumarin; 2 mg/l, Sigma) was added to drinking water of mice beginning 3 days prior to infection. Warfarin containing drinking water was changed every 48 h and treatment was continued until day 10 after infection.

3.2.29 *In vivo* small interfering RNA (siRNA) treatment

CYLD and STAT3 siRNA were obtained from Ambion (CA, USA). A 1.5 mg/mL siRNA solution was prepared by mixing 250 μ L of CYLD and STAT3 siRNA stock solution (3mg/mL), respectively, with 250 μ L of complexation buffer. Invivofectamine 2.0 reagent (Invitrogen, Oregon, USA) was warmed to room temperature and 500 μ l Invivofectamine was added to the siRNA solutions. The Invivofectamine-siRNA duplex mixture was incubated at 50°C for 30 min. The mixture was dialyzed with PBS using Float-A-Lyzer (Spectra/Por, TX USA). The Float-A-Lyzer dialysis device was prepared by soaking in sterile water for 10 min. The Invivofectamine 2.0-siRNA duplex mixture was added to the Float-A-Lyzer dialysis device and incubated at room temperature for 1 h in 1 L of PBS, pH 7.4, with gentle agitation. The samples were then collected. The final volume increases by about 10%, and thus, the final volume is divided by the initial volume of siRNA to determine the final siRNA concentration. 200 μ l of siRNA with a final concentration of 7 mg siRNA/kg mouse was injected into the tail vein 24 to 48 h before i.v. infection with *L. monocytogenes*.

3.2.30 Statistics

Statistical significance was determined using the two-tailed Student *t* test or nonparametric Mann-Whitney rank sum test using Statistica5 software (StatSoft, OK, USA). All experiments were performed at least twice. *P* values of <0.05 were considered significant.

4. Results

4.1.1 Function of PKC-θ in murine listeriosis

4.1.1.1 PKC-θ is essential for the generation of *L. monocytogenes*-specific, but not for LCMV-specific CD4 and CD8 T cells

In good agreement with previously published data (Berg-Brown et al., 2004), the number of LCMVgp₃₃₋₄₁-specific CD8 T cells was identical in spleens of LCMV-infected WT and PKC-θ^{-/-} (Fig. 1A) as revealed by pentamer staining. However, the number of CD8 T cells specific for the MHC class I OVA₂₅₇₋₂₆₄ epitope was significantly reduced in PKC-θ^{-/-} mice as compared to WT animals after infection with LMova (Fig. 7A). Importantly, the number of gp₃₃₋₄₁-specific CD8 T cells was also reduced in PKC-θ-deficient mice after infection with transgenic *L. monocytogenes*-expressing the LCMV gp₃₃₋₄₁ CD8 T cell epitope (Fig. 7A).

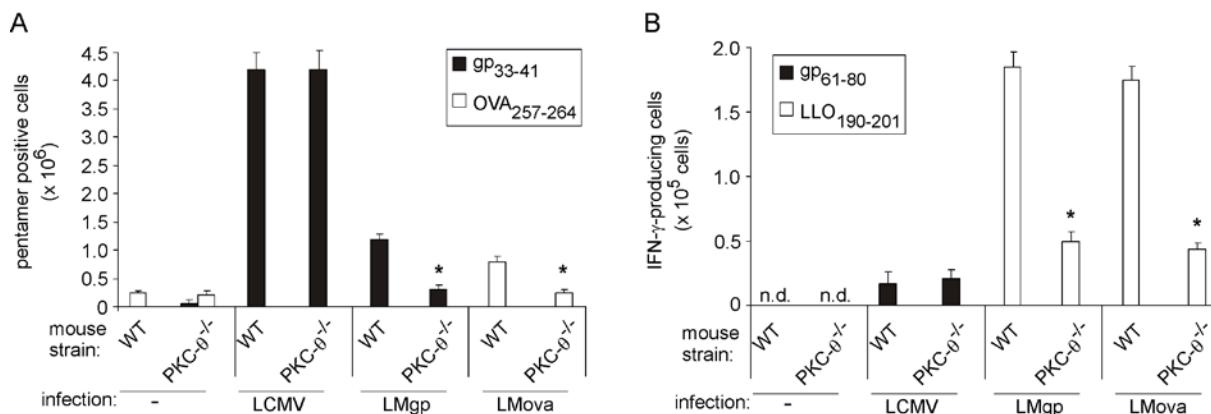


Figure 7. Reduced numbers of pathogen-specific CD8 and CD4 T cells in *Listeria*, but not LCMV infection of PKC-θ^{-/-} mice. WT and PKCθ^{-/-} C57BL/6 mice were infected with 1x10⁵ PFU of LCMV, 1x10⁵ LMgp (transgenic for the LCMV gp₃₃₋₄₁ epitope) and 1x10⁵ LMova, respectively. (A) The number of splenic gp₃₃₋₄₁-, and OVA₂₅₇₋₂₆₄-specific CD8 T cells was determined in LCMV, LMgp, and LMova infected (d8 p.i.) as well as non-infected WT and PKC-θ^{-/-} mice by staining with anti-CD8-FITC in combination with OVA₂₅₇₋₂₆₄ (SIINKFEKL) or gp₃₃₋₄₁ (KAVYNFATM)-PE-conjugated pentamers, and analyzed by flow cytometry. Data are means + SD of three mice per experimental groups. * p ≤ 0.02 for PKC-θ^{-/-} vs. WT mice. (B) The number of gp₆₁₋₈₀- and LLO₁₉₀₋₂₀₁-specific cells was determined in spleen cells of non-infected and infected (day 8 p.i.) WT and PKC-θ^{-/-} mice (day 8 p.i.) by an IFN-γ ELISPOT. Data are means + SD of three mice per experimental groups. “n.d.” is for “not detectable”. * p ≤ 0.001 for PKC-θ^{-/-} vs. WT mice.

Additional ELISPOT assays confirmed that numbers of pathogen-specific CD8 T cells were normal in LCMV infection, but not in listeriosis of PKC-θ^{-/-} mice (data not shown). In parallel to CD8 T cells, the number of cells specific for the LCMV-gp₆₁₋₈₀ MHC class II epitope was unaffected by PKC-θ-deficiency in LCMV infection, whereas the number of cells specific

for the *L. monocytogenes*-derived LLO₁₉₀₋₂₀₁ MHC class II epitope was significantly reduced in both LMova- and LMgp-infected PKC-θ^{-/-} mice (Fig. 7B). Collectively, PKC-θ plays an important role for the normal generation of *L. monocytogenes*-specific CD4 and CD8 T cells. Importantly, the reduction of *L. monocytogenes*-specific T cells in PKC-θ^{-/-} mice depends on the pathogen rather than on the epitope, because PKC-θ^{-/-} mice mounted a reduced CD8 T cell response against the gp₃₃₋₄₁ epitope upon infection with LMgp, but not after infection with LCMV.

4.1.1.2 Reduced numbers of MHC class Ia-, MHC class Ib-, and MHC class II-restricted *L. monocytogenes*-specific T cells in primary and secondary listeriosis of PKC-θ^{-/-} mice

To analyze whether PKC-θ regulates the kinetics of *L. monocytogenes*-specific T cells, we infected C57BL/6 WT and PKC-θ^{-/-} mice with LMova and quantified the number of LMova-specific T cells at different time points after primary and secondary infection. The number of OVA₂₅₇₋₂₆₄-specific, MHC class Ia-restricted CD8 T cells was significantly reduced in PKC-θ^{-/-} mice (Fig. 8A) at all time points between d 5 and d 50 after primary infection. In addition, the number of fMIGWII-specific MHC class Ib-restricted CD8 T cells was significantly reduced in acute listeriosis of PKC-θ^{-/-} mice (Fig. 8B). In parallel to CD8 T cells, the number of *L. monocytogenes*-specific IFN-γ-producing CD4 T cells was significantly reduced in listeriosis of PKC-θ^{-/-} mice at days 7 and 9 p.i. (Fig. 8C). Upon secondary infection at d 50 after primary infection, numbers of OVA₂₅₇₋₂₆₄-specific CD8 T cells were reduced at any time point between d 1 and d 21 after reinfection with LMova (Fig. 8D). Moreover, numbers of LLO₁₉₀₋₂₀₁-specific CD4 T cells was also reduced in PKC-θ^{-/-} mice, although differences were only significant at d 5 after reinfection (Fig. 8E). In summary, these findings illustrate that PKC-θ is important for an optimal expansion of both *L. monocytogenes*-specific CD8 and CD4 T cells in primary and secondary listeriosis.

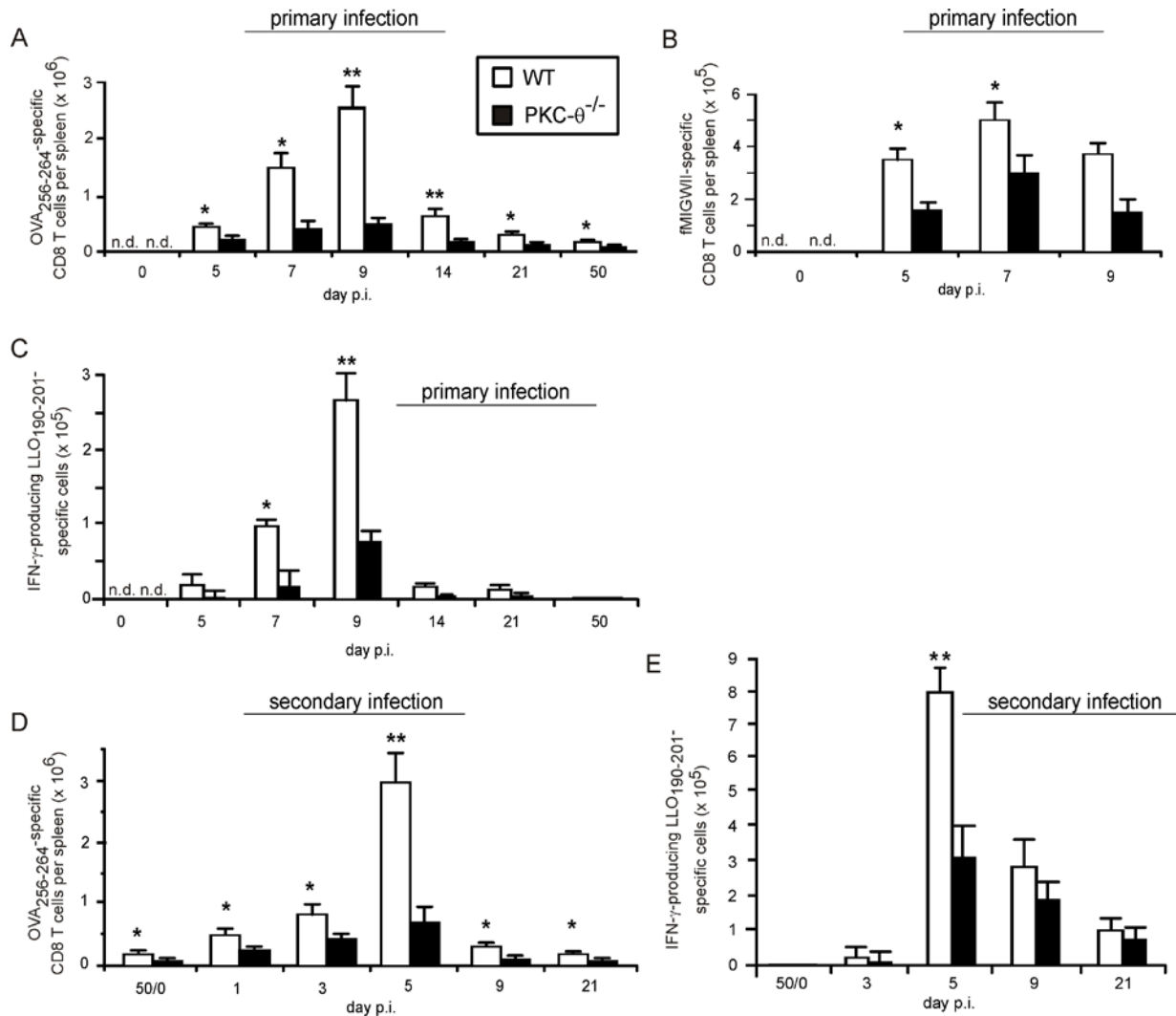


Figure 8. Kinetics of *L. monocytogenes*-specific T cells in WT and PKC-θ^{-/-} mice. The number of OVA₂₅₇₋₂₆₄-specific (A, D) and fMIGWII-specific (B) CD8 T cells was determined in the spleen of C57BL/6 WT and PKC-θ^{-/-} mice by staining with OVA₂₅₇₋₂₆₄-PE pentamer (A, D) and fMIGWII-specific tetramer (B) in combination with anti-CD8-FITC after primary (A, B) and secondary (D) infection with LMova. (C, E) The frequency of LLO₁₉₀₋₂₀₁-specific splenic CD4 T cells was determined by an IFN-γ ELISPOT after primary (C) and secondary (E) infection with LMova. Data represent the means ± SD of 3 to 4 mice per experimental group. “n.d.” is for “not detectable”. * $p \leq 0.05$, and ** $p \leq 0.001$ for PKC-θ^{-/-} vs. WT mice.

4.1.1.3 Impaired control of *L. monocytogenes* in PKC-θ^{-/-} mice

To study whether the reduced T cell responses in PKC-θ^{-/-} mice correspond to an impaired pathogen control, we determined colony forming units (CFUs) in liver and spleen. After primary infection with WT *L. monocytogenes*, PKC-θ^{-/-} mice harboured significantly increased numbers of *L. monocytogenes* in the liver and spleen starting at d5 p.i. (Fig. 9A, B). Thus, the inability of PKC-θ^{-/-} mice to control *L. monocytogenes* became evident at the same time point when stronger

T cell responses were detectable in WT mice. Upon secondary infection, PKC- $\theta^{-/-}$ mice had also increased numbers of *L. monocytogenes* in liver and spleen, and as observed in primary infection, differences became significant in the liver earlier than in the spleen (Fig. 9C, D). These data indicate that PKC- θ is functionally relevant for control of *L. monocytogenes* in primary and secondary infection *in vivo*.

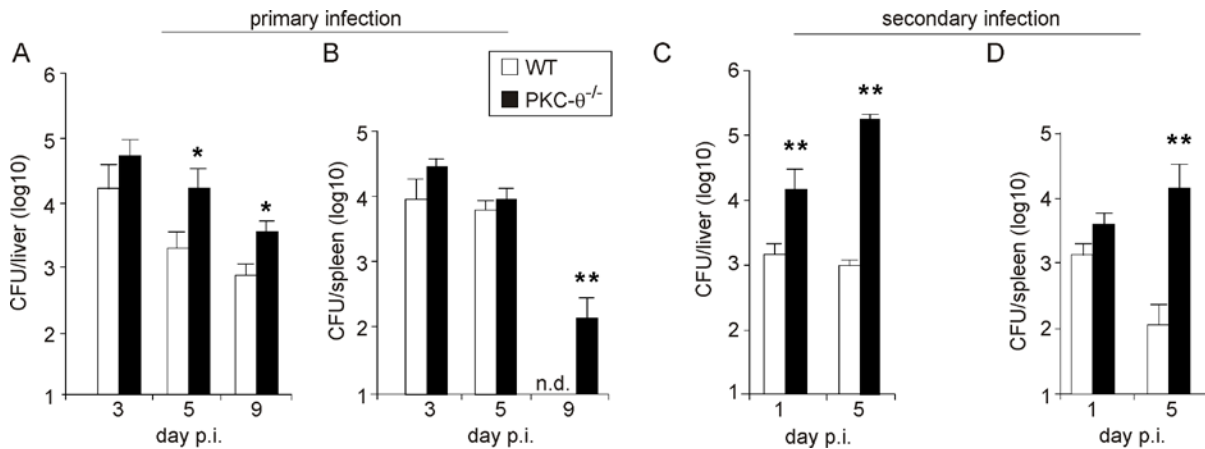


Figure 9. Impaired control of *L. monocytogenes* in PKC- $\theta^{-/-}$ mice during primary and secondary infection. CFUs were determined in liver and spleen of C57BL/6 WT and PKC- $\theta^{-/-}$ mice after primary infection with 1×10^4 (A, B) and secondary infection with 1×10^6 (C, D) WT *L. monocytogenes*. CFUs were determined in 4 mice per experimental group at the indicated time points p.i. Data represent the mean + SD. “n.d.” is for “not detectable”. * $p \leq 0.05$, and ** $p \leq 0.005$ for PKC- $\theta^{-/-}$ vs. WT mice.

4.1.1.4 The reduction of *L. monocytogenes*-specific CD8 and CD4 T cells in PKC- $\theta^{-/-}$ mice is organ-dependent

To analyze whether the reduction of *L. monocytogenes*-specific CD8 and CD4 T cells is a general or an organ-specific finding, we determined the numbers of *L. monocytogenes*-specific CD8 and CD4 T cells in spleen, liver, mLN, and blood of LMova-infected C57BL/6 WT and PKC- $\theta^{-/-}$ mice at d 9 after primary infection with LMova. The percentage of OVA₂₅₇₋₂₆₄-specific CD8 T cells was reduced in spleen, liver, mLN, and blood of PKC- $\theta^{-/-}$ mice (Fig. 10A). A quantitation of the number of OVA₂₅₇₋₂₆₄-specific CD8 T cells revealed that this reduction was significant in all organs analyzed (B). In parallel to CD8 T cells, numbers of *L. monocytogenes*-specific IFN- γ -producing CD4 T cells were significantly reduced in spleen, liver, mLN, and blood of PKC- $\theta^{-/-}$ mice (Fig. 10C). Thus, the reduction of *L. monocytogenes*-specific T cells in

the spleen of PKC- $\theta^{-/-}$ (Fig. 7 and 8) is not caused by a failure of PKC- $\theta^{-/-}$ T cells to home to the spleen or by an increased egress from the spleen.

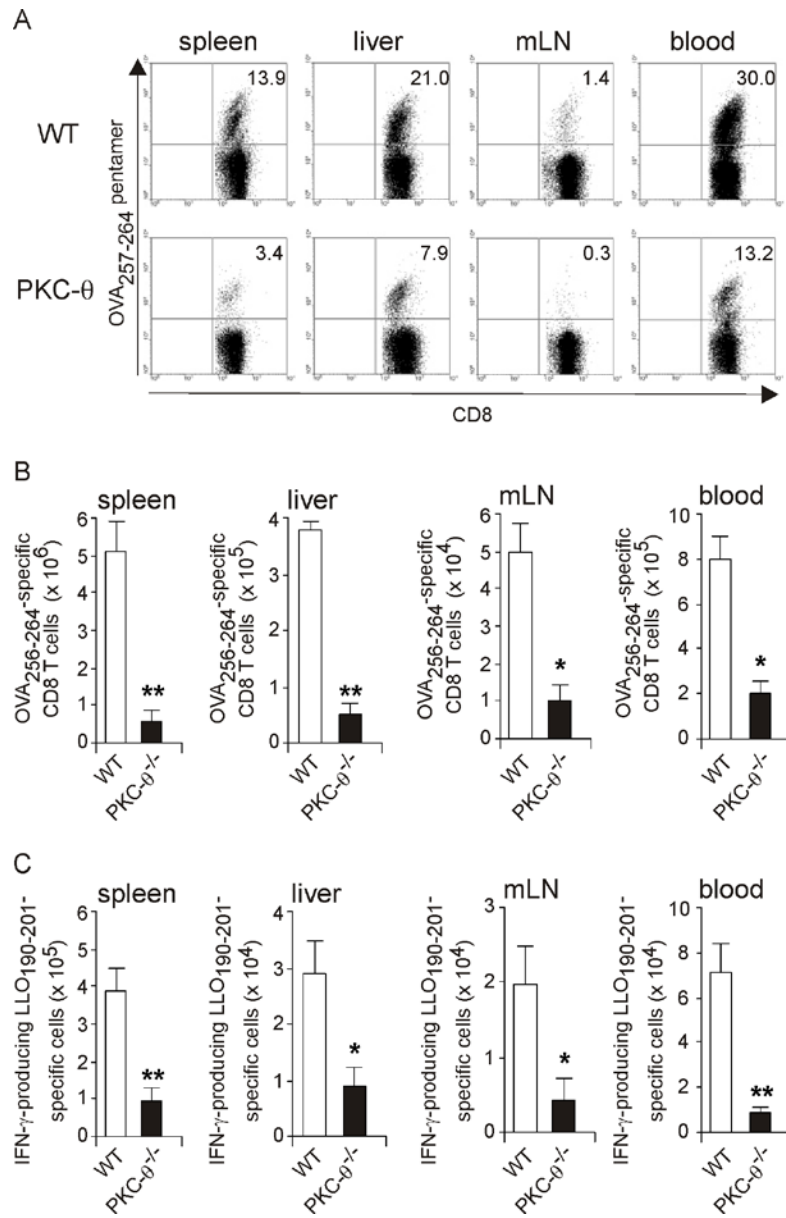


Figure 10. Reduced numbers of *L. monocytogenes*-specific CD8 and CD4 T cells in different organs of PKC- $\theta^{-/-}$ mice. The number of OVA₂₅₇₋₂₆₄-specific (A, B) CD8 T cells and LLO₁₉₀₋₂₀₁-specific CD4 T cells (C) was determined in the spleen, liver, mLN, and blood of C57BL/6 WT and PKC- $\theta^{-/-}$ mice at d 9 after primary infection with 5x10⁴ LMova. (A) Leukocytes were isolated from the various organs of 6 mice per experimental group and the leukocytes of each organ were pooled and stained with OVA₂₅₇₋₂₆₄-PE pentamer in combination with anti-CD8-FITC. Dot plots of OVA₂₅₇₋₂₆₄-PE pentamer and CD8-FITC are shown after gating on CD8⁺ cells. (B) The percentage of OVA₂₅₇₋₂₆₄-specific CD8 T cells was determined for each mouse and organ individually as illustrated in (A) and the absolute number of OVA₂₅₇₋₂₆₄-specific CD8 T cells per organ was calculated. Data show the mean ± SD of 6 mice per organ and experimental group. (C) The number of LLO₁₉₀₋₂₀₁-specific splenic CD4 T cells was determined by an IFN- γ ELISPOT. Data represent the mean ± SD of 6 mice per experimental group. * p ≤ 0.05, and ** p ≤ 0.001 for PKC- $\theta^{-/-}$ vs. WT mice.

4.1.1.5 The role of PKC-θ for the generation of *L. monocytogenes*-specific T cells and bacterial control is independent of the host genetic background

Immunity to *L. monocytogenes* is partially dependent on the host genetic background (Cheers and McKenzie, 1978). To assess whether the role of PKC-θ for the generation of *L. monocytogenes*-specific cells and control of the bacterium is influenced by the host genetic background, we additionally infected BALB/c WT and PKC-θ^{-/-} with WT *L. monocytogenes* (Fig. 11). As observed for mice on the C57BL/6 background (Fig. 9), BALB/c PKC-θ^{-/-} mice harboured significantly more *L. monocytogenes* in spleen and liver as compared to WT animals on day 9 p.i. (Fig. 11A). In addition, the number of *L. monocytogenes*-specific CD8 and CD4 T cells was significantly reduced in spleen and liver of BALB/c PKC-θ^{-/-} mice as compared to the corresponding WT mice (Fig. 11B, C). These findings illustrate, that the important function of PKC-θ for an optimal T cell response and pathogen control in listeriosis is independent of the host genetic background.

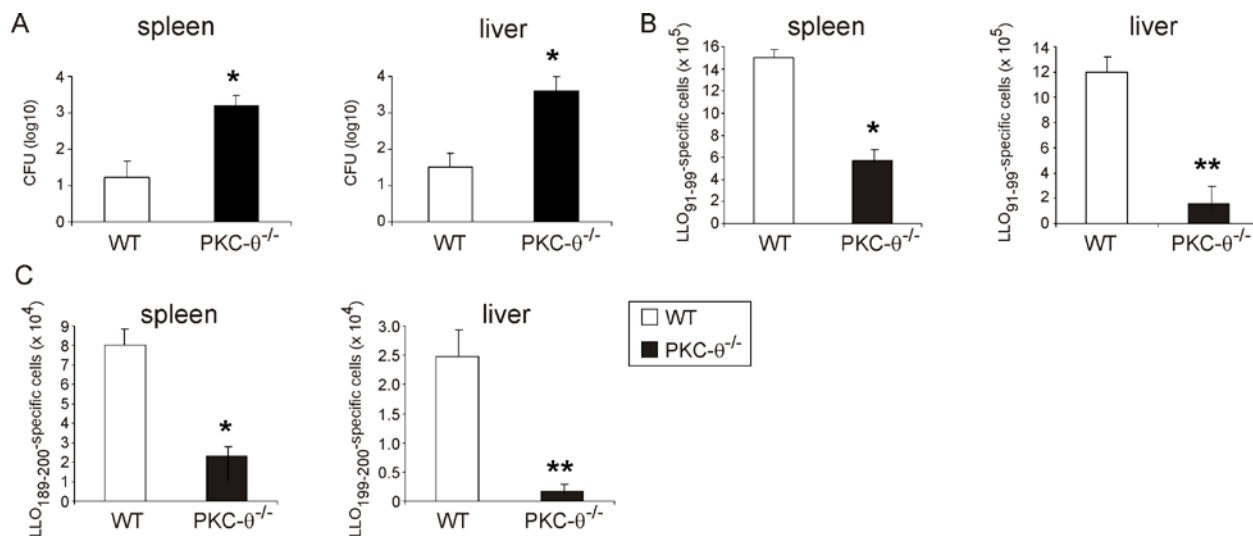


Figure 11. The immune response against *L. monocytogenes* is also severely impaired in PKC-θ^{-/-} mice of the BALB/c background. BALB/c WT and PKC-θ^{-/-} mice were i.p infected with 1×10^4 WT *L. monocytogenes* and analyzed at d 9 after infection. (A) CFUs were determined in spleen and liver of 5 mice per group (mean + SD, * p < 0.01). (B) The number of LLO₉₁₋₉₉ and (C) LLO₁₈₉₋₂₀₀-specific cells was determined in spleen and liver of 5 mice per group by IFN-γ ELISPOT assays (mean + SD, * p < 0.01, ** p < 0.005).

4.1.1.6 Adoptive transfer of WT T cells compensates for PKC-θ-deficiency in listeriosis

To validate that the impaired control of *L. monocytogenes* in PKC-θ^{-/-} mice was caused by an insufficient T cell response, we adoptively transferred purified polyclonal WT T cells into PKC-θ^{-/-} mice before infection with LMova and monitored the bacterial load in these animals. In fact, CFUs were significantly reduced in spleen (Fig. 12A) and liver (Fig. 12B) of PKC-θ^{-/-} mice supplemented with WT T cells as compared to PKC-θ^{-/-} supplemented either with PKC-θ^{-/-} T cells or without adoptive transfer. Importantly, the bacterial load in PKC-θ^{-/-} mice supplemented with WT T cells was as low as in infected WT control mice (Fig. 12A, B).

Additional western blot analysis showed that PKC-θ was present in spleen cells of non-infected and infected WT mice as well as in LMova-infected PKC-θ^{-/-} mice supplemented with WT T cells, whereas it was as expected absent in PKC-θ^{-/-} mice (Fig. 12C). Moreover, phosphorylated PKC-θ, already detectable in non-infected WT spleens at varying signal intensities (compare exp.1 and 2), was enhanced in infected WT controls as well as in PKC-θ^{-/-} mice supplemented with WT T cells (Fig. 12C).

Since *L. monocytogenes* secretes virulence factors, in particular LLO, which may impact on the Ag-presenting capacity of DCs and may reduce T cell responsiveness upon contact with APCs (Foulds et al., 2002), we studied whether an immunization with WT DCs loaded with OVA₂₅₇₋₂₆₄ and LLO₁₉₀₋₂₀₁ peptides induces normal T cell responses in PKC-θ^{-/-} mice. In good agreement with data from Hamilton and Harty (Hamilton and Harty, 2002), WT mice generated an OVA₂₅₇₋₂₆₄-specific CD8 T cell and LLO₁₉₀₋₂₀₁-specific CD4 T cell response (Fig. 12D, E). However, numbers of OVA₂₅₇₋₂₆₄-specific CD8 and LLO₁₉₀₋₂₀₁-specific CD4 T cells were significantly reduced in PKC-θ^{-/-} mice (Fig. 12D, E).

These findings indicate that the impaired control of *L. monocytogenes* in PKC-θ^{-/-} mice is due to an intrinsic defect of T cells and can be restored by transfer of WT T cells . In contrast, an immunization with peptide-loaded, mature activated WT-DCs does not compensate for lack of T-cellular PKC-θ-expression for the induction of OVA₂₅₇₋₂₆₄-specific CD8 and LLO₁₉₀₋₂₀₁-specific CD4 T cells.

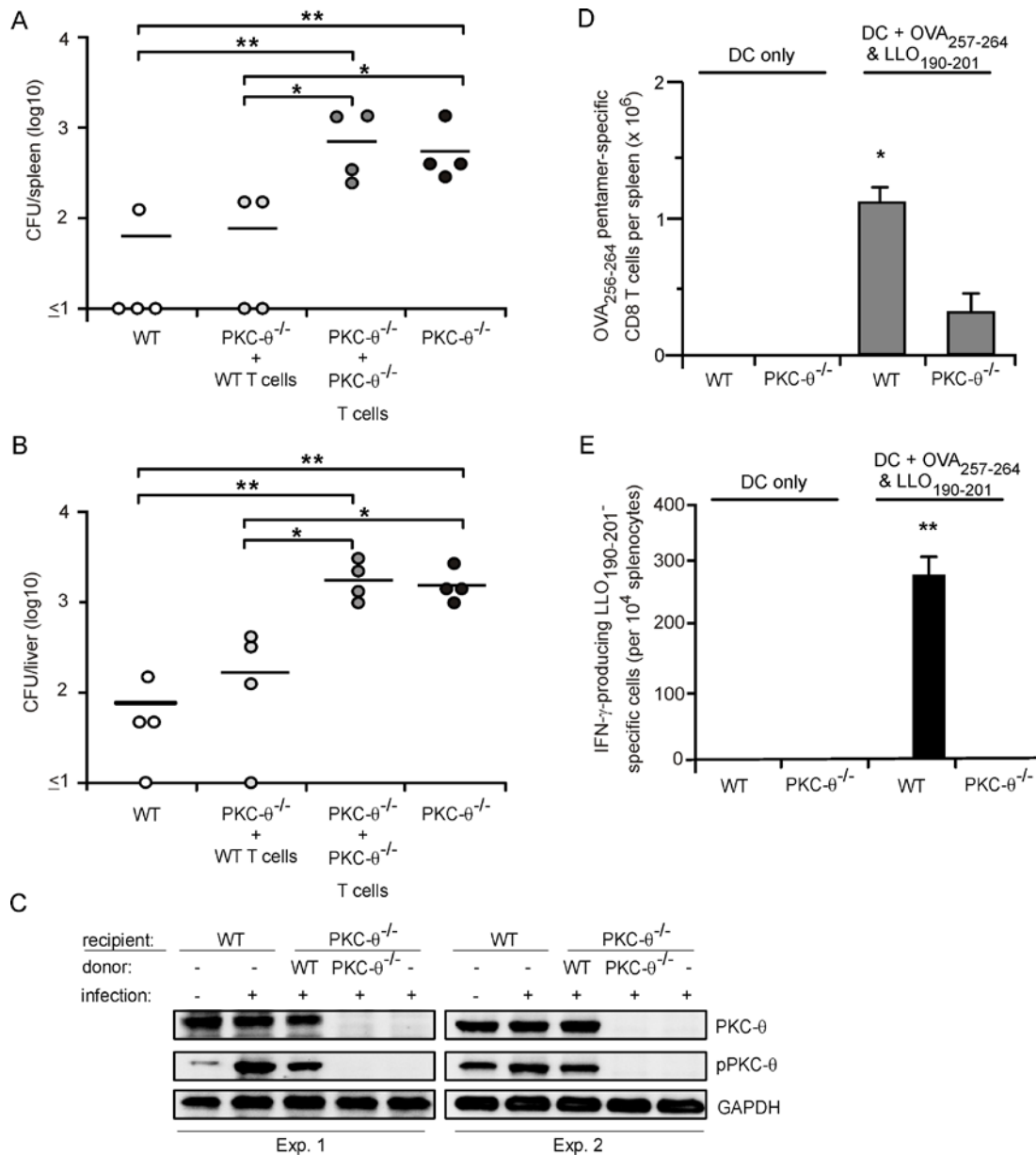


Figure 12. WT T cells compensate for PKC-θ-deficiency in listeriosis, but peptide-loaded WT DCs do not induce a normal expansion of peptide-specific T cells in PKC-θ^{-/-} mice. (A, B) On d 8 after infection with WT *L. monocytogenes*, CFUs were determined in spleen (A) and liver (B) of (i) C57BL/6 WT mice, (ii) PKC-θ^{-/-} mice, (iii) PKC-θ^{-/-} mice supplemented with 2×10^7 polyclonal WT T cells, and (iv) PKC-θ^{-/-} mice supplemented with 2×10^7 polyclonal PKC-θ^{-/-} T cells. Adoptive T cell transfers were performed one day prior to infection. CFUs of individual mice are shown and the horizontal bar represents the mean value. * $p \leq 0.05$, and ** $p \leq 0.004$. (C) Western blot analysis of PKC-θ, phospho-PKC-θ, and GAPDH expression in MACS-isolated splenic T cells of non-infected WT mice and WT LM-infected WT, PKC-θ^{-/-}, PKC-θ^{-/-} mice supplemented with either polyclonal WT or PKC-θ^{-/-} T cells. T cells were isolated from infected mice at d 8 p.i. Results of one representative mouse per group from two independent experiments with three mice each are shown. (D,E) WT and PKC-θ^{-/-} were immunized with OVA₂₅₇₋₂₆₄ and LLO₁₉₀₋₂₀₁ peptide-loaded BMDCs or with non-peptide-loaded DCs. The number of OVA₂₅₇₋₂₆₄-specific CD8 T cells was determined by OVA₂₅₇₋₂₆₄-PE pentamer staining (D) and the number of LLO₁₉₀₋₂₀₁-specific cells was determined by an IFN-γ-ELISPOT (E) at d 7 after immunization. Data show the mean + SD of four mice per experimental group. * $p \leq 0.01$, and ** $p \leq 0.006$ for PKC-θ^{-/-} vs. WT mice.

4.1.1.7 PKC-θ is important for proliferation and survival of *L. monocytogenes*-specific CD8 T cells, but its function can be partially compensated by neighbouring WT cells

To determine the impact of PKC-θ on proliferation, apoptosis and activation of *L. monocytogenes*-specific T cells we crossed PKC-θ^{-/-} mice with OVA₂₅₇₋₂₆₄-specific TCR transgenic OT-I mice and adoptively transferred MACS-purified CSFE-labeled PKC-θ^{-/-} or WT OT-I CD8 T cells into WT (Fig. 13A) or PKC-θ^{-/-} (Fig. 13B) recipients prior to infection with LMova. In non-infected mice, only small numbers of transferred WT and PKC-θ^{-/-} OT-I T cells proliferated in both WT and PKC-θ^{-/-} recipients (Fig. 13A, B). Upon infection with LMova, 84.5 % of transferred WT OT-I T cells proliferated in WT recipients (Fig. 13A), and a comparable percentage (79.9 %) of transferred WT OT-I T cells proliferated in LMova-infected PKC-θ^{-/-} recipients (Fig. 13B). In contrast, proliferation of PKC-θ^{-/-} OT-I CD8 T cells was reduced in LMova-infected recipients: only 55.6 % of adoptively transferred PKC-θ^{-/-} OT-I CD8 T cells proliferated in LMova-infected WT mice (Fig. 13A), and PKC-θ^{-/-} OT-I CD8 T cells did not proliferate in LMova-infected PKC-θ^{-/-} recipients (Fig. 13B).

To determine the impact of PKC-θ on the survival of *L. monocytogenes*-specific CD8 T cells, we stained adoptively transferred PKC-θ^{-/-} and WT OT-I T cells with 7-AAD and annexin-V. In non-infected mice, the vast majority both WT and PKC-θ^{-/-} OT-I T cells died independent of PKC-θ expression of the host within 2 days after adoptive transfer (Fig. 13A, B). In contrast, ~80 % of proliferating WT OT-I T cells survived (annexinV⁻/7-AAD⁻) in both LMova-infected WT and PKC-θ recipients 2 days after infection. Proliferating PKC-θ^{-/-} OT-I T cells were also partially rescued from death (62.1 % annexinV⁻/7-AAD⁻) in LMova-infected WT recipients (Fig. 13A), which is in contrast to the few proliferating PKC-θ^{-/-} T cells in LMova-infected PKC-θ^{-/-} recipients (Fig. 13B). Non-proliferating PKC-θ^{-/-} and WT OT-I T cells did not survive in LMova-infected mice independent of the PKC-θ expression of the recipient.

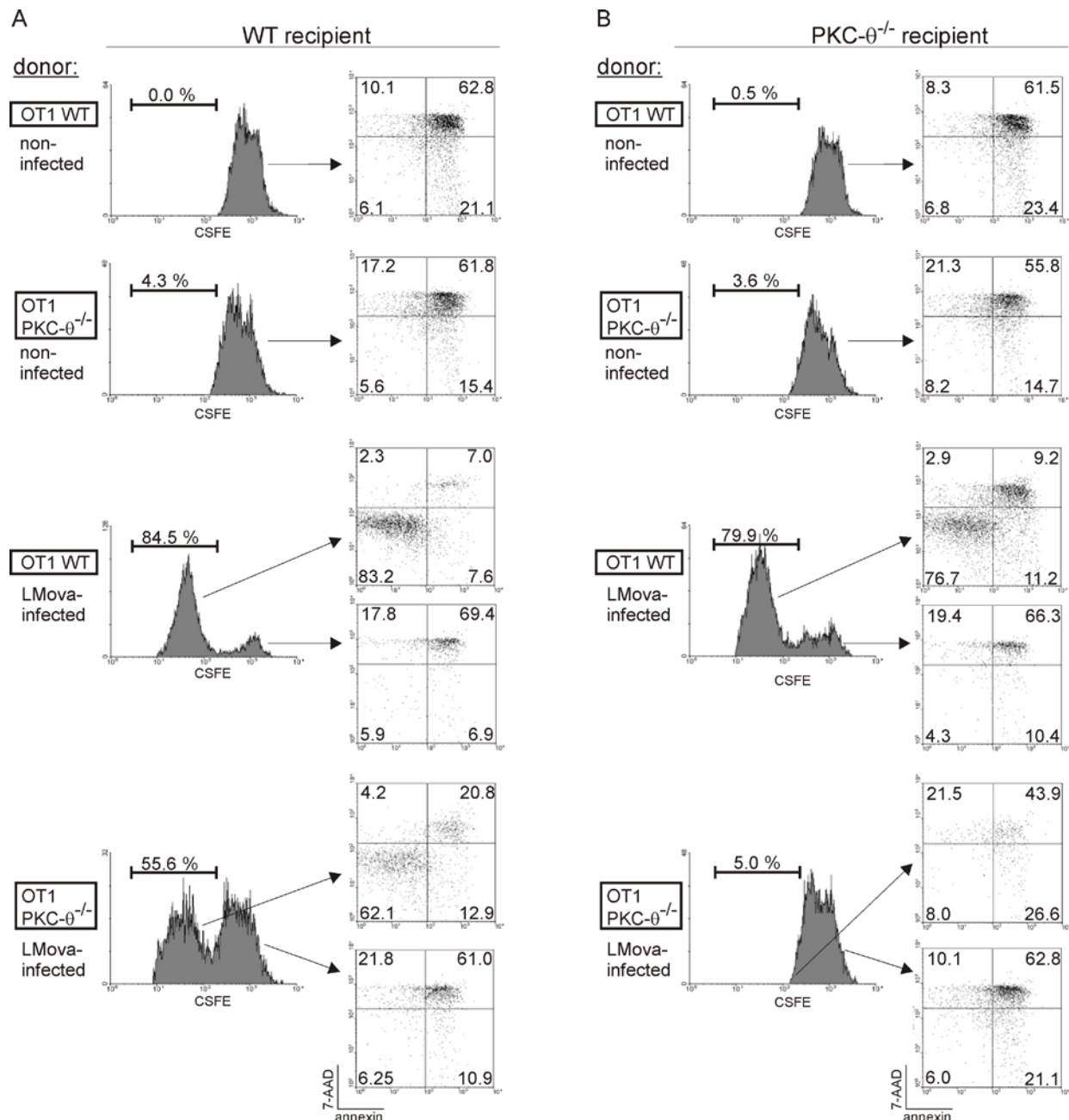


Figure 13. Decreased proliferation and survival of PKC- $\theta^{-/-}$ OT-I CD8 T cells in LMova-infected mice is partially rescued in WT hosts. MACS-purified, CSFE-labeled WT and PKC- $\theta^{-/-}$ OT-I CD8 T cells were adoptively transferred into WT (A) or PKC- $\theta^{-/-}$ (B) recipients. Recipients were left uninfected or were infected with 5×10^4 LMova one day after adoptive transfer. Representative histograms show CSFE profiles of adoptively transferred CD8 T cells 48 h after infection and the percentage of proliferating cells is presented. Dot plots show results for annexin-V/7-AAD staining of proliferating and non-proliferating cells as indicated by arrows. The percentage of annexin-V and 7-AAD positive or negative cells is presented. Three to four recipient mice were analyzed per group and representative data are shown.

C

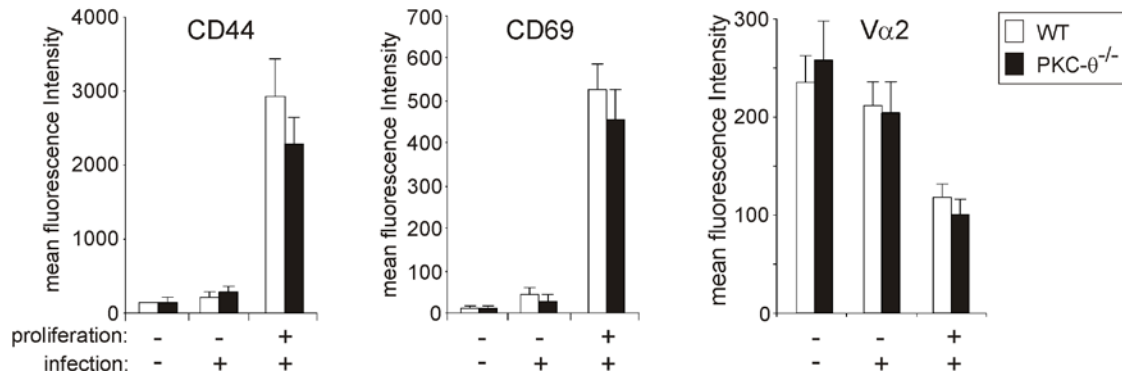


Figure 13. (C) The activation of CSFE $^{+}$ CD8 T cells adoptively transferred into WT mice was analyzed by staining with anti CD44, anti-CD69 and anti-V α 2 antibodies, respectively, followed by flow cytometry at d 2 after infection with 5×10^4 LMova. Three to four recipient mice were analyzed per group and the mean + SD is shown.

In addition, both proliferating WT and PKC-θ $^{-/-}$ OT-I T cells equally upregulated CD44 and CD69 activation markers and down-regulated the V α 2 TCR in LMova-infected WT recipients (Fig. 13C).

In parallel, we also performed adoptive transfer experiments with OVA-specific WT and PKC-θ $^{-/-}$ OT-II CD4 T cells, which provided essentially the same results with respect to proliferation, survival and activation as demonstrated for OT-I CD8 T cells (data not shown).

These findings illustrate (i) that a WT milieu partially rescues proliferation and survival of PKC-θ $^{-/-}$ *L. monocytogenes* -specific T cells, and (ii) that a cell autonomous expression of PKC-θ by *L. monocytogenes* -specific T cells is sufficient for proliferation and survival of these T cells in a PKC-θ-deficient host.

4.1.1.8 Externally supplemented IL-2, but not inhibition of caspases partially restores proliferation of PKC-θ $^{-/-}$ T cells *in vitro*

To identify parameters, which might mediate the compensatory effect of a WT milieu on PKC-θ $^{-/-}$ T cell proliferation and survival, we used an *in vitro* system composed of LMova-infected WT BMDCs and MACS-purified WT or PKC-θ $^{-/-}$ OT-I T cells.

After co-incubation with non-infected WT BMDCs, only a very small number of CSFE-labeled WT or PKC-θ $^{-/-}$ OT-I cells proliferated (Fig. 14A). In contrast, stimulation of WT OT-I T cells with LMova-infected BMDCs resulted in proliferation of more than 50 % of the WT T cells, whereas PKC-θ $^{-/-}$ OT-I cells still did not proliferate (Fig. 14A). However, addition of IL-2

induced proliferation of 40 % of PKC- $\theta^{-/-}$ OT-I cells stimulated with LMova-infected WT BMDCs. The proliferation of WT OT-I cells did not further increase after addition of IL-2. As observed for non-infected recipients *in vivo* (Fig. 13), only small numbers of WT and PKC- $\theta^{-/-}$ OT-I cells co-incubated with non-infected BMDCs survived as revealed by annexin-V/7-AAD staining (Fig. 14A). Stimulation with LMova-infected BMDCs resulted in proliferation and an increased survival of OT-I T cells (34.5 % annexinV⁻/7-AAD⁻), whereas the number of annexin-V⁻/7-AAD⁻ PKC- $\theta^{-/-}$ remained unchanged (14.6 %) after WT BMDC-LMova stimulation.

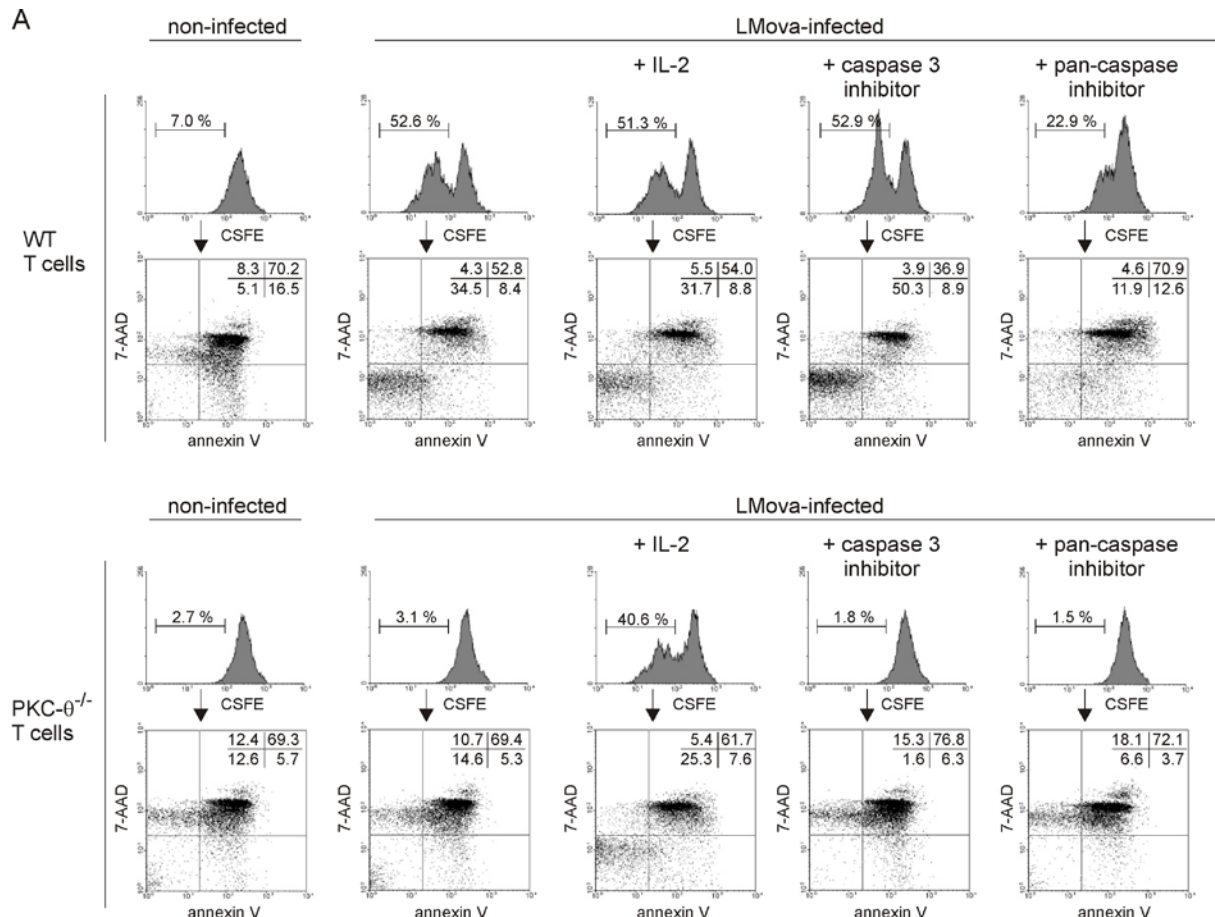


Figure 14. IL-2, but not caspase inhibitors enhance proliferation of PKC- $\theta^{-/-}$ OT-I CD8 T cells after stimulation with LMova-infected WT BMDCs *in vitro*.(A) Uninfected and LMova-infected WT BMDCs were co-incubated with MACS-purified, CSFE-labeled WT or PKC- $\theta^{-/-}$ OT-I CD8 T cells. Cultures were left untreated or were supplemented with either IL-2, a caspase-3 inhibitor or the pan-caspase inhibitor Z-VAD. Triplicate wells were analyzed and representative histograms show CSFE profiles of OT-I CD8 T cells 48 h after infection. The percentage of proliferating cells is presented. Dot plots show results for annexin-V/7-AAD staining of CSFE⁺ CD8 T cells and the percentage of cells in each quadrant is presented.

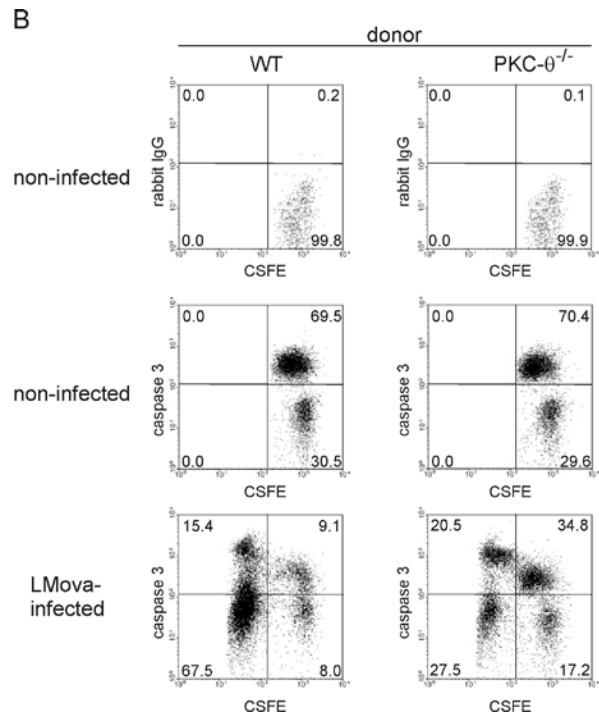


Figure 14. (B) MACS-purified, CSFE-labeled WT and $\text{PKC-}\theta^{-/-}$ OT-I T cells were adoptively transferred into WT recipients. Recipients were left uninfected or were infected with 5×10^4 LMova. 48 h after infection, spleen cells were stained for active caspase-3 and CD8. Controls included staining with isotype-matched control antibodies. Dot plots show the CSFE profile of transferred CD8 T cells in combination with anti-caspase-3 staining or control staining. The percentage of cells per quadrant is shown. Three recipients per group were analyzed and a representative dot plot is shown.

However, the addition of IL-2 to $\text{PKC-}\theta^{-/-}$ OT-I T cells stimulated with LMova-infected BMDC resulted in an increased survival rate of the T cells (25.3 %, Fig. 14A). The addition of IL-2 did not modify the survival rate of WT OT-I cells stimulated with LMova-infected BMDCs.

These findings illustrate (i) that LMova-infected WT BMDCs only induce the proliferation and survival of WT OT-I cells, but are not sufficient to compensate for a T cellular $\text{PKC-}\theta$ -deficiency and (ii) that IL-2 partially restores proliferation and survival of *L. monocytogenes*-specific $\text{PKC-}\theta^{-/-}$ T cells stimulated with LMova-infected WT BMDCs.

Our data presented in Fig. 14 indicate that $\text{PKC-}\theta$ prevents the apoptosis of activated *L. monocytogenes*-specific T cells. To further analyze the impact of $\text{PKC-}\theta$ on apoptosis of *L. monocytogenes*-specific T cells, we determined the presence of active caspase-3 in WT and $\text{PKC-}\theta^{-/-}$ OT-I T cells after adoptive transfer to WT recipients. In non-infected WT recipients, about 70 % of transferred WT and $\text{PKC-}\theta^{-/-}$ OT-I T cells were positive for active caspase-3 (Fig. 14B), which corresponds to the percentage of annexin-V/7-AAD positive cells (Fig. 13). Upon infection with LMova, 82.9 % of WT OT-I cells proliferated and only approximately 1/5 of the

proliferating cells was positive for active caspase-3 (Fig. 14B). In contrast and as observed before (Fig. 13), only 48 % of PKC- $\theta^{-/-}$ OT-I cells proliferated in LMova-infected WT recipients and approximately 50 % of these proliferating cells were active caspase-3⁺ (Fig. 14B).

To study the functional role of caspases, we treated co-cultures of LMova-infected BMDC and OT-I cells with either a caspase-3 inhibitor or the pan-caspase inhibitor Z-VAD (Fig. 14A). Caspase-3 inhibition had no influence on proliferation of WT OT-I cells, although strongly increasing the number of surviving annexin-V⁻/7-AAD⁻ OT-I cells. In contrast, the pan-caspase-inhibitor strongly inhibited the proliferation of WT OT-I T cells by more than 50 % (52.6 % proliferation without and 22.9 % proliferation with Z-VAD). In addition, the pan-caspase inhibitor decreased the survival rate of WT OT-I cells. In PKC- $\theta^{-/-}$ OT-I T cells, neither the pan-caspase nor the caspase-3 inhibitor induced proliferation or prevented the death of these T cells.

These *in vitro* findings illustrate (i) that the reduced proliferation and survival of PKC- $\theta^{-/-}$ T cells is caspase-independent, and (ii) that caspases other than caspase-3 are required to allow a normal proliferation and survival of WT T cells.

4.1.2 Role of PKC-θ in murine toxoplasmosis

The *Listeria* and LCMV experiments have revealed that PKC-θ played a crucial role for the induction of protective T cell response in bacterial but not in viral infections. To study whether PKC-θ is important for T cell response in parasitic infections, the infection of mice with the intracellular protozoan parasite *T. gondii* was studied.

4.1.2.1 Infection with *T. gondii* induces sustained phosphorylation of PKC-θ in CD4 and CD8 T cells.

WB analysis showed that (non-activated) PKC-θ was expressed in CD4 as well as CD8 T cells of both non-infected (d 0) as well as *T. gondii*-infected mice (Fig. 15). In uninfected mice, activated PKC-θ was weakly expressed in CD4 and CD8 T cells (Fig. 15). Upon infection, PKC-θ was strongly activated in both CD4 and CD8 T at days 7, 14 and 21 post infection (p.i.) (Fig. 15). These findings illustrate a sustained activation of PKC-θ in CD4 and CD8 T cells of *T. gondii*-infected mice and provide the basis to analyze the functional role of PKC-θ in toxoplasmosis.

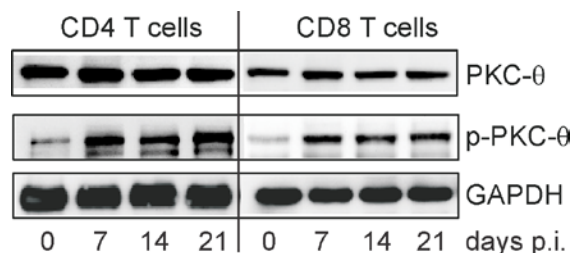


Figure 15. Sustained activation of PKC-θ in CD4 and CD8 T cells in toxoplasmosis. WB analysis of PKC-θ expression and phosphorylation in CD4 and CD8 T cells of non-infected as well as *T. gondii*-infected (d 7, 14, and 21 p.i.) WT mice was performed. CD4 and CD8 T cells were selectively isolated by MACS from 4 mice per time point. Representative blots are shown.

4.1.2.2 BALB/c PKC $\theta^{-/-}$ mice succumb to a necrotizing *Toxoplasma* encephalitis (TE)

To analyze whether PKC-θ plays a critical role for survival of toxoplasmosis, BALB/c PKC-θ $^{-/-}$ and WT mice were infected with *T. gondii* cysts. Whereas 92 % of PKC-θ $^{-/-}$ mice succumbed to the infection up to d 40 p.i., only 8 % of WT mice died up to d 60 p.i. (Fig 16A). A detailed histopathological examination revealed that BALB/c PKC-θ $^{-/-}$ mice died from a necrotizing TE with huge amounts of intracerebral parasites (Fig. 16B). In contrast, BALB/c WT mice harboured only low numbers of parasites in the brain without tissue necrosis. A quantification of

intracerebral toxoplasms revealed that the number of parasites was significantly increased in the brain of BALB/c $\text{PKC-}\theta^{-/-}$ mice as compared to WT controls at day 21 p.i. (Fig. 16C). These findings demonstrate that $\text{PKC-}\theta$ is essential for intracerebral parasite control and survival of toxoplasmosis in BALB/c mice. In the following experiments, BALB/c $\text{PKC-}\theta^{-/-}$ and WT mice were used to analyze the role of $\text{PKC-}\theta$ in toxoplasmosis.

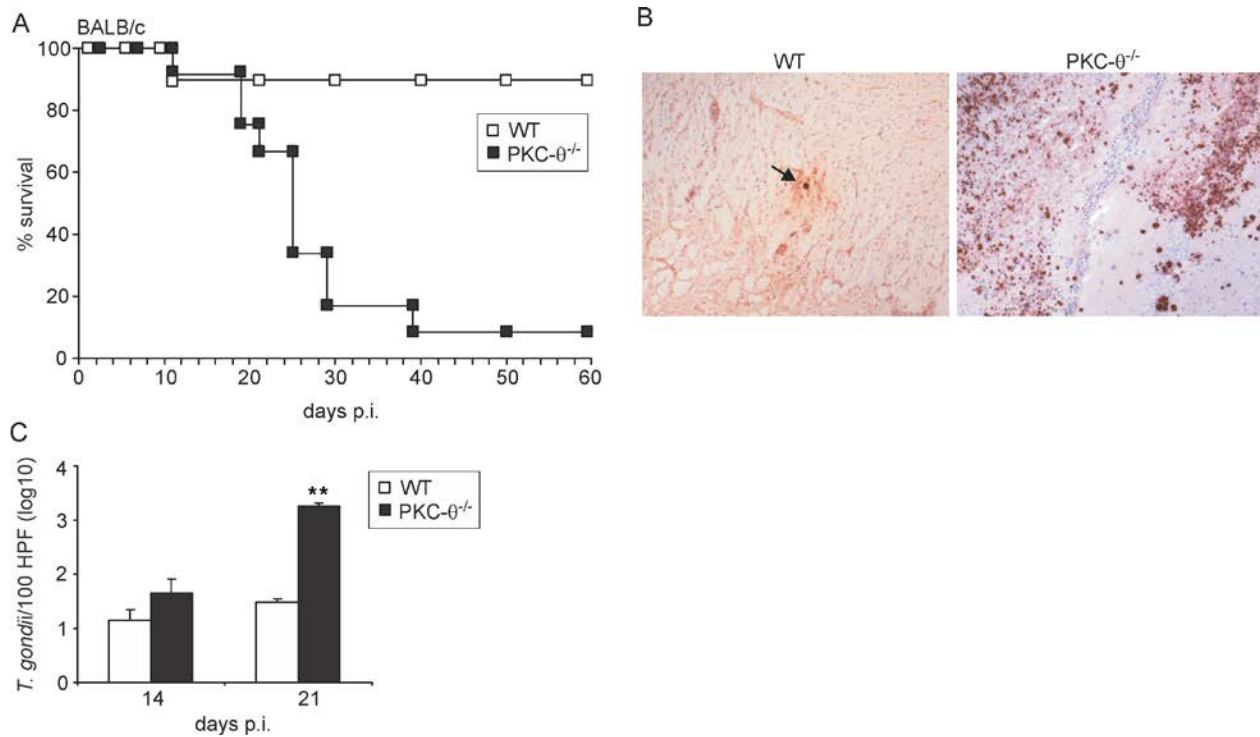


Figure 16. Reduced survival and impaired parasite control of *T. gondii*-infected BALB/c $\text{PKC-}\theta^{-/-}$ mice. BALB/c and C57BL/6 WT and $\text{PKC-}\theta^{-/-}$ mice were orally infected with *T. gondii*. (A) Significantly more BALB/c $\text{PKC-}\theta^{-/-}$ mice succumbed to the infection as compared to BALB/c WT animals (* $p < 0.005$) up to d 60 p.i. Ten mice were analyzed per mouse strain. (B) A histopathological analysis revealed that BALB/c $\text{PKC-}\theta^{-/-}$ mice had developed a severe necrotizing TE with huge amounts of intracerebral parasites at day 21 p.i. In contrast, BALB/c WT mice harboured only few parasitic cysts (arrow) at this stage of infection. Anti-*T. gondii* immunostaining, slight counterstaining with hemalum, original magnification 100x. (C) The numbers of *T. gondii* in 100 high-power fields per mouse brain were determined microscopically. Four mice were analyzed per group at d 14 and 21 p.i. and data represent the mean + SD (* $p < 0.01$).

4.1.2.3 Reduced numbers of CD4 and CD8 T cells in spleen and brain of *T. gondii*-infected $\text{PKC-}\theta^{-/-}$ mice

To determine whether $\text{PKC-}\theta$ plays a role for the recruitment of leukocytes to the brain and affects leukocyte numbers in the spleen in toxoplasmosis, intracerebral and splenic leukocytes were isolated from uninfected as well as *T. gondii*-infected mice at d 21 and d 42 p.i. Uninfected $\text{PKC-}\theta^{-/-}$ and WT mice harboured equal numbers of CD4 and CD8 T cells, B cells, macrophages,

and granulocytes in their brains and spleens, respectively (Fig. 17A, 17B). Upon infection with *T. gondii*, numbers of these leukocyte populations increased in both strains of mice (Fig 17A, 17B). However, numbers of CD4 and CD8T cells were significantly increased in spleen and brain of WT animals at d 21 and d 42 p.i., respectively. In addition, B cells were increased in spleen and brain of WT as compared to PKC- $\theta^{-/-}$ mice. Numbers of splenic and intracerebral granulocytes and macrophages did not differ between PKC- $\theta^{-/-}$ and WT mice at both time points after infection (Fig 17A, 17B). Since PKC- θ is predominantly expressed in T cells and numbers of CD4 and CD8 T cells were strongly reduced in spleen and brain of *T. gondii*-infected PKC- $\theta^{-/-}$ mice, we further focussed on the impact of PKC- θ on *T. gondii*-specific T cells.

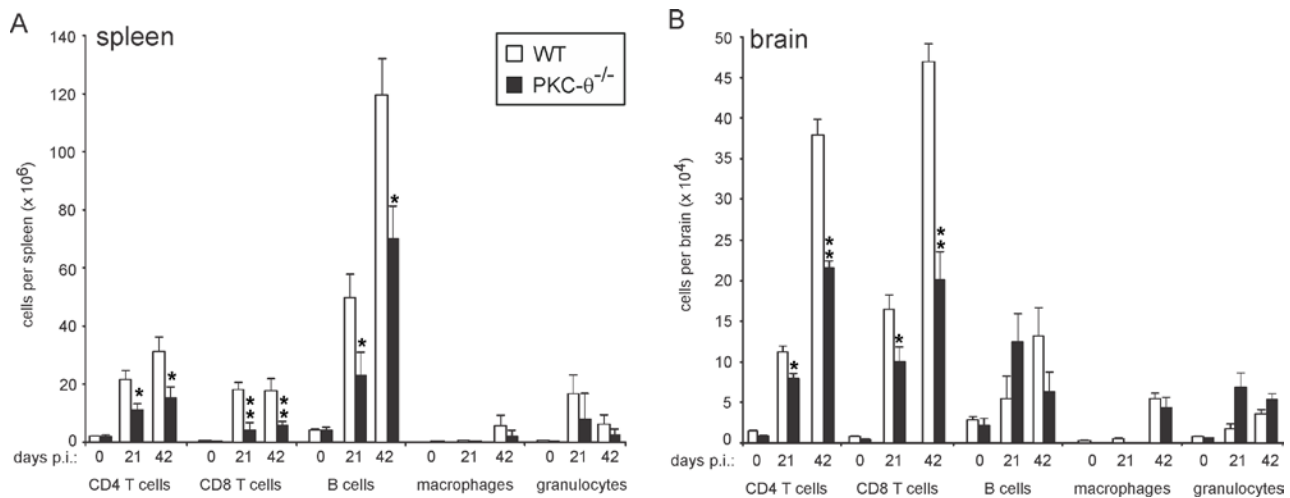


Figure 17. Reduced numbers of CD4 and CD8 T cells in spleen and brain of *T. gondii*-infected PKC- $\theta^{-/-}$ mice. Leukocyte populations were phenotyped in the spleen (A) and brain (B) of uninfected and *T. gondii*-infected WT and PKC- $\theta^{-/-}$ mice by flow cytometry at the indicated time points. Six mice per group and time points were analyzed. Data represent the mean + SD for each cell population (* p < 0.05, ** p < 0.01).

4.1.2.4 Diminished *T. gondii*-specific CD4 and CD8 T cell response in PKC- $\theta^{-/-}$ mice

To analyze whether PKC- θ regulates *T. gondii*-specific CD8 T cells, we determined the frequency and number of *T. gondii*-specific Gra6-HF10-specific CD8 T cells in spleen and brain mice by DimerX staining at d 7, 14 and 21 p.i. (Fig. 18A, B). Flow cytometry revealed that both the percentage (Fig. 18A) and the number (Fig. 18B) of Gra6-HF10-specific CD8 T cells increased in the spleen of WT mice and reached a maximum at d 21 p.i. which is in accordance with data from Blanchard et al.(2008). Additional ELISPOT experiments showed that numbers of *T. gondii*-specific IFN- γ producing CD4 and CD8 T cells were also significantly reduced in spleen and brain of PKC- $\theta^{-/-}$ mice (Fig. 18C, D). Since IFN- γ -production of CD4 and CD8 T

cells is crucial to control *T. gondii* in the CNS, these findings imply that the insufficient generation of IFN- γ -producing T cells in the absence of PKC- θ accounts for the lethal necrotizing TE in PKC- $\theta^{-/-}$ mice.

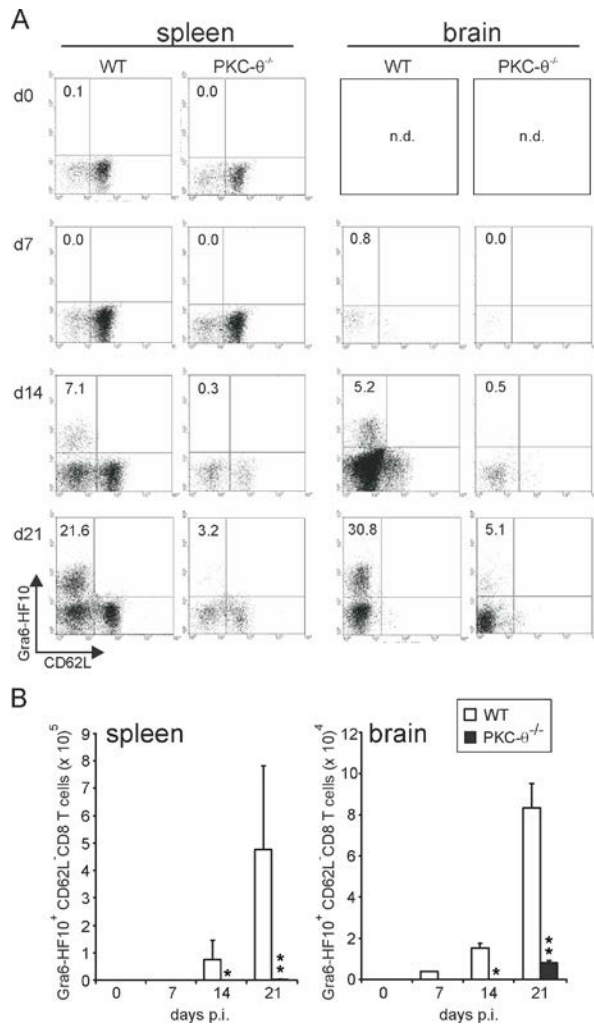


Figure 18. Impaired *T. gondii*-specific T cell responses in PKC- $\theta^{-/-}$ mice. (A) Splenic and intracerebral leukocytes were isolated and stained with Gra6-HF10 DimerX and anti-CD62L in combination with anti-CD8 at the indicated time points. Leukocytes were gated on CD8 T cells and dot plots show Gra6-HF10- and CD62L-stained CD8⁺ T cells. The percentage of Gra6-HF10⁺ CD62L⁻ is indicated in each dot plot. Six mice were analyzed per time point and experimental group and representative dot plots are shown. (B) The mean number + SD of *T. gondii*-specific CD8 T cells in the spleen and brain of WT and PKC- $\theta^{-/-}$ mice was calculated from the percentage of Gra6-HF10⁺ CD62L⁻ CD8 T cells and the absolute number of CD8 T cells. Six mice were analyzed per group and time point (* p < 0.05, ** p < 0.01).

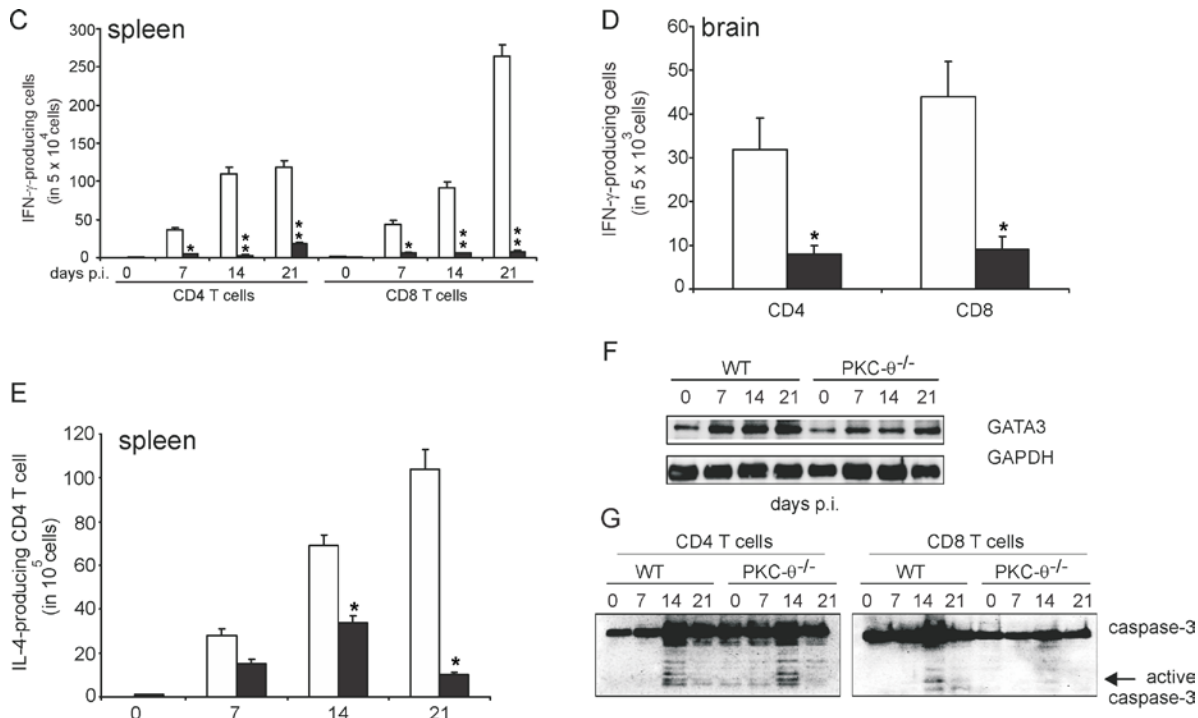


Figure 18. (C) and intracerebral (D) CD4 and CD8 T cells was determined by an ELISPOT assay. Splenic and intracerebral CD4 and CD8 T cells were isolated by MACS before analysis. Intracerebral leukocytes were analyzed at d 21 p.i. Data show the mean + SD of six mice per group (* $p < 0.05$, ** $p < 0.01$). (E) The frequency of IL-4-producing *T. gondii*-specific, MACS-isolated splenic CD4 T cells was determined by an IL-4 ELISPOT assay at the indicated time points. Four mice were analyzed per experimental group and time point. Data show the mean + SD (* $p < 0.05$). (F) Proteins were isolated from MACS-isolated splenic CD4 T cells of WT and PKC-θ⁻/⁻ and stained for GATA3 and GAPDH by WB. Representative blots are shown. (G) CD4 and CD8 T cells were isolated from spleens of three to five mice per experimental group by MACS at the indicated time points. WB analysis for caspase-3 and active caspase-3 was performed and representative data are shown.

Since it has been reported that PKC-θ is important for the development of Th2 cells upon infection with *Nippostrongylus brasiliensis* and *Leishmania major* (Marsland et al., 2004), we studied the effect of PKC-θ on Th2 responses in toxoplasmosis by IL-4 ELISPOT assay of CD4 T cells. Numbers of *T. gondii*-specific IL-4 producing CD4 T cells were significantly reduced in PKC-θ⁻/⁻ mice at all time points after infection (Fig. 18E). In parallel, the expression of the transcription factor GATA3, which induces Th2 responses, was strongly upregulated in CD4 T cells of WT animals, whereas upregulation of GATA3 expression was lower in CD4 T cells of *T. gondii*-infected PKC-θ⁻/⁻ mice at d 7, 14, and 21 p.i. (Fig. 18F). Thus, *T. gondii*-specific Th2 responses were reduced in the absence of PKC-θ.

The reduced absolute number of CD4 and CD8 T cells as well as parasite-specific CD4 and CD8 T cells may be caused by an increased apoptosis of PKC-θ-deficient T cells. Therefore, we isolated CD4 and CD8 T cells from both strains of mice and analyzed the expression of

active caspase-3. Both WT and PKC- $\theta^{-/-}$ mice expressed equally low levels of activated caspase-3 at d 14 p.i. At all other time points, active caspase-3 was not detectable by WB. However, a further *in vitro* analysis of T cell proliferation and apoptosis was precluded by the extreme low number of parasite-specific CD4 and CD8 T cells in PKC- $\theta^{-/-}$ mice. (Fig. 18G).

4.1.2.5 Reduced cytokine responses in PKC- $\theta^{-/-}$ mice

To study the impact of the reduced number of IFN- γ -producing *T. gondii*-specific T cells on cytokine production, a quantitative RT-PCR analysis was performed at d 21 p.i. IFN- γ mRNA was significantly reduced in spleen and brain of *T. gondii*-infected PKC- $\theta^{-/-}$ mice (Fig. 19A). In addition, mRNA expression of TNF was reduced in PKC- $\theta^{-/-}$ mice (Fig. 19B). Interestingly IL-10 mRNA, which is mainly produced by conventional Foxp3-Th1 cells in toxoplasmosis (Jankovic et al., 2007), was also significantly reduced in spleen and brain of PKC- $\theta^{-/-}$ mice (Fig. 19C). Furthermore, iNOS and IGTP, two important IFN- γ -regulated anti-parasitic effector molecules, were significantly reduced in PKC- $\theta^{-/-}$ mice (Fig. 19C, D). In conclusion, mRNA production of essentially protective cytokines and IFN- γ -regulated anti-parasitic effector molecules were significantly diminished in PKC- $\theta^{-/-}$ mice.

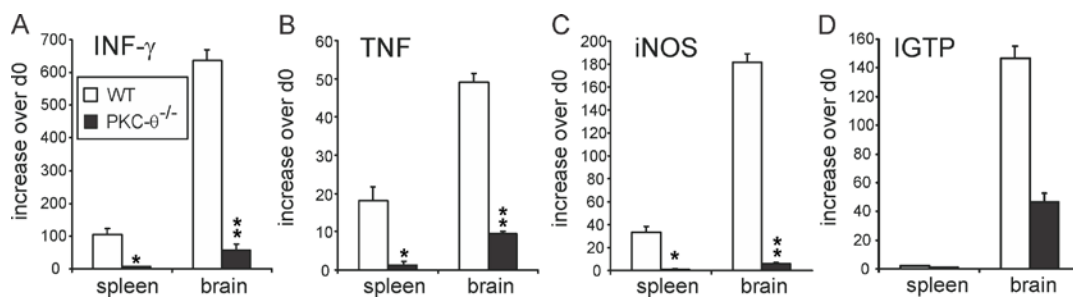


Figure 19. Reduced production of cytokines and anti-parasitic effector molecules in *T. gondii*-infected PKC- $\theta^{-/-}$ mice. A quantitative RT-PCR analysis of IFN- γ (A), TNF (B), iNOS (C) and IGTP (D) mRNA expression was performed in spleen and brain of WT and PKC- $\theta^{-/-}$ mice. Data are expressed as the increase of the respective mRNA from infected (d 21 p.i.) over uninfected mice and were normalized to HPRT expression. Data represent the mean + SD of three to five mice per group and time point (* p < 0.05, ** p < 0.01).

4.1.2.6 Impaired activation of NF- κ B, AP1, and ERK in PKC- $\theta^{-/-}$ mice

The activation and regulation of the transcription factors NF- κ B and AP1 as well as the kinase ERK were studied by WB in T cells of *T. gondii*-infected mice. In these experiments, we

focussed on bulk CD4 and CD8 T cells, since the number of parasite-specific CD4 and CD8 T cells, especially in PKC- $\theta^{-/-}$ mice, was too low to allow a direct *ex vivo* analysis by WB. As shown in Figure 20, CD4 and CD8 T cells of PKC- $\theta^{-/-}$ mice showed an impaired activation of NF- κ B as indicated by a reduced phosphorylation of IKK1/2 and p65.

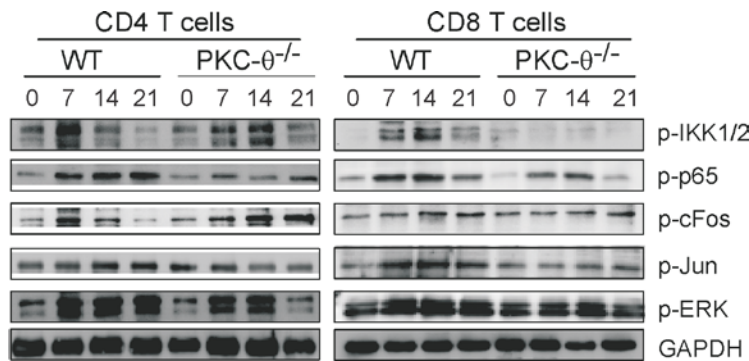


Figure 20. WB analysis of the NF κ B, AP-1, and ERK pathway in CD4 and CD8 T cells. CD4 and CD8 T cells, respectively, were isolated by MACS from spleens of three to five WT and PKC- $\theta^{-/-}$ mice at the indicated time points. After isolation and blotting, proteins were stained for p-IKK1/2, p-p65, p-c-Fos, anti- p-c-Jun, p-ERK, and GAPDH.

In addition, phosphorylation of the AP1 transcription factor c-Jun, but not of c-Fos, was reduced in CD4 and CD8 T cells of PKC- $\theta^{-/-}$ as compared to WT mice. Furthermore, PKC- $\theta^{-/-}$ mice showed a slight reduction of ERK activation both in CD4 and CD8T cells as compared to WT animals. Taken together, these data indicate that in the absence of PKC- θ activation of several important signaling pathways including NF- κ B, AP-1 and ERK was impaired in CD4 and CD8 T cells.

4.1.2.7 Reduced *T. gondii*-specific IgG production in serum and CSF of PKC- $\theta^{-/-}$ mice.

B cells play a protective role in toxoplasmosis and *T. gondii*-specific Ab responses are partially regulated by CD4 T cells (Kang et al., 2000; Lutjen et al., 2006). Therefore, we evaluated *T. gondii*-specific Ab responses in *T. gondii*-infected PKC- $\theta^{-/-}$ and WT mice. At d 21 p.i., equal amounts of *T. gondii*-specific IgM were present in serum and CSF of PKC- $\theta^{-/-}$ and WT mice (Fig. 21A, B). In contrast, *T. gondii*-specific IgG was reduced in serum and CSF of PKC- $\theta^{-/-}$

mice (Fig. 21C, D). These results illustrate that *T. gondii*-specific IgG but not IgM production was partially dependent on PKC-θ.

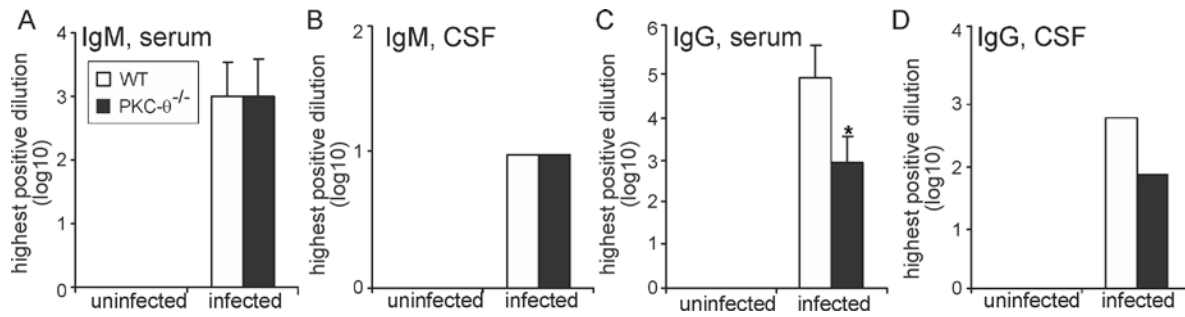


Figure 21. Reduced IgG but normal *T. gondii*-specific IgM production in PKC-θ⁻/⁻ mice. (A-D) *T. gondii*-specific IgM (A, B) and IgG (C, D) Ab were determined in serum (A, C) and CSF (B, D) of WT and PKC-θ⁻/⁻ mice by ELISA at d 21 p.i. The serum and CSF were serially diluted and the highest positive dilution is shown. Serum and CSF were isolated from five to six mice per group and time point. Data show the mean + SD of Ab titers in serum (* p < 0.05). The CSF was pooled from mice of each experimental group to obtain a sufficient amount of CSF and the mean of duplicates is shown.

4.1.2.6 WT T cells compensate for PKC-θ-deficiency in toxoplasmosis

To validate that the lethal course of toxoplasmosis in PKC-θ⁻/⁻ mice was caused by an insufficient T cell response, we adoptively transferred purified polyclonal WT T cells into PKC-θ⁻/⁻ mice before infection with *T. gondii* and monitored survival of these animals. As shown in Fig. 22A, 68% of PKC-θ⁻/⁻ mice reconstituted with WT T cells survived the infection, whereas 100% of both PKC-θ⁻/⁻ mice without T cell transfer or with transfer of PKC-θ⁻/⁻ T cells succumbed to the infection. As shown before, all WT mice (i.e. without T cell transfer) survived the infection. Compared to WT animals, surviving PKC-θ⁻/⁻ mice with adoptive WT T cells transfer harboured equally low numbers of *T. gondii* cysts in their brains at d 60 p.i. (p > 0.05, Fig. 22B). To further analyze whether an adoptive transfer of WT T cells into PKC-θ⁻/⁻ mice improved parasite-specific T cell responses in PKC-θ⁻/⁻ mice, the number of Gra6-HF10-specific CD8 T cells was determined. Both, in spleen (Fig. 22C) and brain (Fig. 22D) the number of Gra6-HF10-specific CD8 T cells was significantly increased in PKC-θ⁻/⁻ mice with WT T cell transfer as compared to PKC-θ⁻/⁻ mice without WT T cell transfer (p < 0.05 for both organs).

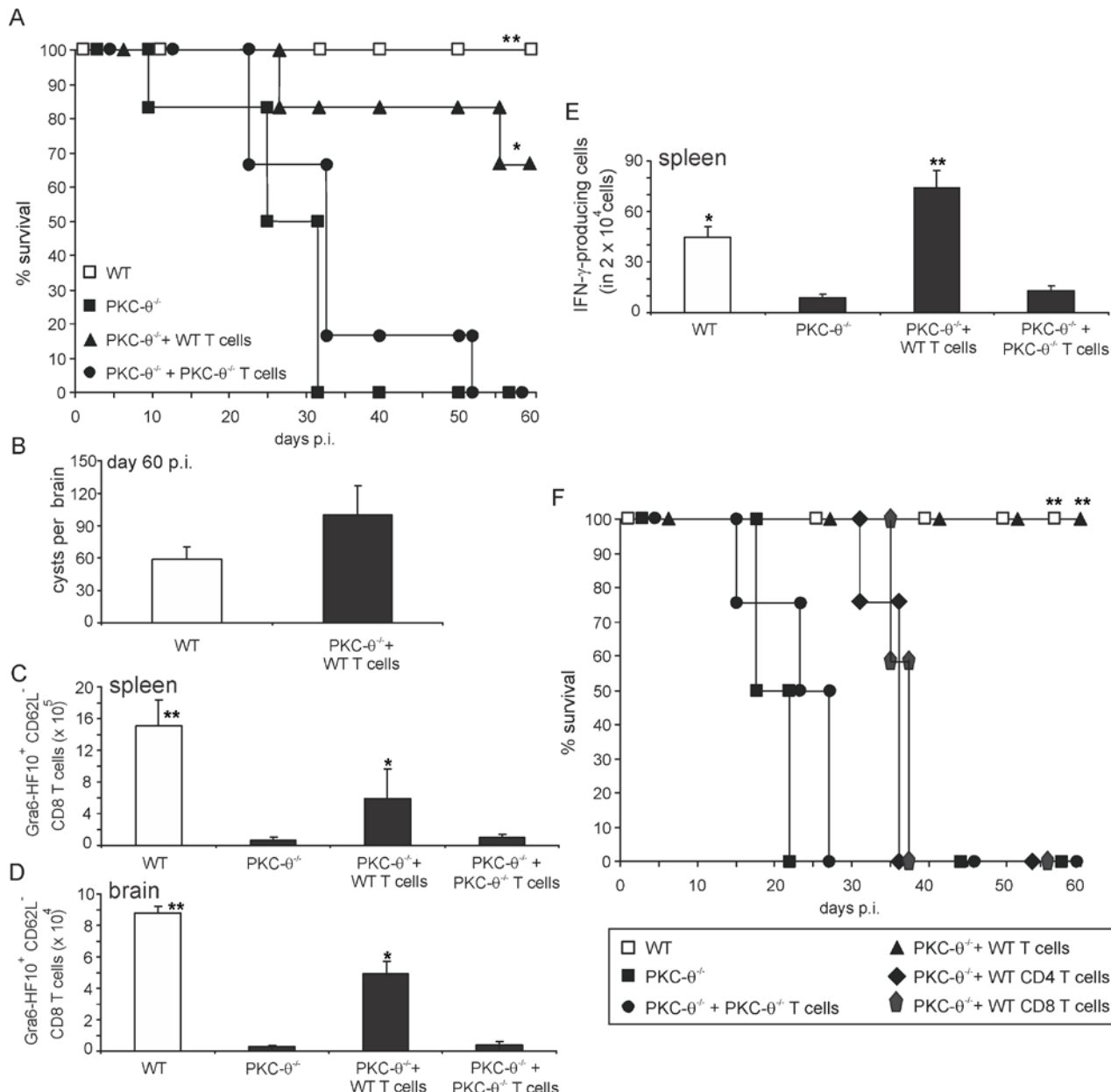


Figure 22. WT T cells compensate for a PKC-θ-deficiency in toxoplasmosis. MACS-purified WT and PKC- $\theta^{-/-}$ T cells were adoptively transferred into PKC- $\theta^{-/-}$ recipients. Recipients as well as control WT and PKC- $\theta^{-/-}$ mice were orally infected with *T. gondii*. (A) The survival of six mice per experimental group was monitored until d 60 p.i. (B) The number of *T. gondii* cysts was determined in WT and PKC- $\theta^{-/-}$ mice with adoptively transferred WT T cells at d 60 p.i. Data represent mean + SD of six surviving WT and four surviving PKC- $\theta^{-/-}$ mice with transfer of WT T cells. (C, D) The number of *T. gondii*-specific Gra6-HF10⁺ and CD62L⁻ CD8 T cells was determined in spleen (C) and brain (D) of the indicated groups of mice by flow cytometry at d 21 p.i. (E) The frequency of IFN- γ ELISPOT assay at d 21 p.i. In C-D data represent the mean + SD of 5 mice per group. (F) MACS-purified WT CD4, WT CD8, and WT CD4 plus CD8 T cells as well as PKC- $\theta^{-/-}$ CD4 and CD8 T cells were adoptively transferred into PKC- $\theta^{-/-}$ recipients. Recipients as well as control WT and PKC- $\theta^{-/-}$ mice were orally infected with *T. gondii*, and the survival of six mice per experimental group was monitored until d 60 p.i. (A-F) * $p < 0.05$, ** $p < 0.01$ for the respective group vs. PKC- $\theta^{-/-}$ mice.

As shown before, numbers of Gra6-HF10-specific CD8 T cells were also significantly increased in spleen and brain of WT mice as compared to PKC- $\theta^{-/-}$ animals. In addition, numbers of *T. gondii*-specific IFN- γ -producing T cells were significantly increased in the spleen of both PKC- $\theta^{-/-}$ with WT T cells transfer and WT mice as compared to PKC- $\theta^{-/-}$ without T cell transfer ($p < 0.01$, Fig. 22E). These, findings demonstrate that WT T cells can significantly protect PKC- $\theta^{-/-}$ mice from lethal toxoplasmosis.

To determine whether adoptively transferred CD4 and/or CD8 WT T cells confer protection against toxoplasmosis in PKC- $\theta^{-/-}$ mice, CD4, CD8, and CD4 plus CD8 T cells, were adaptively transferred to PKC- $\theta^{-/-}$ mice before infection with *T. gondii*. As illustrated in Fig. 22F, only transfer of both T cell populations significantly protected PKC- $\theta^{-/-}$ mice from lethal toxoplasmosis. Although transfer of either CD4 or CD8 WT T cells prolonged the survival time of PKC- $\theta^{-/-}$ mice by a maximum of 10 days, all of these animals succumbed to the infection. Thus, the combined action of both CD4 and CD8 WT T cells was required to compensate efficiently PKC- θ -deficiency in toxoplasmosis of BALB/c mice.

4.2 Regulation of murine listeriosis and toxoplasmosis by CYLD

The PKC-θ experiments demonstrated that this serine/threonine kinase is important to induce an activation of protective T cell response and signaling pathways including NF-κB, NFAT, AP1, and GATA3. To study whether negative regulation of the signaling pathways by deubiquitinating enzymes impact on the course of listeriosis and toxoplasmosis, we studied the impact of CYLD in these diseases.

4.2.1 CYLD does not influence the course of *Toxoplasma* encephalitis

To analyze whether CYLD plays a critical role for survival of toxoplasmosis, C57BL/6 WT and Cyld^{-/-} mice were infected with *T. gondii* cysts. Both C57BL/6 Cyld^{-/-} and WT mice survived the infection up to day 60 p.i. (Fig. 23A). A quantification of intracerebral toxoplasms revealed that the number of parasites did not differ in the brain of C57BL/6 Cyld^{-/-} mice as compared to WT controls at day 60 p.i. (Fig. 23B). These findings demonstrate that CYLD is dispensable during the course of *T. gondii* infection.

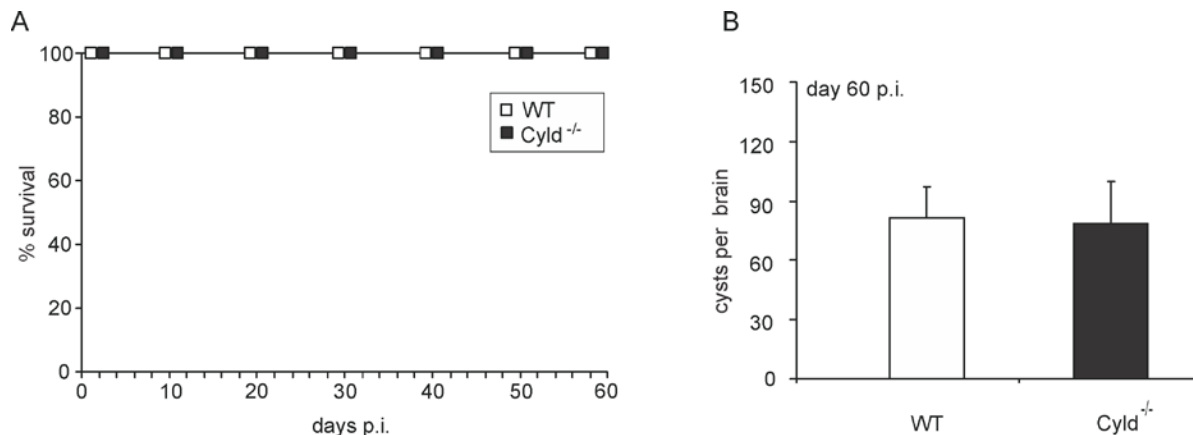


Figure 23. CYLD does not influence the course of murine toxoplasmosis. C57BL/6 WT and Cyld^{-/-} mice were orally infected with *T. gondii*. (A) Survival was analyzed for ten mice per mouse strain. (B) The number of *T. gondii* cysts was determined in WT and Cyld^{-/-} mice at d 60 p.i. Data represent mean + SD of ten WT and Cyld^{-/-} mice.

4.2.2 CYLD does not influence the course of low dose *L. monocytogenes* infection

To investigate the functional role of CYLD in severe listeriosis, WT and *Cyld^{-/-}* mice were i.v. infected with lethal dose of 5×10^4 CFU of *L. monocytogenes*. Whereas all WT mice succumbed up to day 7 post infection (p.i.), 100% of *Cyld^{-/-}* mice survived (Fig. 24A). The bacterial load were similar in liver and spleen of both the mice groups (Fig. 24B, C). These data indicate that CYLD does not influence the course of low dose *L. monocytogenes* infection.

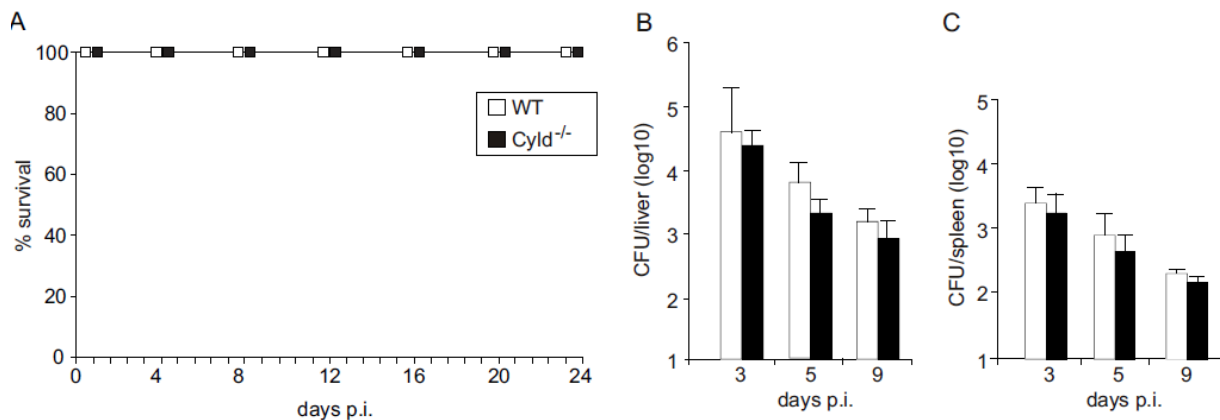


Figure 24. CYLD does not influence the course of low dose *L. monocytogenes* infection . C57BL/6 WT and *Cyld^{-/-}* mice were i.v injected 5×10^4 CFU of *L. monocytogenes* . (A) Survival was analyzed for ten mice per mouse strain. (B) CFUs were determined in 6 mice per experimental group at the indicated time points p.i. Data represent mean + SD of ten WT and *Cyld^{-/-}* mice.

4.2.3 CYLD prevented survival from severe listeriosis and aggravated liver pathology in listeriosis

To investigate whether CYLD plays any role in severe listeriosis, WT and *Cyld^{-/-}* mice were i.v. infected with lethal dose of 5×10^5 CFU of *L. monocytogenes*. Whereas all WT mice succumbed up to day 7 post infection (p.i.), 100% of *Cyld^{-/-}* mice survived (Fig. 25A).

At day 5 p.i., critically ill WT mice showed macroscopically severe liver haemorrhage, which was absent in *Cyld^{-/-}* mice (Fig. 25B). In WT mice, hepatic inflammation was widespread with ill-defined borders of the inflammatory infiltrates and large areas of necrosis were present (Fig. 25C). In addition, numerous *L. monocytogenes* in huge, partially confluent inflammatory infiltrates were scattered throughout the liver of WT mice, being particularly prominent at the border of necroses (Fig. 25C).

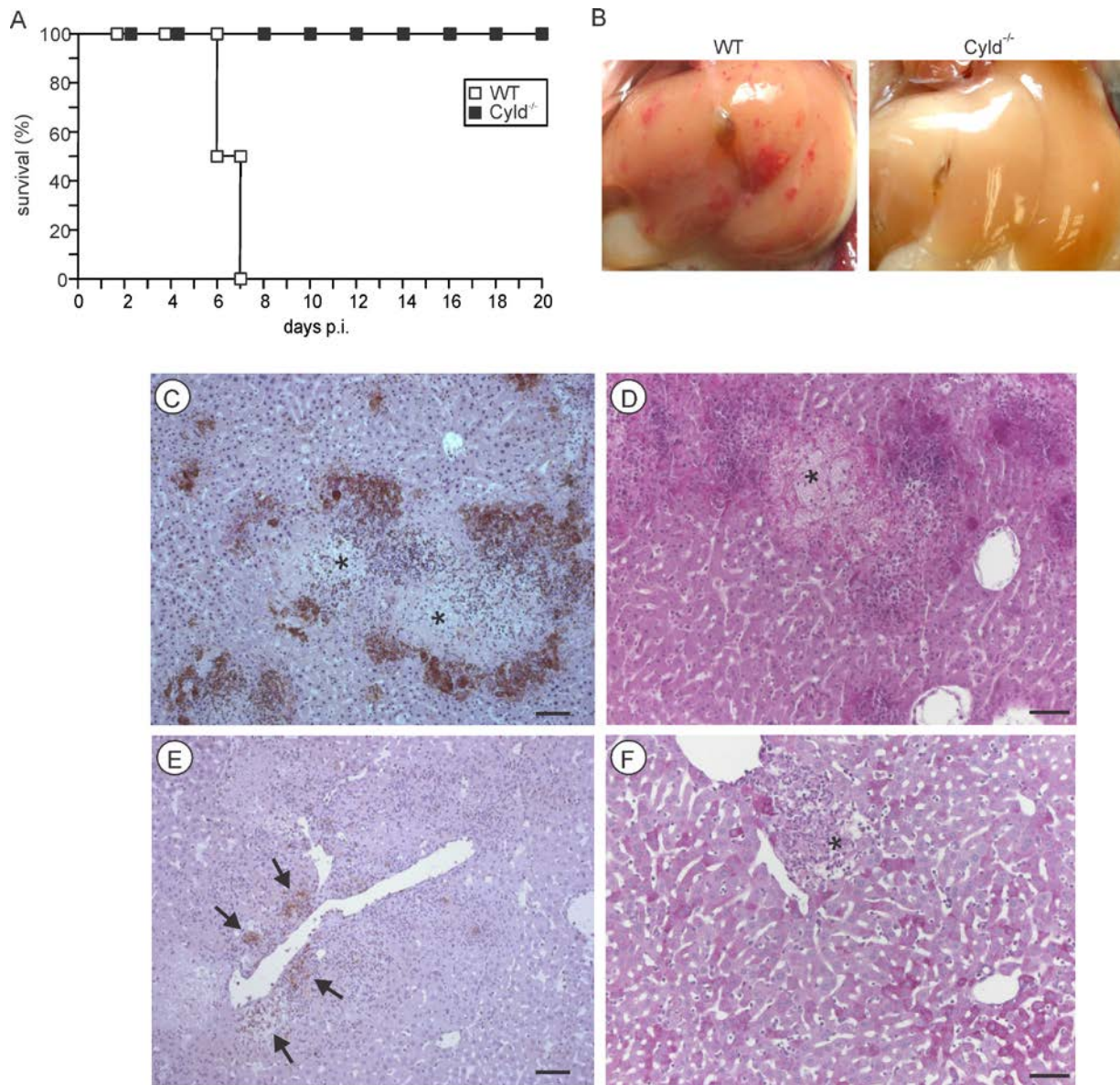


Figure 25. *Cyld*^{-/-} mice are protected from lethal listeriosis and severe liver pathology. (A) C57BL/6 *Cyld*^{-/-} ($n=10$) and WT ($n=10$) mice were infected i.v. with 5×10^5 *L. monocytogenes* and survival rates were monitored until day 20 p.i. ($p < 0.005$ for WT vs. *CYLD*^{-/-} mice). One of two representative experiments is shown. (B) A macroscopic examination of livers from WT and *Cyld*^{-/-} mice showed severe haemorrhage in WT but not in *Cyld*^{-/-} mice at day 5 p.i. (C-F) Histopathology of WT (C, D) and *Cyld*^{-/-} mice (E, F) at day 5 p.i. (C, E) Immunohistochemistry with α -*L. monocytogenes* antiserum in a WT (C) and *Cyld*^{-/-} mouse (E) (slight counterstaining with hemalum, bar 5 μ m). In (C), * marks necrosis surrounded by clusters of *L. monocytogenes*. (D, F) PAS staining of a WT (D) and *Cyld*^{-/-} (F) mouse (bar 10 μ m). In (D), * indicates a large area of necrosis. In (F), * indicates a well-defined inflammatory focus. In (B-F), three mice per group were analyzed and representative data are shown. The experiment was performed twice.

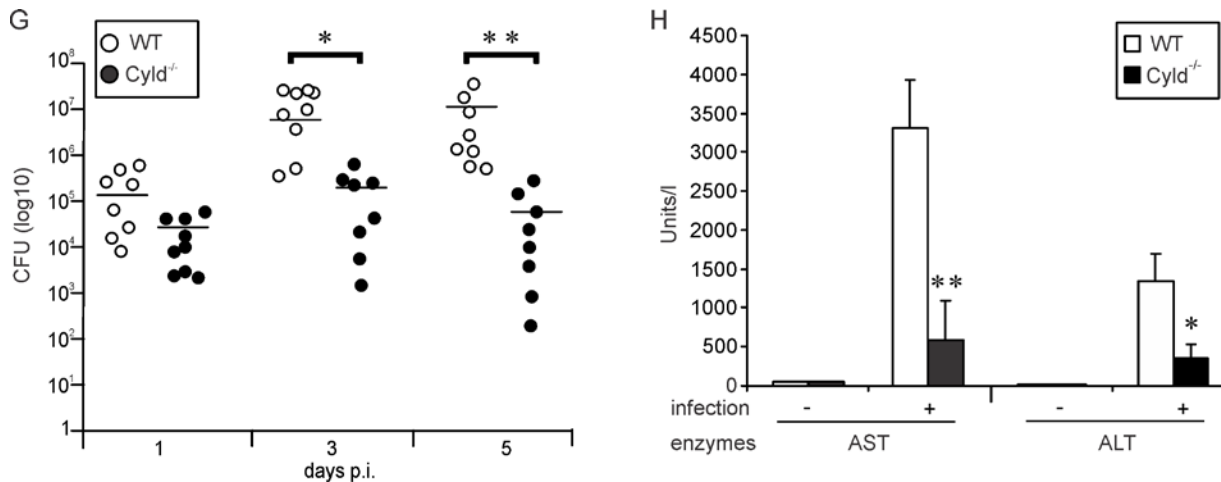


Figure 25. (G) CFUs were determined in the liver of *L. monocytogenes*-infected WT and Cyld^{-/-} mice at the indicated time points p.i. (* p < 0.05, ** p < 0.01). Data show the combined results of two independent experiments with a total of 8-9 mice per experimental group and time point. The mean of each experimental group is shown by a bar and each symbol represents one mouse. (H) The liver enzymes aspartate transaminase (AST) and alanine transaminase (ALT) were determined in serum at day 5 p.i. (* p < 0.05 and ** p < 0.01 for WT vs. Cyld^{-/-} mice). Data show the mean + SD of 5 mice per experimental group from one of two representative experiments.

L. monocytogenes and inflammatory infiltrates contributed to widespread necroses and total loss of glycogen from hepatocytes (Fig. 25D). In contrast to WT mice, necrosis was consistently absent from the liver of Cyld^{-/-} mice (Fig. 25E, F). In addition, Cyld^{-/-} mice harboured remarkably lower numbers of bacteria confined to well delineated granulomas of moderate size (Fig. 25E), which were associated with a focal loss of glycogen confined to the inflammatory lesions (Fig. 25F).

The improved pathogen control of Cyld^{-/-} mice was confirmed by determination of CFU, which revealed significantly lower numbers of *L. monocytogenes* in the liver of Cyld^{-/-} mice at days 3 and 5 p.i. (Fig. 25G). In addition, the more severe liver pathology of WT mice also resulted in disturbance of liver function as revealed by increased serum alanine transaminase (ALT) and aspartate transaminase (AST) levels in *L. monocytogenes*-infected WT mice (Fig. 25H).

4.2.3.1 CYLD impaired IL-6, IFN-γ and NOX2 mRNA production and recruitment of myeloid cells to the liver

To explore the influence of CYLD on cytokine production in listeriosis, serum cytokine levels were determined at day 5 p.i. Levels of IL-6 and IFN-γ were significantly increased in Cyld^{-/-} mice, whereas serum levels of IL-2, IL-4, IL-10, IL-17, and TNF did not differ between the two

mouse strains (Fig. 26A). To further analyze differences in IL-6 and IFN- γ , mRNA expression of these cytokines was analyzed by quantitative RT-PCR in the liver and spleen. Both IL-6 and IFN- γ mRNA were up-regulated in livers (Fig. 26B, C) and spleens (Fig. 26E, F) of infected WT and Cyld^{-/-} mice but only IL-6 mRNA was significantly higher in Cyld^{-/-} as compared to WT mice. In addition, NOX2 mRNA was significantly higher expressed in liver and spleen of *L. monocytogenes*-infected Cyld^{-/-} mice (Fig. 26D, G).

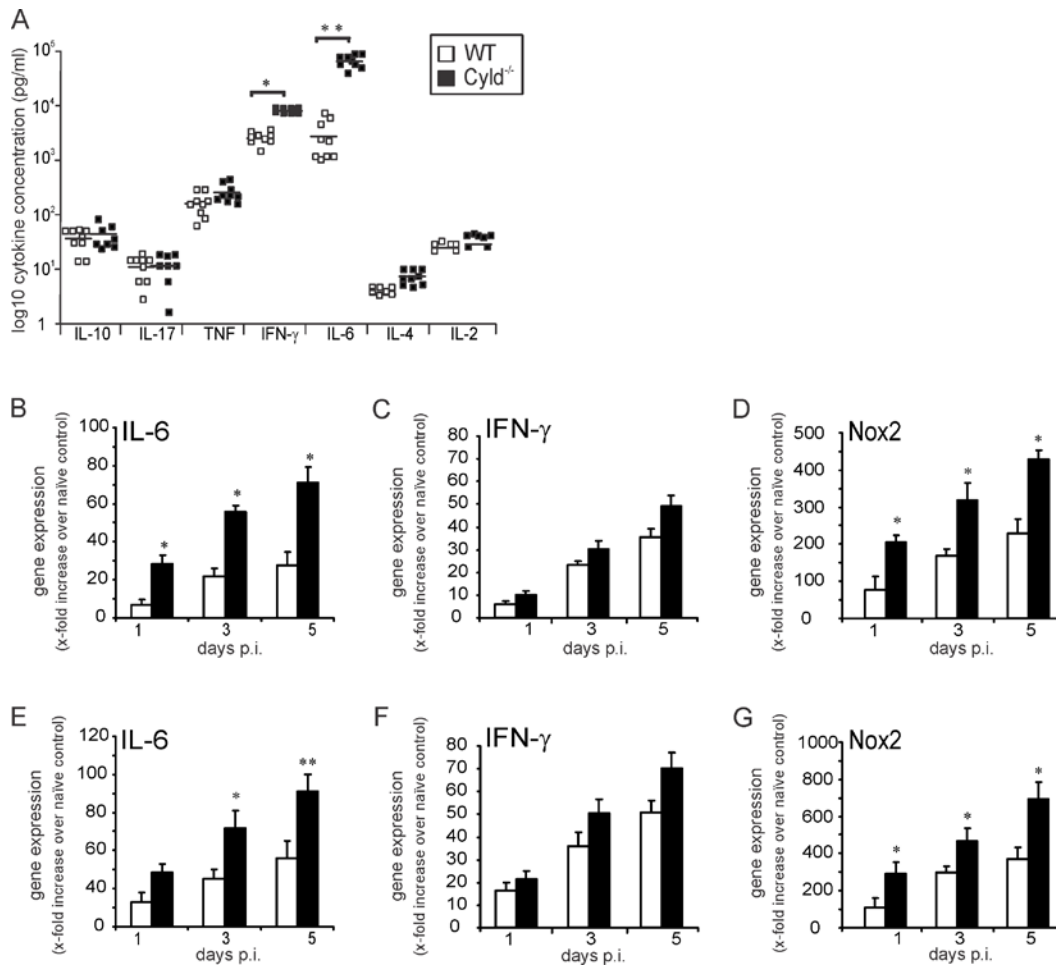


Figure 26. CYLD impairs IL-6 and IFN- γ production and leukocyte recruitment in listeriosis. (A) The serum concentrations of IL-10, IL-17, TNF, IFN- γ , IL-6, IL-4, and IL-2 were determined in *L. monocytogenes*-infected WT and Cyld^{-/-} mice by a cytometric bead assay at day 5 p.i. (* p < 0.05, ** p < 0.01). Symbols represent individual mice from two representative experiments. (B-G) Quantitative RT-PCR analysis of hepatic (B-D) and splenic (E-G) IL-6, IFN- γ , and NOX2 mRNA expression. Data show the increase of the respective mRNA expression of *L. monocytogenes*-infected over uninfected mice of the same mouse strain. Data represent the mean + SD of 5 mice. Data from two representative experiments are shown.

Since the protective action of IL-6 in listeriosis includes the recruitment of myeloid cells, the cellular composition of hepatic inflammatory infiltrates was determined in *Cyld^{-/-}* and WT mice at day 5 p.i. Flow cytometry revealed a significant increase of Ly6G^{high} CD11b^{high} granulocytes, F4/80⁺ CD11b⁺ macrophages and CD8⁺ CD3⁺ T cells in livers of *L. monocytogenes*-infected *Cyld^{-/-}* mice (Fig. 2H).

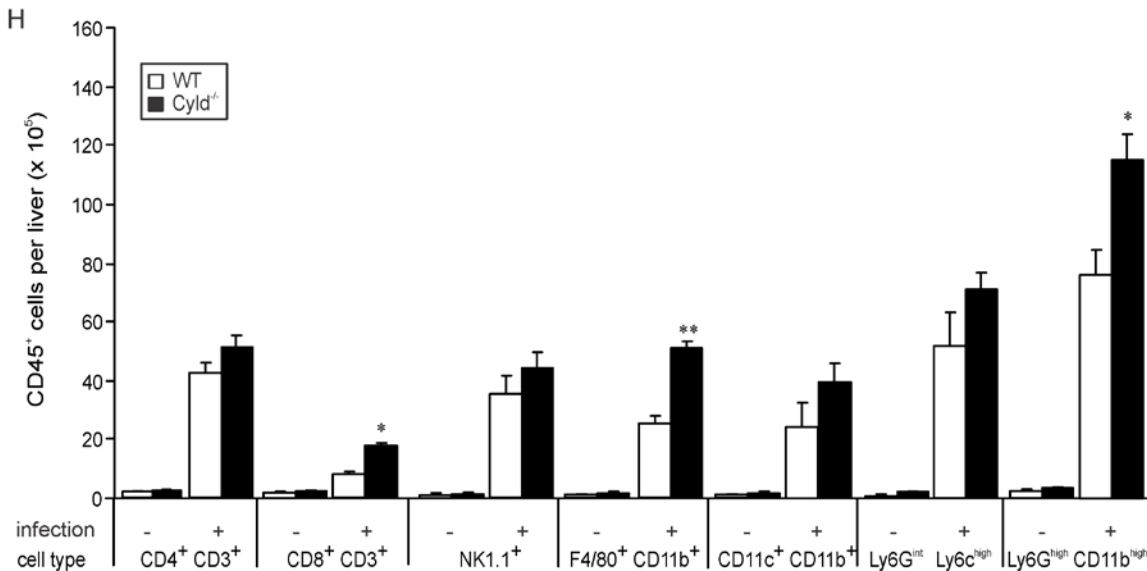


Figure 26. (H) The number of different leukocyte populations was determined in cells isolated from livers of uninfected and *L. monocytogenes* -infected WT and *Cyld^{-/-}* mice. Data show the mean + SD of CD45⁺ cell populations from 5 mice per experimental group. Data from one of two representative experiments are shown (* p < 0.05 and ** p < 0.001 for WT vs. *Cyld^{-/-}* mice).

4.2.3.2 CYLD reduced IL-6, ROS production and killing of *L. monocytogenes* in macrophages by impairing NF-κB activation

To further study the impact of CYLD on IL-6 production and anti-bacterial activity, IFN-γ-stimulated bone marrow-derived macrophages (BMDMs) were infected with *L. monocytogenes*. After 24 h of infection, CFUs were significantly reduced in *Cyld^{-/-}* macrophages (Fig. 27A), which correlated with a significantly increased production of ROS (Fig. 27B). In addition, IL-6 production was significantly increased in *Cyld^{-/-}* macrophages (Fig. 27C). *L. monocytogenes* -infected IFN-γ-stimulated *Cyld^{-/-}* macrophages showed an enhanced activation of NF-κB mediated by an increased phosphorylation of p65 (Fig. 27D, E), which persisted until 24 h p.i. (Fig. 27D, E). Importantly, the improved pathogen control as well as production of ROS and IL-6 of *Cyld^{-/-}* macrophages was dependent on NF-κB, since inhibition of NF-κB activity by an IKK inhibitor abolished these protective macrophage responses (Fig. 27A-C).

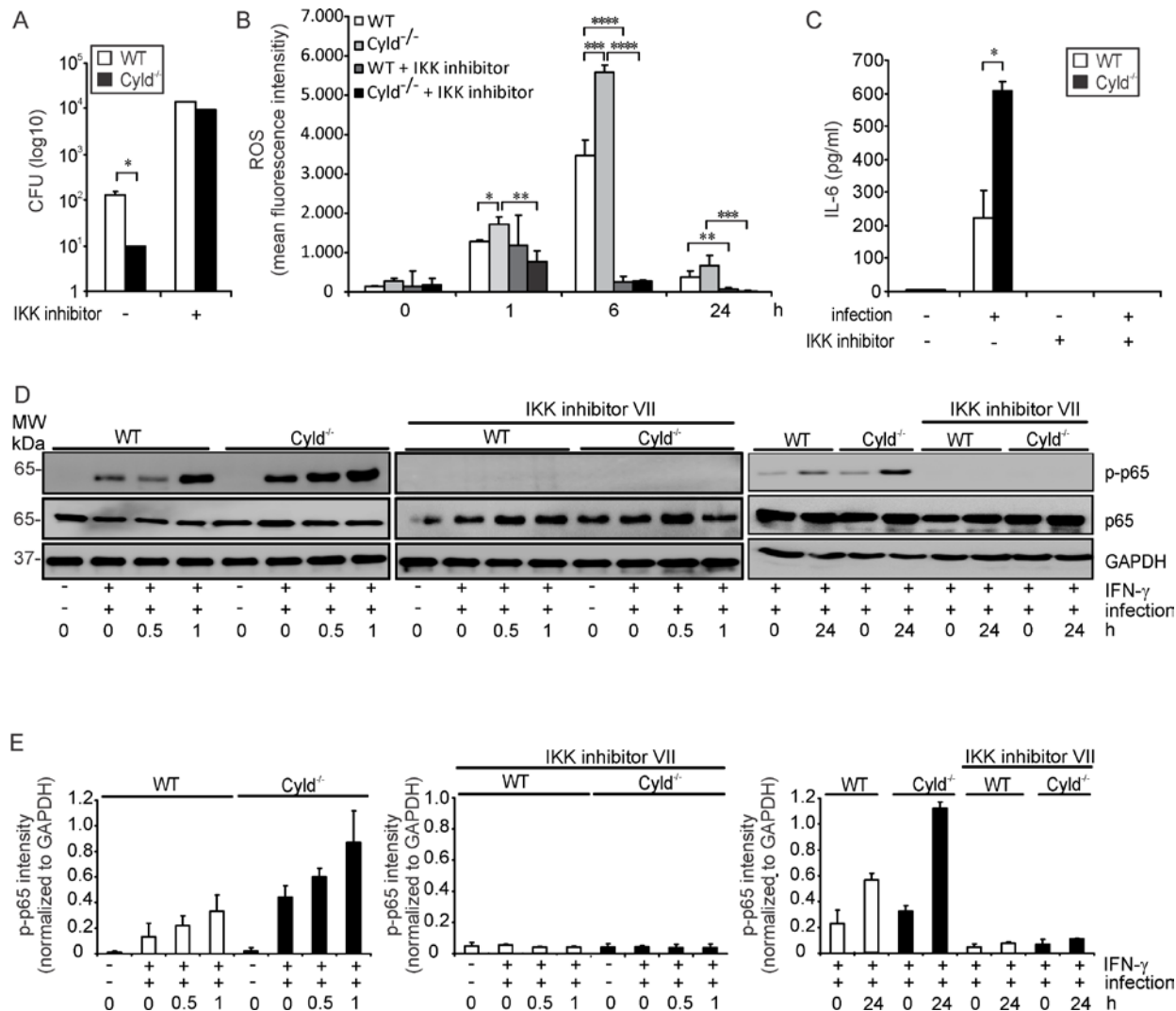


Figure 27. CYLD diminishes NF-κB-dependent IL-6 production, ROS production and pathogen control of *L. monocytogenes*-infected macrophages. (A-C) BMDM were isolated from WT and Cyld^{-/-} mice and stimulated with IFN-γ (100 U/ml). Indicated groups were infected with *L. monocytogenes* (MOI of 5:1) and treated with IKK inhibitor (10 μM for 4 h followed by 1 μM for 20 h), respectively. (A) After 24 h, the amount of intracellular *L. monocytogenes* was determined in 1×10⁶ BMDM. (B) ROS production was analyzed by flow cytometry in *L. monocytogenes*-infected macrophages 24 h after infection. (C) The supernatant was harvested from uninfected and infected macrophages after 24 h and analyzed for IL-6 by CBA. In (A-C), data show the mean + SD of triplicate wells; * p < 0.05, ** p < 0.01, *** p < 0.005, **** p < 0.0001. (D) Proteins were isolated from uninfected and *L. monocytogenes*-infected BMDM at the indicated time points. Cells were stimulated with IFN-γ and IKK inhibitor VII as indicated. WBs were incubated with α-p-p65, α-p65, and α-GAPDH as loading control. Representative WBs from a total of three independent experiments are shown. (E) Quantification of p-p65 intensity (+ SD) was performed from WB data of uninfected and *L. monocytogenes*-infected BMDM, which were stimulated as described in (D). The results present pooled data from 3 independent experiments.

4.2.3.3 CYLD impaired IL-6-mediated STAT3 activation and fibrin production in hepatocytes by deubiquitination of cytoplasmic STAT3

Since *L. monocytogenes*-infected WT mice suffered from haemorrhage, we studied the impact of CYLD on IL-6-induced STAT3 activation and fibrin production in hepatocytes. IL-6 treatment resulted in an increase of CYLD protein in the cytoplasm of WT mice (Fig. 28A). Further, stimulation of WT and *Cyld*^{-/-} hepatocytes with IL-6 resulted in phosphorylation of cytoplasmic STAT3 (Fig. 28A). Within 60 min after stimulation, pSTAT3 declined in the cytosol of *Cyld*^{-/-} but not in WT hepatocytes (Fig. 28A). At 120 min, pSTAT3 was undetectable in the cytoplasm of *Cyld*^{-/-} hepatocytes, whereas it was still present in the cytoplasm of WT hepatocytes (Fig. 28A). In addition, IL-6-stimulation induced translocation of pSTAT3 to the nucleus of hepatocytes from both mouse strains. However, nuclear pSTAT3 amounts were much higher in *Cyld*^{-/-} as compared to WT hepatocytes 60 and 120 min after stimulation (Fig. 28A). In contrast to pSTAT3, non-phosphorylated STAT3 was found constitutively in the cytoplasm and nucleus of WT and *Cyld*^{-/-} hepatocytes (Fig. 28A), which is in accordance with the observation that importin- α 3 constitutively shuttles non-phosphorylated STAT3 between cytoplasm and nucleus (Liu et al., 2005).

To study whether CYLD may regulate nuclear accumulation of pSTAT3 by deubiquitination of STAT3, we immunoprecipitated STAT3 from WT and *Cyld*^{-/-} hepatocytes. Western blot (WB) analysis of immunoprecipitates detected STAT3 in WT and *Cyld*^{-/-} hepatocytes, whereas CYLD was only detectable in WT hepatocytes (Fig. 28B). IL-6 stimulation induced a strong increase of K63-ubiquitination in *Cyld*^{-/-} hepatocytes but only a slight increase in IL-6-stimulated WT hepatocytes. Importantly, the amount of K63-ubiquitinated proteins was strongly augmented in immunoprecipitates of IL-6-stimulated *Cyld*^{-/-} hepatocytes as compared to WT hepatocytes suggesting that CYLD reduced K63-ubiquitination of STAT3 (Fig. 28B). In immunoprecipitates of nuclear STAT3, CYLD was undetectable further indicating that CYLD interacted with STAT3 in the cytosol (Fig. 28B).

Transfection of *Cyld*^{-/-} hepatocytes with MYC-DDK STAT3, HA-WT CYLD (CYLD WT), and catalytically inactive CYLD (CYLD C/S) followed by immunoprecipitation of STAT3 further showed that WT CYLD reduced K63-ubiquitination of STAT3 (Fig. 28C, total lysates). Catalytically inactive CYLD still interacted with STAT3 but failed to reduce K63-ubiquitination of STAT3 (Fig. 28C, D).

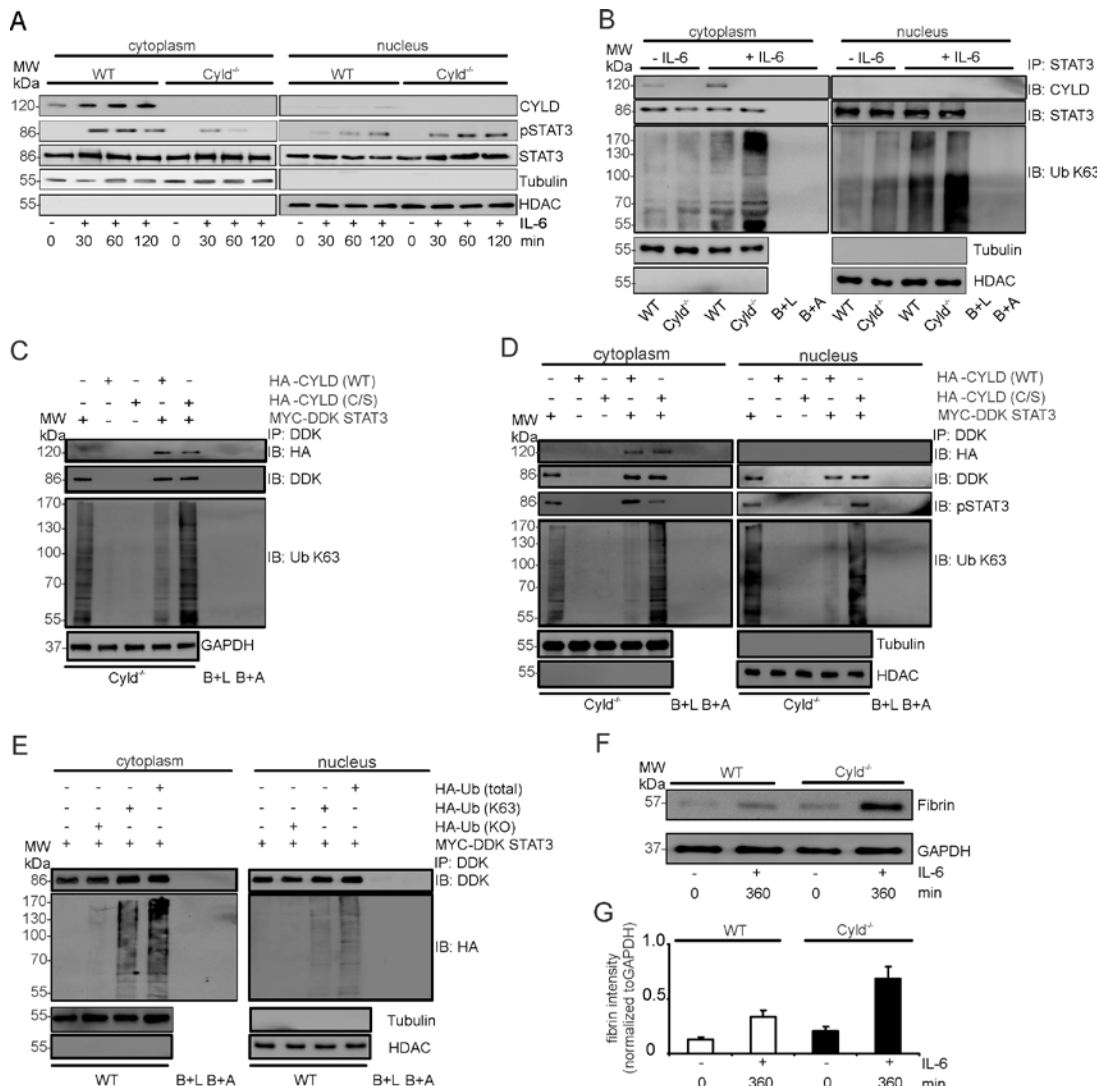


Figure 28. CYLD binds to STAT3 and inhibits nuclear accumulation of activated STAT3 and fibrin production in hepatocytes. (A) Proteins were isolated from the cytoplasm and nucleus, respectively, of WT and Cyl^d^{-/-} hepatocytes. WB were stained with α-tubulin and α-HDAC as marker proteins for the cytoplasm and nucleus, respectively. (B) Cytoplasmic and nuclear protein lysates of unstimulated and IL-6-stimulated (200 ng/ml) WT and Cyl^d^{-/-} hepatocytes were immunoprecipitated with STAT3. Immunoprecipitates were stained for CYLD, STAT3, and K63-linked ubiquitin. The purity and amount of cytoplasmic and nuclear proteins was controlled by staining lysates for tubulin and HDAC, respectively, before immunoprecipitation. Beads plus lysate without antibody before immunoprecipitation (B+L) and beads plus STAT3 antibody without lysates (B+A) were used as controls. (C, D) Cyl^d^{-/-} hepatocytes were transfected with MYC-DDK STAT3, HA-CYLD (WT), mutant HA-CYLD (C/S) lacking catalytic activity as indicated. After IL-6 stimulation (1 h), total (C), cytoplasmic (D) and nuclear (D) lysates were immunoprecipitated with α-DDK. Immunoprecipitates were stained for the indicated proteins. (E) WT hepatocytes were transfected with MYC-DDK STAT3, ubiquitin with all lysine residues (HA-Ub total), ubiquitin with K63 only (HA-Ub K63), and ubiquitin with no lysine residues (HA-Ub KO) as indicated. After IL-6 stimulation (1 h), cytoplasmic and nuclear proteins were isolated and immunoprecipitated with α-DDK. Immunoprecipitates were stained for the indicated proteins. (F) WB analysis of fibrin production in unstimulated (0 min) and IL-6 stimulated (360 min) cultivated WT and Cyl^d^{-/-} hepatocytes. (G) Quantification of fibrin (+ SD) was performed from WB data of unstimulated and IL-6-stimulated WT and Cyl^d^{-/-}, respectively, hepatocytes. Representative results from one of three experiments are shown.

STAT3 and CYLD interacted in the cytoplasm but not in the nucleus of IL-6-stimulated hepatocytes (Fig. 28D). The amount of nuclear pSTAT3 was strongly increased in hepatocytes transfected with catalytically inactive CYLD (Fig. 28D). Further analysis of the interaction between ubiquitin and STAT3 showed that ubiquitin with only K63 (HA Ub (K63)) bound efficiently to STAT3 in IL-6-stimulated WT hepatocytes, whereas ubiquitin with no lysine residues (HA-Ub (KO)) failed to interact with STAT3 (Fig. 28E).

Since IL-6 induces STAT3-dependent fibrin synthesis by hepatocytes (Zhang et al., 1995), we studied the CYLD-dependent regulation of IL-6-induced fibrin production in cultivated WT and *Cyld*^{-/-} hepatocytes. Interestingly, IL-6-induced fibrin synthesis was strongly enhanced in *Cyld*^{-/-} as compared to WT hepatocytes (Fig. 28F, G). Thus, IL-6 induced up-regulation of CYLD expression and promoted deubiquitination of K63-ubiquitinated STAT3, which limited the amount of nuclear pSTAT3, thereby, reducing fibrin production.

4.2.3.3 CYLD reduced activation of p65, JAK2, STAT3, and p38 MAPK as well as fibrin production in livers of *L. monocytogenes*-infected WT mice

In listeriosis, IL-6 production and STAT3 activation are initiated within the 5 h p.i. (Gregory et al., 1998). Therefore, we studied the impact of CYLD on STAT3 K63-ubiquitination in livers of *L. monocytogenes*-infected mice 6 h p.i. (Fig. 29A). Infection with *L. monocytogenes* increased K63-ubiquitination of STAT3, which was augmented in *Cyld*^{-/-} as compared to WT mice. Thus, CYLD regulated STAT3 ubiquitination also *in vivo*. In good agreement with an inhibitory role of CYLD on NF-κB activity in macrophages (Fig. 27D) and on STAT3 activation in hepatocytes (Fig. 28A, D), increased hepatic CYLD production of *L. monocytogenes*-infected WT mice correlated with a reduced and delayed phosphorylation of p65, JAK2 and STAT3 as compared to *Cyld*^{-/-} mice (Fig. 29B). In addition, phosphorylation of p38 MAPK was reduced in livers of WT mice. Expression of PAI-1, which is induced by MAP kinases, was only slightly reduced in WT mice. Importantly, fibrin deposition was increased in *Cyld*^{-/-} as compared to WT mice at day 3 and 5 p.i. (Fig. 29C, D).

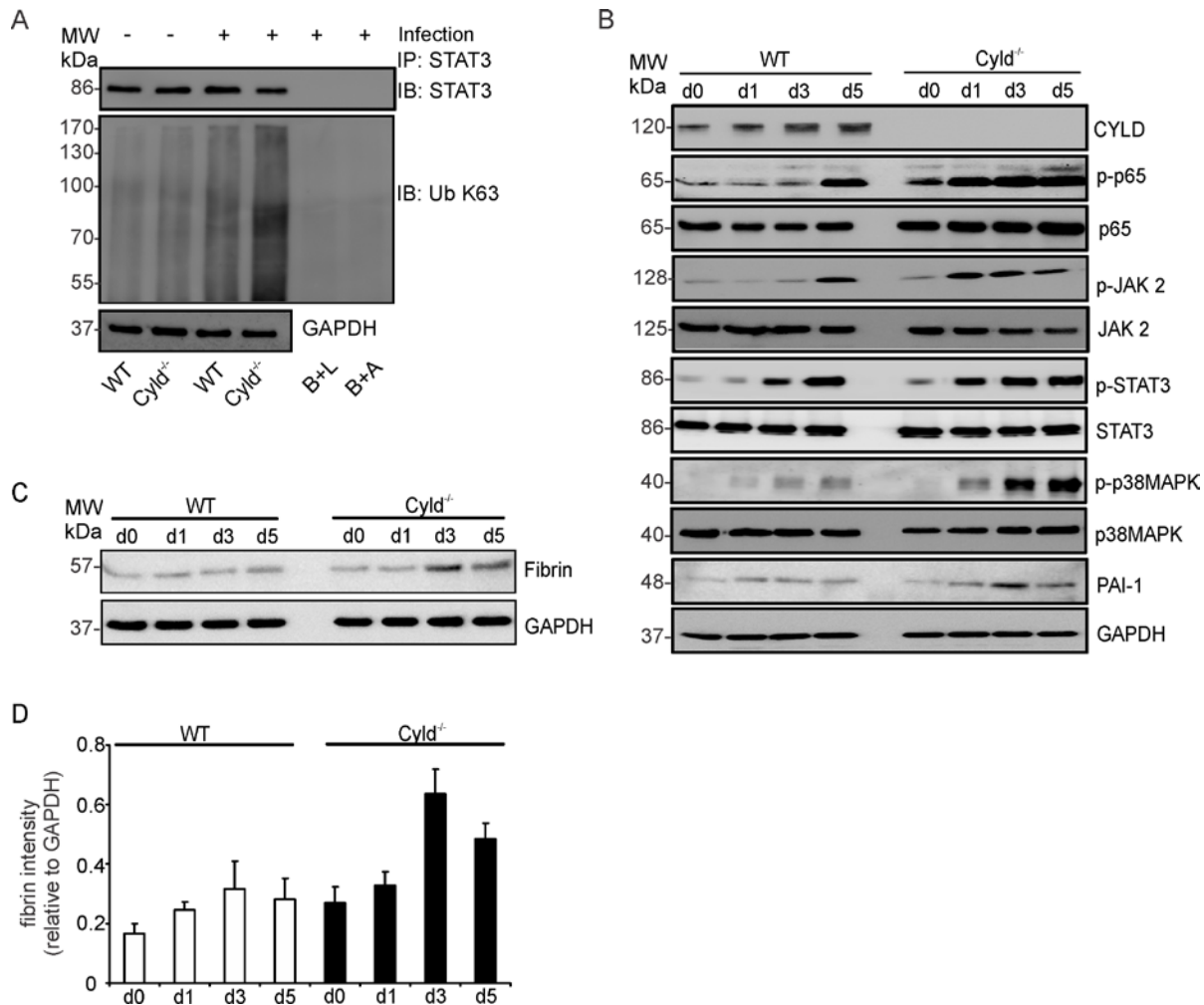


Figure 29. Reduced activation of p65, JAK2, STAT3, p38 MAPK and fibrin production in livers of *Listeria*-infected WT mice. (A) Proteins were isolated from livers of uninfected (d0) and *L. monocytogenes* -infected WT and Cyld^{-/-} mice (6 h p.i.). Protein lysates were immunoprecipitated with STAT3 and WB was performed for STAT3 and K63-linked ubiquitin. (B, C) Proteins were isolated from livers of uninfected (d0) and *L. monocytogenes*-infected WT and Cyld^{-/-} mice at days 1, 3, and 5 p.i. WB were incubated with α -CLYD, α -p-p65, α -p65, α -pSTAT3, α -STAT3, α -p-p38MAPK, α -p38MAPK, and α -PAI-1 (B) and fibrin (C). GAPDH was used as loading control. Three to four mice were analyzed per group and representative data from one of two independent experiments are shown. (D) Quantification of fibrin (+ SD) was performed from WB data of uninfected and *L. monocytogenes*-infected WT and Cyld^{-/-}, respectively. The results present 3 mice per group and time point.

4.2.3.4 The protection of *Cyld*^{-/-} mice against lethal listeriosis is dependent on IL-6, STAT3 and fibrin

To study whether the IL-6 induced STAT3 activation protected *Cyld*^{-/-} mice from lethal listeriosis by increased fibrin production, *in vivo* IL-6, STAT3 and fibrin neutralization experiments were performed. Neutralization of endogenous IL-6 by i.p. administration of the monoclonal MP5-20F3 antibody 1 h before i.v. *L. monocytogenes* infection completely abolished the protective effect of *Cyld*-deficiency and all α-IL-6-treated *Cyld*^{-/-} mice succumbed up to day 5 p.i. (Fig. 30A).

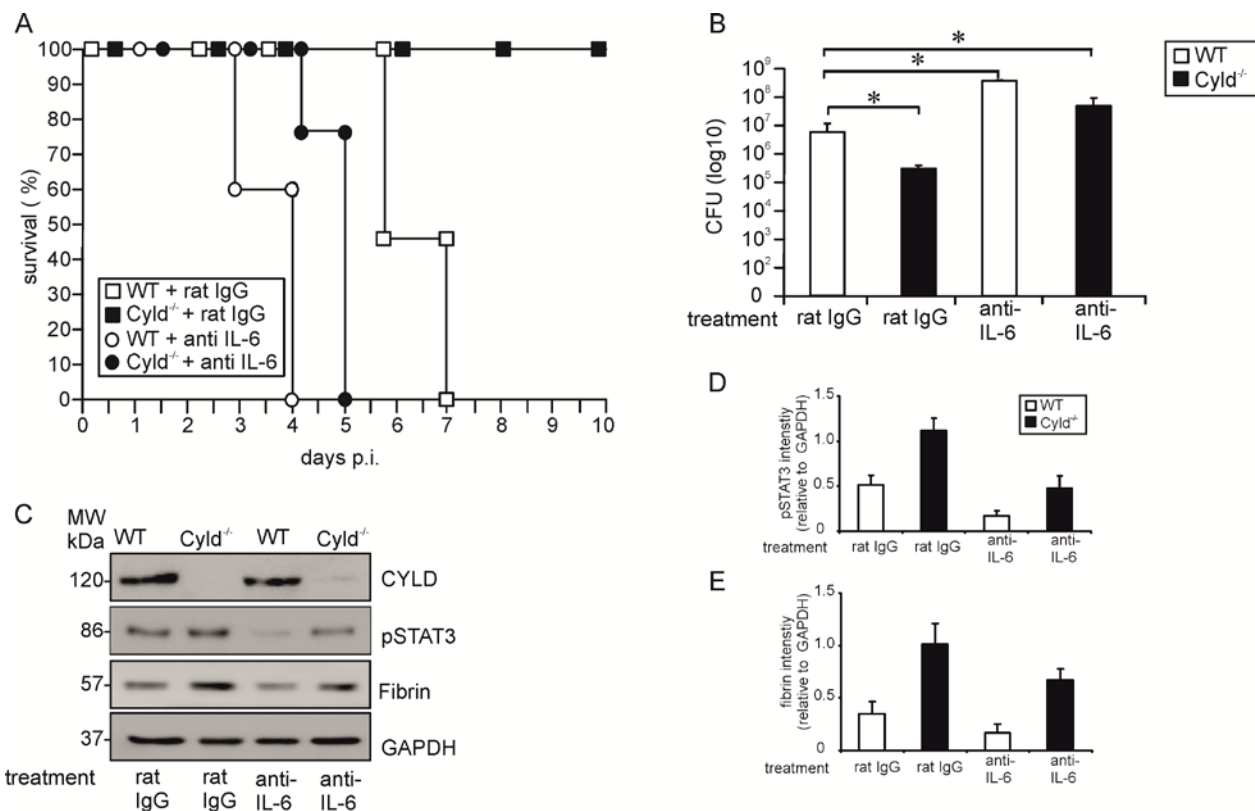


Figure 30. IL-6 neutralization abolishes increased STAT3 activation, fibrin production, survival and pathogen control in *L. monocytogenes*-infected *Cyld*^{-/-} mice. (A) The survival rates of rat IgG and α-IL-6-treated *L. monocytogenes*-infected WT and *Cyld*^{-/-} mice (n=7 per experimental group) are shown. The survival rate of IgG-treated *Cyld*^{-/-} mice ($p < 0.05$) but not of the other groups was significantly increased as compared to rat IgG-treated WT mice. (B) CFUs were determined in the liver of *L. monocytogenes*-infected rat IgG and IL-6-treated WT and *Cyld*^{-/-} mice at day 5 p.i. (n=5 per experimental group; * $p < 0.05$). Data show the mean + SD from one of two representative experiments. (C) Proteins were isolated from livers of infected rat IgG and IL-6-treated WT and *Cyld*^{-/-} mice (n=3 per experimental group) at day 5 p.i. WB analysis for CYLD, pSTAT3, fibrin and GAPDH was performed and representative data are shown. (D, E). Quantification of hepatic pSTAT3 (D) and fibrin (E) (+ SD)

In addition, 100% of α -IL-6- and rat IgG-treated WT mice, respectively, succumbed, whereas all control antibody-treated $Cyld^{-/-}$ mice survived (Fig. 30A). The improved pathogen control of $Cyld^{-/-}$ mice was abolished by IL-6 neutralization and α -IL-6-treated $Cyld^{-/-}$ mice had even significantly higher CFUs than rat IgG-treated WT mice at day 3 p.i. (Fig. 30B). Furthermore in $Cyld^{-/-}$ mice, IL-6 neutralization resulted in reduction of hepatic pSTAT3 (Fig. 30C, D) and fibrin (Fig. 30E) as compared to rat IgG-treated $Cyld^{-/-}$ mice. In WT mice, IL-6 neutralization only slightly reduced pSTAT3 without affecting fibrin (Fig. 30C, E) indicating that IL-6 induced pSTAT3 is strongly regulated by CYLD, which limits STAT3 activity and STAT3-dependent fibrin production.

4.2.3.5 Inhibition of STAT3 reduces fibrin production, survival and pathogen control in *L. monocytogenes*-infected $Cyld^{-/-}$ mice.

To further study the impact of CYLD on IL-6-induced, STAT3-dependent fibrin production, STAT3 small interfering (si) RNA experiments were performed. I.v. treatment of $Cyld^{-/-}$ mice with STAT3 siRNA 24 h before infection resulted in 80% reduction of total STAT3 in the liver (Fig. 31A, B), which caused reduced fibrin deposition in $Cyld^{-/-}$ mice (Fig. 31A, C). In contrast, fibrin deposition was not reduced in control siRNA-treated and untreated infected $Cyld^{-/-}$ mice (Fig. 31A, C). Importantly, STAT3 siRNA treatment induced 100% mortality of *L. monocytogenes*-infected $Cyld^{-/-}$ mice, thus, resembling WT mice (Fig. 31D). In contrast, control siRNA and untreated $Cyld^{-/-}$ mice, respectively, survived the infection (Fig. 31D). Knockdown of STAT3 in $Cyld^{-/-}$ mice also abolished the improved pathogen control of $Cyld^{-/-}$ in comparison to WT mice (Fig. 31E). In contrast, control siRNA-treated and untreated $Cyld^{-/-}$ mice had significantly lower CFUs as compared to WT mice (Fig. 31E) illustrating that siRNA-treatment did not unspecifically effect pathogen control. It has been reported that STAT3, in addition to NF- κ B, contributes to IL-6 production (Samavati et al., 2009). Accordingly, knockdown of STAT3 significantly reduced serum IL-6 levels in *L. monocytogenes*-infected $Cyld^{-/-}$ mice as compared to mock-treated infected $Cyld^{-/-}$ mice as well as untreated infected $Cyld^{-/-}$ mice (Fig. 31F). In STAT3 siRNA-treated $Cyld^{-/-}$ mice IL-6 levels were still increased as compared to untreated WT mice (Fig. 31F).

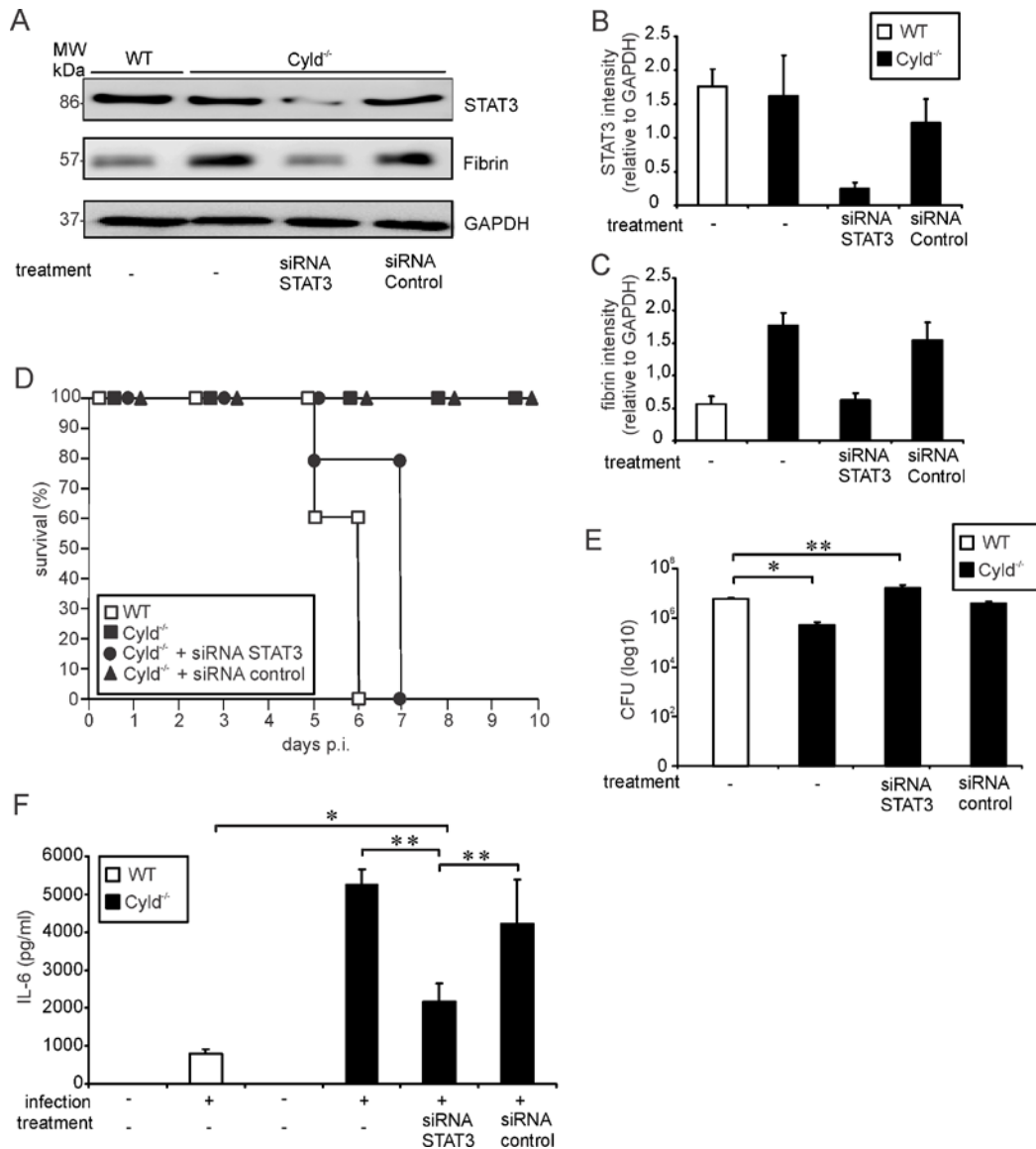


Figure 31. Inhibition of STAT3 reduces fibrin production, survival and pathogen control in *L. monocytogenes*-infected *Cyld^{-/-}* mice. (A) Proteins were isolated from infected livers of untreated WT and *Cyld^{-/-}* mice as well as STAT3 siRNA and control siRNA-treated *Cyld^{-/-}* mice at day 5 p.i. (n=3 experimental group). WB analysis for CYLD, pSTAT3, fibrin and GAPDH was performed and representative data are shown. (B, C) Quantification of total STAT3 (B) and fibrin (C) (+ SD) was performed from WB data of livers from *L. monocytogenes*-infected WT and *Cyld^{-/-}* mice, which were treated as indicated. The results present n=3 mice per experimental group. (D) The survival rates of infected WT and *Cyld^{-/-}* as well as STAT3 siRNA and control siRNA-treated *Cyld^{-/-}* mice are shown. The survival of *Cyld^{-/-}* and control siRNA-treated *Cyld^{-/-}* mice but not of STAT3 siRNA-treated *Cyld^{-/-}* mice was significantly increased as compared to WT animals (p < 0.05 for both groups, n=5 per experimental group). Survival was monitored until day 10 p.i. One of two representative experiments is shown. (E) CFUs were determined in the liver of *L. monocytogenes*-infected untreated WT and *Cyld^{-/-}* mice as well as STAT3 siRNA and control siRNA-treated *Cyld^{-/-}* mice at day 5 p.i. (* p < 0.05, ** p < 0.01; n=5 per experimental group). Data show the mean + SD and one of two representative experiments. (F) The serum concentration of IL-6 was determined by a cytometric bead assay at day 5 p.i. Data show the mean + SD of 5 mice per experimental group and from one of two representative experiments (* p < 0.05, ** p < 0.01).

4.2.3.6 Inhibition of fibrin production abolished protection and increased the hepatic bacterial load of *Cyld*^{-/-} mice.

To prove that the increased IL-6/STAT-3-dependent fibrin production protected *Cyld*^{-/-} mice from lethal listeriosis, fibrin deposition was inhibited by treatment with warfarin, a vitamin K antagonist. Warfarin treatment strongly reduced hepatic fibrin levels of both *L. monocytogenes*-infected WT and *Cyld*^{-/-} mice (Fig. 32A, B).

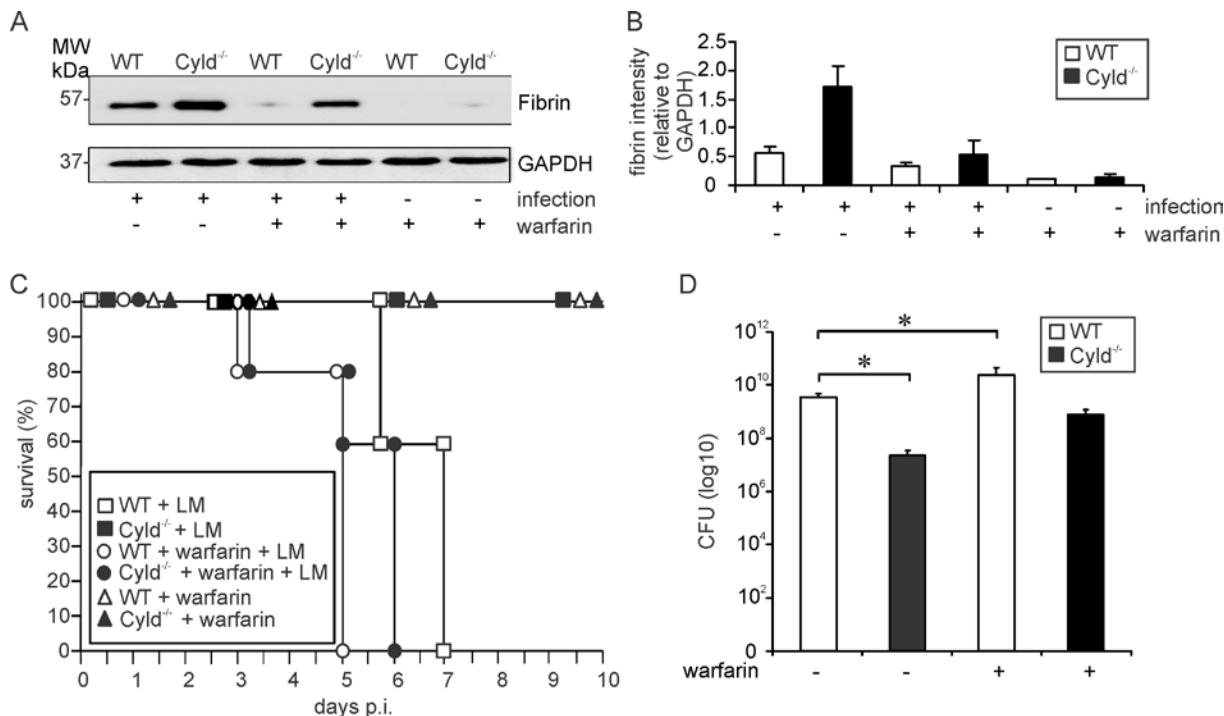


Figure 32. Inhibition of fibrin production abolished protection and increased the hepatic bacterial load of *Cyld*^{-/-} mice. (A) WB analysis of hepatic fibrin production in uninfected and infected WT and *Cyld*^{-/-} mice. GAPDH was used as loading control. (B) Quantification of fibrin (+ SD) was performed from WB data of uninfected and *L. monocytogenes*-infected WT and *Cyld*^{-/-}, respectively, which were treated with warfarin as indicated. The results present 3 mice per experimental group. (C) The survival rate of uninfected and infected mice, which were treated with warfarin as indicated, was monitored until day 10 of infection (n=10 per experimental group). Survival of infected *Cyld*^{-/-}, uninfected *Cyld*^{-/-} mice treated with warfarin, and WT mice treated with warfarin, respectively, was significantly increased as compared to infected WT mice without warfarin treatment ($p < 0.001$ for all groups). (D) CFUs were determined in the liver of *L. monocytogenes*-infected WT and *Cyld*^{-/-} mice, which were treated with warfarin as indicated, at day 5 p.i. (* $p < 0.05$, n=5 per experimental group). Data show the mean + SD. In (C) and (D) one of two representative experiments is shown.

Suppression of fibrin production completely abolished protection from severe listeriosis in *L. monocytogenes*-infected *Cyld*^{-/-} mice and warfarin-treated *Cyld*^{-/-} and WT mice died up to day 5 and 6 p.i., respectively (Fig. 32C). Untreated infected WT mice died later, i.e. until day 7 p.i.,

indicating that the low amounts of fibrin produced in WT mice still had a minor protective effect. Concomitantly, inhibition of fibrin production in WT mice resulted in increased hepatic CFUs as compared to non-treated WT animals (Fig. 32D). In *Cyld*^{-/-} mice, warfarin treatment resulted in an increase of hepatic CFUs, which were no longer significantly reduced as compared to untreated WT mice. Overall, α -IL6, STAT3 siRNA, and warfarin treatment further illustrated that CYLD impaired IL-6/STAT3-induced fibrin production resulting in impaired pathogen control and death from severe listeriosis.

4.2.3.7 Inhibition of CYLD partially protected WT mice from lethal listeriosis

To explore whether knockdown of CYLD can protect WT mice from lethal listeriosis, WT mice were treated with *Cyld* siRNA 24 h prior to *L. monocytogenes* infection. WB analysis showed a 90% CYLD knockdown in livers of *Cyld* siRNA-treated WT mice, whereas treatment with control siRNA had no effect on CYLD protein levels of WT mice at day 5 p.i. (Fig. 33A, B). CYLD knockdown resulted in an increase of pSTAT3 (Fig. 33A, C) as well as fibrin (Fig. 33A, D) in *L. monocytogenes*-infected WT mice.

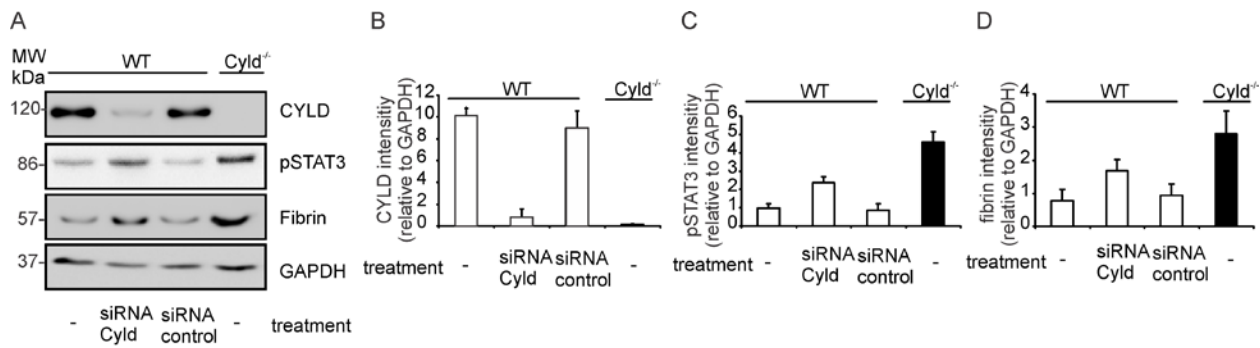


Figure 33. Therapeutic *Cyld* siRNA treatment protects WT mice from lethal listeriosis. (A) WT and *Cyld*^{-/-} mice were i.v. infected with 5×10^5 *L. monocytogenes*. Infected mice were treated as indicated 24 h p.i. At day 5 p.i., proteins were isolated from the liver (n=3 per experimental group) and CYLD, pSTAT3 fibrin, and GAPDH production was analyzed by WB. (B, C, D) Quantification of CYLD (B), pSTAT3 (C) and fibrin (D) (+ SD) was performed from WB data of the indicated groups. The results present 3 mice per experimental group.

The increased pSTAT3 and fibrin levels of *Cyld* siRNA-treated, infected WT mice were associated with 50% survival, whereas all mock-treated and untreated WT mice succumbed (Fig. 33E). Thus, CYLD inhibition significantly reduced mortality of WT mice. Furthermore, siRNA-mediated CYLD inhibition significantly reduced CFUs in WT mice as compared to untreated and mock-treated WT animals, respectively (Fig. 33F). Macroscopic analysis of livers revealed strongly reduced hepatic haemorrhage in *Cyld* siRNA-treated WT mice as compared to untreated

as well as mock-treated WT animals (Fig. 33G). In conclusion, these findings identify CYLD as a potential therapeutic target in severe listeriosis.

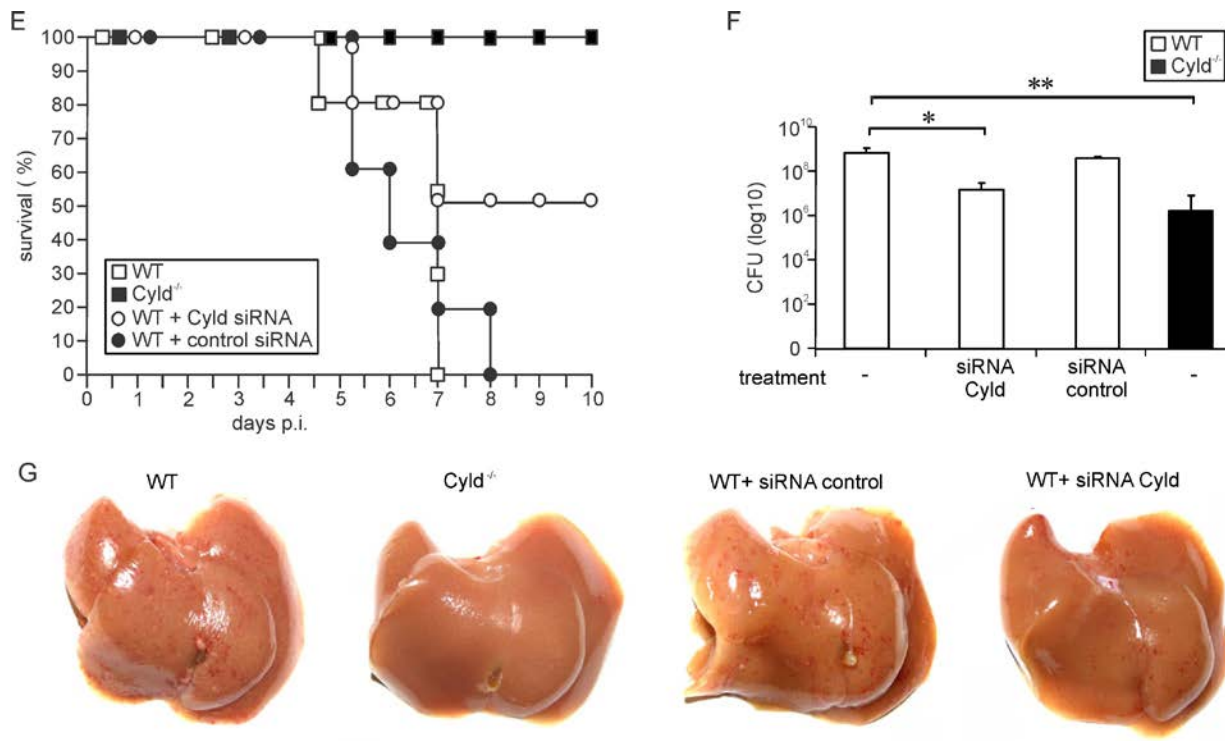


Figure 33. Therapeutic Cyld siRNA treatment protects WT mice from lethal listeriosis. (E) The survival rates of *L. monocytogenes*-infected untreated Cyld^{-/-} and Cyld siRNA-treated WT mice were significantly increased as compared to untreated WT mice ($p < 0.01$ for Cyld^{-/-} vs. WT mice, $p < 0.05$ for Cyld siRNA treated WT vs. WT mice). Ten mice per group were analyzed until day 10 p.i. (F) CFUs were determined in the liver at day 5 p.i. Five mice were analyzed per group and data show the mean \pm SD (* $p < 0.05$, ** $p < 0.01$). In (A-G) data from one of two representative experiments are shown. (G) Macroscopic analysis showed haemorrhage of untreated and control siRNA-treated infected WT mice. Haemorrhage was reduced in WT mice treated with Cyld siRNA and was absent from untreated Cyld^{-/-} mice.

4.2.3.8 Cyld-deficiency is protective in cerebral listeriosis

To investigate the functional role of CYLD in cerebral listeriosis, WT and Cyld^{-/-} mice were infected intracerebrally with 5×10^2 *L. monocytogenes*. Whereas all WT mice succumbed up to day 4 post infection (p.i.), 60% of Cyld^{-/-} mice survived (Fig. 34A) demonstrating that CYLD prevents the initiation of protective host responses in cerebral listeriosis. *L. monocytogenes* infection also resulted in brain haemorrhage of WT but not of Cyld^{-/-} mice (Fig. 34B). The

bacterial loads were identical in both mice strains (Fig. 34C), illustrating a more general anti-haemorrhagic function of CYLD independent of pathogen control.

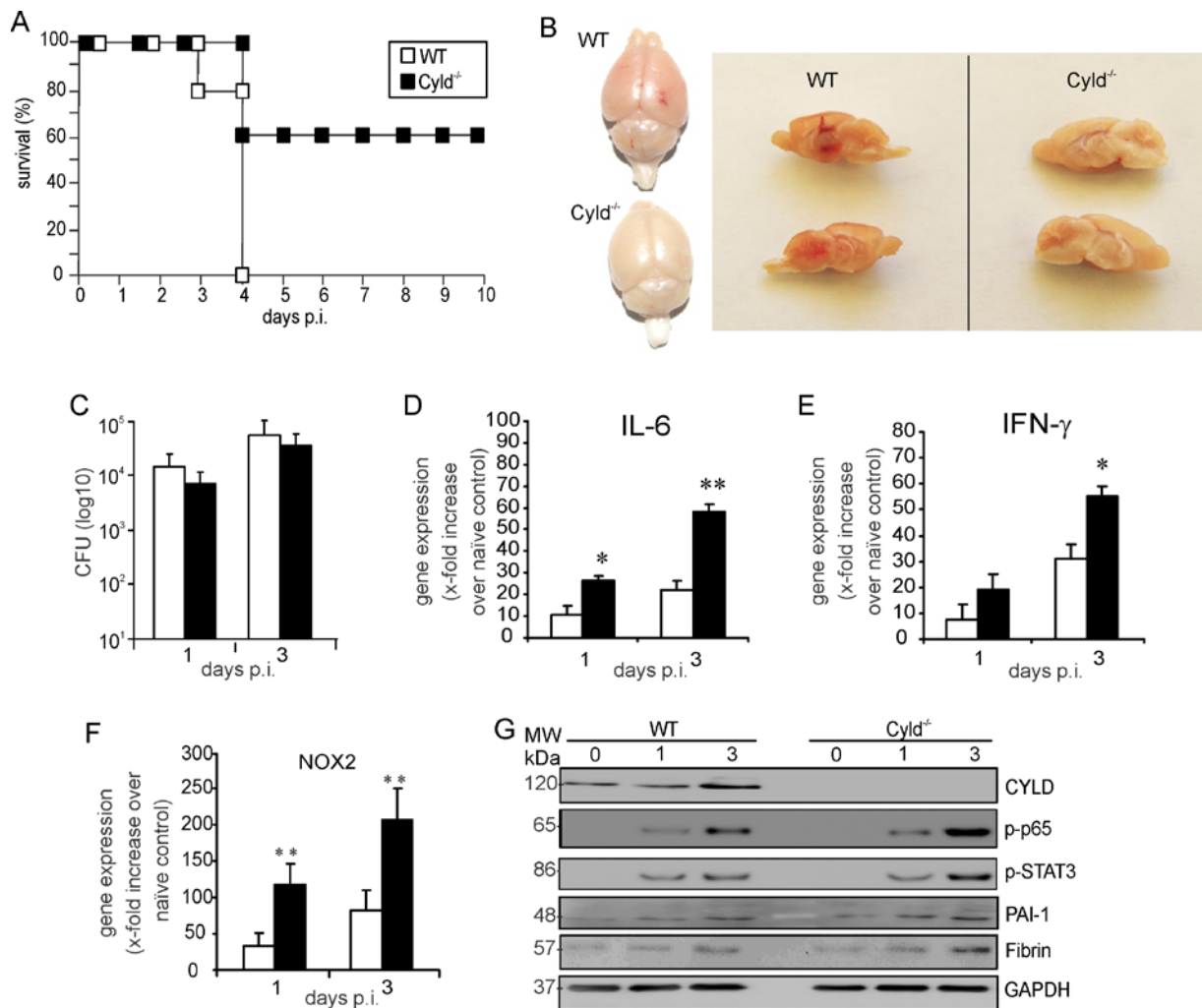


Figure 34. Protective effects of Cyld-deficiency on cerebral listeriosis. (A) Ten C57BL/6 Cyld^{-/-} and WT mice were infected intracerebrally with 5×10^2 *L. monocytogenes* and survival rates were monitored until day 10 p.i. Survival of Cyld^{-/-} mice was significantly increased as compared to WT animals ($p < 0.01$). (B) Increased intracerebral haemorrhage in WT as compared to Cyld^{-/-} mice at day 3 after intracerebral infection. Representative finding, individual mice from 5 mice per experimental group are shown. (C) CFU were determined in the brain of *L. monocytogenes*-infected WT and Cyld^{-/-} mice at day 1 and 3 p.i. Data show the mean \pm SD of 5 mice per experimental groups. (D-F) Quantitative RT-PCR analysis of intracerebral IL-6 (D), IFN- γ (E), and NOX2 (F) mRNA (* $p < 0.05$, ** $p < 0.01$). Data represent the increase of the respective mRNA expression of *L. monocytogenes*-infected over uninjected mice of the same mouse strain. Data show the increase of the respective mRNA expression of *L. monocytogenes*-infected over uninjected mice of the same mouse strain. Data represent the mean \pm SD of 5 mice. (G) Proteins were isolated from the brains of uninfected (d0) and infected (d1 and 3 p.i.) WT and Cyld^{-/-} mice. Proteins were analyzed by WB for CYLD, p-p65, pSTAT3, PAI-1, fibrin and GAPDH. Three to four mice were analyzed per group and representative data are shown. In (A-G) one of two independent experiments is shown.

In addition, NOX2 mRNA was significantly higher expressed in *L. monocytogenes*-infected Cyld^{-/-} mice. Impaired IL-6, IFN- γ , and NOX2 mRNA production by CYLD was also observed in cerebral listeriosis (Fig. 34D-F). In cerebral listeriosis, Cyld-deficiency also resulted in an increased phosphorylation of p65 and STAT3 as well as fibrin deposition (Fig. 34G). In contrast, PAI-1 was only slightly elevated in Cyld^{-/-} mice (Fig. 34G).

5. Discussion

The present study identified that stimulation of protective host responses in listeriosis and toxoplasmosis is dependent on the activation of immunostimulatory PKC-θ, which was crucial for the activation of T cells. In contrast, CYLD suppressed inflammatory reactions. Interestingly this immunosuppressive role of CYLD was detrimental in lethal high dose infection with *L. monocytogenes*.

Role of PKC-θ in listeriosis and toxoplasmosis

With respect to PKC-θ, we showed that PKC-θ played an important role in conferring protection against both bacterial (*L. monocytogenes*) and parasitic (*T. gondii*) infections. In both diseases, numbers of pathogen-specific T cells were significantly reduced in the absence of PKC-θ at all time points. *L. monocytogenes*-specific CD8 T cells were reduced at the peak of the primary immune response (d 9 p.i.), late after primary infection (d 50 p.i.) and early after secondary infection (d 1 after reinfection) illustrating that both effector and memory CD8 T cells are PKC-θ-dependent in listeriosis. Furthermore, our data also provide the first evidence that the development of MHC class Ib-restricted CD8 T cells, which play a protective role in primary, but not secondary listeriosis (Kerksiek et al., 1999; Kerksiek et al., 2003), is PKC-θ-dependent.

Upon *T. gondii* infection, the numbers of *T. gondii*-specific Gra6-HF10-specific CD8 T cells were reduced at the peak of the T cell response (d 21 p.i.). In addition, the number of IFN-γ-producing CD4 and CD8 T cells were reduced during *T. gondii* infection. Since IFN-γ-producing CD4 and CD8 T cells are absolutely essential for the control of *T. gondii* (Gazzinelli et al., 1992), the diminished T cell response of PKC-θ^{-/-} mice resulted in a lethal necrotizing TE. IFN-γ-producing *L. monocytogenes*-specific CD4 T cells were also reduced in both primary and secondary listeriosis of PKC-θ^{-/-} mice. However, numbers of *L. monocytogenes*-specific CD4 T cells did not differ late after primary infection (d 14 to d 50 p.i.) and after the peak of the secondary *L. monocytogenes*-specific CD4 T cell response (d 9 and d 21 p.i.) indicating that PKC-θ may play a lesser important role for the maintenance of *L. monocytogenes*-specific CD4 T cells as compared to *L. monocytogenes*-specific CD8 T cells. Currently the mechanism resulting in a constantly increased number of *T. gondii*-specific WT CD4 T cells but equal numbers of memory *L. monocytogenes*-specific WT and PKC-θ^{-/-} CD4 T cells are unknown.

However, it may well be that the persistent antigen affiliation in toxoplasmosis continuously stimulates *T. gondii*-specific CD4 T cells and keep them at high numbers, whereas the pool of *L. monocytogenes*-specific CD4 T cells contracts sharply to the level of *L. monocytogenes*-specific PKC- $\theta^{-/-}$ CD4 T cells after elimination of *L. monocytogenes*. In addition, CD4 T cells are of minor importance for the elimination of *Listeria* compared to CD8 T cells (Kaufmann et al., 1997). This is in contrast to toxoplasmosis, where both T cell populations are equally important (Gazzinelli et al., 1996). Thus, PKC- θ seems to be of variable importance in T cell populations for pathogen control.

PKC- θ also plays a critical role for the induction of autoimmune T cells in various models of autoimmune disorders (Marsland et al., 2007; Salek-Ardakani et al., 2005; Tan et al., 2006) which is in marked contrast to several viral infections in which PKC- θ is dispensable for a protective T cell response (Marsland et al., 2004; Berg-Brown et al., 2004; Giannoni et al., 2005; Marsland et al., 2005). This suggests that during viral diseases the strong stimulation of T cells by the inflammatory milieu and highly activated DCs is sufficient to compensate for a T cellular PKC- θ -deficiency, whereas, in general, in autoimmune disorders T cell stimulation remains below this critical level of T cell activation. In analogy, in listeriosis, the stimulation of pathogen-specific T cells by the inflammatory milieu and DCs may be weaker than in viral infections, preventing normal activation and proliferation of T cells in the absence of PKC- θ . The assumption that external factors including the inflammatory milieu and the activation status of DCs partially determines the functional importance of PKC- θ for the activation and proliferation of Ag-specific T cells is further corroborated by the observation that infection with LCMV, but not immunization with DCs loaded with LCMV-specific peptides induced proliferation of LCMV-specific T cells in PKC- $\theta^{-/-}$ mice (Berg-Brown et al., 2004). Also in our experiments, an immunization with OVA₂₅₇₋₂₆₄ and LLO₁₉₀₋₂₀₁-peptide-loaded WT DCs was insufficient to induce normal numbers of OVA-specific CD8 and LLO-specific CD4 T cells in PKC- $\theta^{-/-}$ mice. The assumption that the inflammatory milieu, but not the T cell stimulating antigen determines the functional importance of PKC- θ for T cell activation is illustrated by the observation that *Listeria* expressing LCMV also induce a diminished LCMV-specific T cell response in PKC- $\theta^{-/-}$ mice

Both murine listeriosis and toxoplasmosis are characterized by a strong protective Th1 response, while Th2 CD4 T cell response plays only a protective role in toxoplasmosis but is absent in listeriosis. In listeriosis, the Th2 polarizing cytokine IL-4, which is produced by CD4 NK T cells early after infection, is downregulated by IL-12 produced by the macrophages, thereby inhibiting the Th2 response (Kaufmann et al., 1997). While in toxoplasmosis, in addition to the strong Th1 response, additional IL-4 producing Th2 cells develop and contribute to the optimal control of the parasite and survival of toxoplasmosis (Suzuki et al., 1996). In our experiments, the *T. gondii*-specific Th2 response was also PKC-θ-dependent, since in the absence of PKC-θ the frequency of IL-4-producing CD4 T cells was greatly diminished. Interestingly, GATA3, which is of key importance for the Th2 differentiation of CD4 T cells (Mowen and Glimcher, 2004), was also reduced in CD4 T cells of PKC-θ^{-/-} mice. These data extend previous *in vitro* observations in anti-CD3/CD28-stimulated CD4 T cells, which also revealed that PKC-θ is involved in the upregulation of GATA3 (Stevens et al., 2006). In addition, Th2 differentiation of *Leishmania* and *Nippostrongylus brasiliensis*-specific CD4 T cells is PKC-θ-dependent (Marsland et al., 2004). However, in contrast to *T. gondii*-specific Th1 cells, the development of *Leishmania*-specific Th1 responses was PKC-θ independent (Marsland et al., 2004). These findings further illustrate that not only the “class” of the pathogen, i.e. virus, bacteria or parasites, but also the specific pathogen has an impact on the function of PKC-θ for the induction of different Th subtypes. Again, the reason for these differences have not been resolved yet, but antigen abundance, strength of DC activation and the magnitude of Th1/Th2 polarizing cytokines may play a role.

In listeriosis and toxoplasmosis, the reduced numbers of pathogen-specific T cells in PKC-θ^{-/-} mice may either be caused by an impaired proliferation or survival of T cells. Both, survival and proliferation of T cells are critically regulated by PKC-θ after TCR stimulation (Manicassamy et al., 2006; Saibil et al., 2007; Sun et al., 2000). In listeriosis the inhibition of caspase-3 had no influence on the percentage of proliferating WT T cells. Thus, apoptosis of WT T cells was not linked to the number of proliferating cells under these conditions. In contrast to caspase-3 inhibition, treatment with a pan-caspase inhibitor strongly reduced proliferation of WT OT-I T cells, which is completely compatible with a function of caspases, especially caspase-8, upstream of caspase-3 for the proliferation of T cells (Chun et al., 2002; Kennedy et al., 1999). In toxoplasmosis the lack of increased activation of caspase-3 in splenic CD4 and CD8 T cells of

PKC- $\theta^{-/-}$ implies that an increased rate of apoptosis was not responsible for the reduced numbers of *T. gondii*-specific CD4 and CD8 T cells. However, the very low numbers of *T. gondii*-specific T cells in PKC- $\theta^{-/-}$ mice prevented a further *in vivo* functional analysis of T cell proliferation and apoptosis.

To analyze under which experimental conditions PKC- $\theta^{-/-}$ mice develop an improved pathogen-specific T cell response, we performed additional *in vivo* and *in vitro* experiments. The observation that PKC- $\theta^{-/-}$ mice reconstituted with polyclonal WT T cells controlled both listeriosis and toxoplasmosis illustrates that T cell autonomous expression of PKC- θ is sufficient to compensate for PKC- θ deficiency.

Role of deubiquitinase CYLD in listeriosis and toxoplasmosis

With respect to PKC- θ , pathogen control and survival were reduced in the absence of PKC- θ following low dose infection with *L. monocytogenes* and *T. gondii*. Therefore, we studied first the pathogen control and survival of Cyld $^{-/-}$ mice employing the same experimental conditions for both infectious diseases. However, Cyld $^{-/-}$ mice had a normal pathogen control and survival as compared to WT mice in both listeriosis and toxoplasmosis. These findings indicate that Cyld deficiency provided no significant advantage under these experimental conditions. However, upon infection with a lethal dose of *L. monocytogenes*, Cyld $^{-/-}$ mice were completely protected from death whereas all WT mice succumbed. Survival of Cyld $^{-/-}$ mice was in part dependent on IL-6–STAT3-dependent production of fibrin.

Our data show that inhibition of STAT3 by STAT3 siRNA treatment, which reduced hepatic fibrin levels, as well as inhibition of fibrin production by warfarin treatment abolished survival of Cyld $^{-/-}$ mice demonstrating the functional importance of the STAT3/CYLD/fibrin pathway. Furthermore, the increased p38 activation and PAI-1 production in *L. monocytogenes*-infected Cyld $^{-/-}$ mice indicates that CYLD also negatively regulates fibrin deposition and fosters haemorrhage by the inhibition of this anti-fibrinolytic pathway as reported before in *Streptococcus pneumoniae*-induced acute lung injury (Lim et al., 2007b). Taken together, both increased STAT3-dependent fibrin production as well as inhibition of fibrinolysis by PAI-1 contribute to the reported protective function of fibrin in listeriosis. In addition to STAT3, p38, PAI-1 and fibrin, CYLD negatively regulated activation of the NF- κ B pathway as illustrated by reduced p65 phosphorylation. This is in good agreement with previous studies demonstrating

that CYLD inhibits several signal transduction molecules including TRAF2, TRAF6, RIP1, and IKK- γ (Massoumi, 2010), which all contribute to NF- κ B activation upon stimulation. TNF, a potent activator of these signal transduction molecules, was produced in both *L. monocytogenes*-infected WT and Cyld $^{-/-}$ mice without significant differences. Noteworthy, activated NF- κ B induces IL-6 production, and, consequently, Cyld $^{-/-}$ mice had significantly increased hepatic and serum IL-6 levels. These increased IL-6 levels were a central part of the protective effect of Cyld-deficiency, since IL-6 neutralization completely abrogated protection of Cyld $^{-/-}$ mice from lethal listeriosis. Kupffer cell-derived IL-6 is an activator of hepatocyte STAT3 in listeriosis (Gregory et al., 1998) and, thus, the increased activation of STAT3 in livers of Cyld $^{-/-}$ mice is caused both by increased IL-6 production as well as the lacking CYLD-mediated deubiquitination of STAT3.

Previous studies have shown that the protective effect of endogenous IL-6 in low-dose *L. monocytogenes* infection included a better control and containment of *L. monocytogenes* in the liver as well as an increased neutrophilia (Dalrymple et al., 1995). In good agreement, we also observed better control and containment in Cyld $^{-/-}$ mice increased IL-6 levels. The present study extends these findings and identifies that the inhibition of IL-6-dependent STAT3 activation by CYLD prevents survival of severe listeriosis in WT animals. Interestingly, neutralization of IL-6 resulted in a very rapid death of Cyld $^{-/-}$ mice with very high bacterial load, which was higher as in Cyld $^{-/-}$ mice treated with STAT3 siRNA and warfarin, respectively. It is well established that IL-6 activates both the gp130/STAT3 and the gp130/SHP-2/ERK signaling pathways. Since the IL-6/gp130/STAT3 (our study) and the IL-6/gp130/SHP2/ERK pathways (Kamimura et al., 2002) play a protective role in listeriosis, this explains the more severe phenotype upon IL-6 neutralization as compared to STAT3 inhibition in Cyld $^{-/-}$ mice.

The present study clearly shows a positive effect of fibrin production in severe listeriosis. A protective function of fibrin has also been observed in murine toxoplasmosis (Johnson et al., 2003), in which fibrin inhibited immunopathology, as well as in *Yersinia enterocolotica* infection (Luo et al., 2011). However, excessive fibrin production may also have deleterious consequences in infectious diseases. Especially disseminated intravascular coagulation is a life-threatening complication in sepsis. In this context it is of note that *L. monocytogenes* is a facultative intracellular bacterium which mostly causes infections of organs. In fact, more than 60% of *L. monocytogenes* can be found in the liver as short as 10 min after i.v. infection (Gregory et al.,

1996). Thus, murine lethal systemic listeriosis is merely a severe organ infection but not sepsis. Protection from hepatic listeriosis is dependent on the formation of granuloma-like lesions in the liver and our histological findings show that *Cyld*^{-/-} mice had small granuloma-like lesions indicating that the increased fibrin production in these animals contributed to the containment of *L. monocytogenes* in the liver parenchyma. In contrast, WT mice suffered from widespread distribution of *L. monocytogenes* and the absence of granuloma-like lesions in the liver parenchyma, which caused disseminated liver necrosis. Importantly, lethal listeriosis of WT mice was also characterized by vascular occlusion and intravascular fibrotic plaques, a finding which was absent from *Cyld*^{-/-} mice. These findings imply that fibrin deposition in the liver parenchyma and intravascular hepatic fibrin deposition were independent of each other and that CYLD mainly affected fibrin production in the liver parenchyma, which may be explained by the strong effect of CYLD on IL-6-induced fibrin production by hepatocytes.

The observation that siRNA-mediated inhibition of CYLD in WT mice increased hepatic p-STAT3 and fibrin levels, diminished haemorrhage and significantly increased survival indicates that inhibition of CYLD might be a therapeutic option in severe listeriosis and potentially other infectious diseases including acute lung injury induced by *S. pneumoniae*, which also show an improved outcome in *Cyld*^{-/-} mice. In this context our observation is of note that in cerebral listeriosis, which is also one of the most dangerous clinical manifestations of human listeriosis, *Cyld*^{-/-} mice were also significantly protected from death and exhibited higher expression of IL-6 mRNA, activation of NF-κB, STAT3 and PAI-1, fibrin deposition, and prevention of haemorrhage. Thus, in listeriosis, the negative effect of CYLD on host protection is not restricted to systemic listeriosis and the liver but of more general importance.

In conclusion, the present studies show that both PKC-θ and CYLD strongly regulate the activation of host cells in infectious diseases and in particular exert a strong effect on NF-κB-dependent immune responses. Thus, both the induction of immune responses by PKC-θ as well as the inhibition of immune responses by CYLD exert a strong important effect on infectious diseases. However, the functional importance of both PKC-θ and CYLD is largely dependent on the cell type, the underlying pathogen as well as the experimental disease conditions.

References

- Adhikari A, Xu M, Chen ZJ (2007) Ubiquitin-mediated activation of TAK1 and IKK. *Oncogene* 26:3214-3226.
- Ambroise-Thomas P, Pelloux H (1993) Toxoplasmosis - congenital and in immunocompromised patients: a parallel. *Parasitol Today* 9:61-63.
- Arendt CW, Albrecht B, Soos TJ, Littman DR (2002) Protein kinase C-theta;; signaling from the center of the T-cell synapse. *Curr Opin Immunol* 14:323-330.
- Baker RG, Hayden MS, Ghosh S (2011) NF-kappaB, inflammation, and metabolic disease. *Cell Metab* 13:11-22.
- Barnden MJ, Allison J, Heath WR, Carbone FR (1998) Defective TCR expression in transgenic mice constructed using cDNA-based alpha- and beta-chain genes under the control of heterologous regulatory elements. *Immunol Cell Biol* 76:34-40.
- Beinke S (2004) Functions of NF-kappaB1 and NF-kappaB2 in immune cell biology. *Biochem J* 382(Pt 2):393-409
- Berg-Brown NN, Gronski MA, Jones RG, Elford AR, Deenick EK, Odermatt B, Littman DR, Ohashi PS (2004) PKCtheta signals activation versus tolerance in vivo. *J Exp Med* 199:743-752.
- Bohne W, Heesemann J, Gross U (1993) Coexistence of heterogeneous populations of *Toxoplasma gondii* parasites within parasitophorous vacuoles of murine macrophages as revealed by a bradyzoite-specific monoclonal antibody. *Parasitol Res* 79:485-487.
- Bradford,M.M. 1976. A rapid and sensitive method for the quantitation of microgram quantities of protein utilizing the principle of protein-dye binding. *Anal. Biochem.* 72: 248-254.
- Braun L, Cossart P (2000) Interactions between *Listeria monocytogenes* and host mammalian cells. *Microbes Infect* 2:803-811.
- Buchmeier NA, Schreiber RD (1985) Requirement of endogenous interferon-gamma production for resolution of *Listeria monocytogenes* infection. *Proc Natl Acad Sci* 82:7404-7408.
- Caamano J, Alexander J, Craig L, Bravo R, Hunter CA (1999) The NF-kappa B family member RelB is required for innate and adaptive immunity to *Toxoplasma gondii*. *J Immunol* 163:4453-4461.
- Caamano J, Tato C, Cai G, Villegas EN, Speirs K, Craig L, Alexander J, Hunter CA (2000) Identification of a role for NF-kappa B2 in the regulation of apoptosis and in maintenance of T cell-mediated immunity to *Toxoplasma gondii*. *J Immunol* 165:5720-5728.

- Cai G, Radzanowski T, Villegas EN, Kastelein R, Hunter CA (2000) Identification of STAT4-dependent and independent mechanisms of resistance to *Toxoplasma gondii*. *J Immunol* 165:2619-2627.
- Chang JT, Palanivel VR, Kinjyo I, Schambach F, Intlekofer AM, Banerjee A, Longworth SA, Vinup KE, Mrass P, Oliaro J, Killeen N, Orange JS, Russell SM, Weninger W, Reiner SL (2007) Asymmetric T lymphocyte division in the initiation of adaptive immune responses. *Science* 315:1687-1691.
- Cheers C, McKenzie IF (1978) Resistance and susceptibility of mice to bacterial infection: genetics of listeriosis. *Infect Immun* 19:755-762.
- Chen ZJ (2005) Ubiquitin signalling in the NF- κ B pathway. *Nat Cell Biol*. 27(8):758-65.
- Chun HJ, Zheng L, Ahmad M, Wang J, Speirs CK, Siegel RM, Dale JK, Puck J, Davis J, Hall CG, Skoda-Smith S, Atkinson TP, Straus SE, Lenardo MJ (2002) Pleiotropic defects in lymphocyte activation caused by caspase-8 mutations lead to human immunodeficiency. *Nature* 419:395-399.
- Dalrymple SA, Lucian LA, Slattery R, McNeil T, Aud DM, Fuchino S, Lee F, Murray R (1995) Interleukin-6-deficient mice are highly susceptible to *Listeria monocytogenes* infection: correlation with inefficient neutrophilia. *Infect Immun* 63:2262-2268.
- Deckert M, Soltek S, Geginat G, Lutjen S, Montesinos-Rongen M, Hof H, Schluter D (2001) Endogenous interleukin-10 is required for prevention of a hyperinflammatory intracerebral immune response in *Listeria monocytogenes* meningoencephalitis. *Infect Immun* 69:4561-4571.
- Dinauer MC, Deck MB, Unanue ER (1997) Mice lacking reduced nicotinamide adenine dinucleotide phosphate oxidase activity show increased susceptibility to early infection with *Listeria monocytogenes*. *J Immunol* 158:5581-5583.
- Dubey JP (1977) Persistence of *Toxoplasma gondii* in the tissues of chronically infected cats. *J Parasitol* 63:156-157.
- Dubey JP (1980) Persistence of encysted *Toxoplasma gondii* in caprine livers and public health significance of toxoplasmosis in goats. *J Am Vet Med Assoc* 177:1203-1207.
- Dubey JP (1985) Persistence of encysted *Toxoplasma gondii* in tissues of equids fed oocysts. *Am J Vet Res* 46:1753-1754.
- Dubey JP (1998) Structures of *Toxoplasma gondii* tachyzoites, bradyzoites, and sporozoites and biology and development of tissue cysts. *Clin Microbiol Rev* 11: 267-29
- Dubey JP, Frenkel JK (1972) Cyst-induced toxoplasmosis in cats. *J Protozool* 19:155-177.
- Esch KJ, Petersen CA (2013) Transmission and epidemiology of zoonotic protozoal diseases of companion animals. *Clin Microbiol Rev* 26:58-85.

- Fischer HG, Bonifas U, Reichmann G (2000) Phenotype and functions of brain dendritic cells emerging during chronic infection of mice with *Toxoplasma gondii*. *J Immunol* 164:4826-4834.
- Foulds KE, Zenewicz LA, Shedlock DJ, Jiang J, Troy AE, Shen H (2002) Cutting edge: CD4 and CD8 T cells are intrinsically different in their proliferative responses. *J Immunol* 168:1528-1532.
- Gazzinelli R, Xu Y, Hieny S, Cheever A, Sher A (1992) Simultaneous depletion of CD4+ and CD8+ T lymphocytes is required to reactivate chronic infection with *Toxoplasma gondii*. *J Immunol* 149:175-180.
- Gazzinelli RT, Wysocka M, Hieny S, Scharton-Kersten T, Cheever A, Kuhn R, Muller W, Trinchieri G, Sher A (1996) In the absence of endogenous IL-10, mice acutely infected with *Toxoplasma gondii* succumb to a lethal immune response dependent on CD4+ T cells and accompanied by overproduction of IL-12, IFN-gamma and TNF-alpha. *J Immunol* 157:798-805.
- Ghosh S (2002) Missing pieces in the NF-kappaB puzzle. *Cell* 109 Suppl:S81-96.
- Giannoni F, Lyon AB, Wareing MD, Dias PB, Sarawar SR (2005) Protein kinase C theta is not essential for T-cell-mediated clearance of murine gammaherpesvirus 68. *J Virol* 79:6808-6813.
- Gilmore TD (2006) Introduction to NF-kappaB: players, pathways, perspectives. *Oncogene* 25:6680-6684.
- Gong B (2007) The role of ubiquitin C-terminal hydrolase L1 in neurodegenerative disorders. *Drug News Perspect.* 206:365-70
- Gregory SH, Sagnimenti AJ, Wing EJ (1996) Bacteria in the bloodstream are trapped in the liver and killed by immigrating neutrophils. *J Immunol* 157:2514-2520.
- Gregory SH, Wing EJ, Danowski KL, van RN, Dyer KF, Twardy DJ (1998) IL-6 produced by Kupffer cells induces STAT protein activation in hepatocytes early during the course of systemic listerial infections. *J Immunol* 160:6056-6061.
- Grenningloh R, Darji A, Wehland J, Chakraborty T, Weiss S (1997) Listeriolysin and IrpA are major protein targets of the human humoral response against *Listeria monocytogenes*. *Infect Immun* 65:3976-3980.
- Guan H, Moretto M, Bzik DJ, Gigley J, Khan IA (2007) NK cells enhance dendritic cell response against parasite antigens via NKG2D pathway. *J Immunol* 179:590-596.
- Hamilton SE, Harty JT (2002) Quantitation of CD8+ T cell expansion, memory, and protective immunity after immunization with peptide-coated dendritic cells. *J Immunol* 169:4936-4944.
- Hamon M, Bierne H, Cossart P (2006) *Listeria monocytogenes*: a multifaceted model. *Nat Rev Microbiol* 4:423-434.

- Harhaj EW, Dixit VM (2012) Regulation of NF-kappaB by deubiquitinases. *Immunol Rev* 246:107-124.
- Harty JT, Bevan MJ (1995) Specific immunity to Listeria monocytogenes in the absence of IFN gamma. *Immunity* 3:109-117.
- Havell EA (1989) Evidence that tumor necrosis factor has an important role in antibacterial resistance. *J Immunol* 143:2894-2899.
- Hayashi K, Altman A (2007) Protein kinase C theta (PKCtheta): a key player in T cell life and death. *Pharmacol Res* 55:537-544.
- Hayden MS (2004) Signaling to NF-kappaB *Genes Dev* 18:2195-224
- Hayden MS, Ghosh S (2011) NF-kappaB in immunobiology. *Cell Res* 21:223-244.
- Hershko A (1998) The ubiquitin system. *Annu Rev Biochem* 67:425-79
- Hicke L (2003) Regulation of membrane protein transport by ubiquitin and ubiquitin-binding proteins *Annu Rev Cell Dev Biol* 19:141-72
- Hochstrasser M (1995) Ubiquitin, proteasomes, and the regulation of intracellular protein degradation *Curr Opin Cell Biol* 7:215-23
- Hof H, Nichterlein T, Kretschmar M (1997) Management of listeriosis. *Clin Microbiol Rev* 10:345-357.
- Hogquist KA, Jameson SC, Heath WR, Howard JL, Bevan MJ, Carbone FR (1994) T cell receptor antagonist peptides induce positive selection. *Cell* 76:17-27.
- Hunter CA, Subauste CS, Van Cleave VH, Remington JS (1994) Production of gamma interferon by natural killer cells from Toxoplasma gondii-infected SCID mice: regulation by interleukin-10, interleukin-12, and tumor necrosis factor alpha. *Infect Immun* 62:2818-2824.
- Isakov N (2012) PKC-θ is a Key Regulator of T-cell Behavior and a Drug Target for T cell-mediated Diseases. *J Clin Cell Immunol* S12:008.
- Jankovic D, Kullberg MC, Feng CG, Goldszmid RS, Collazo CM, Wilson M, Wynn TA, Kamanaka M, Flavell RA, Sher A (2007) Conventional T-bet(+)Foxp3(-) Th1 cells are the major source of host-protective regulatory IL-10 during intracellular protozoan infection *J Exp Med* 204:273-283.
- Jin D, Takamoto M, Hu T, Taki S, Sugane K (2009) STAT6 signalling is important in CD8 T-cell activation and defence against Toxoplasma gondii infection in the brain. *Immunology* 127:187-195.

- Jin W, Reiley WR, Lee AJ, Wright A, Wu X, Zhang M, Sun SC (2007) Deubiquitinating enzyme CYLD regulates the peripheral development and naive phenotype maintenance of B cells. *J Biol Chem* 282:15884-15893.
- Johnson LL, Berggren KN, Szaba FM, Chen W, Smiley ST (2003) Fibrin-mediated protection against infection-stimulated immunopathology. *J Exp Med* 197:801-806.
- Kaech SM, Ahmed R (2001) Memory CD8+ T cell differentiation: initial antigen encounter triggers a developmental program in naive cells. *Nat Immunol* 2:415-422.
- Kamimura D, Fu D, Matsuda Y, Atsumi T, Ohtani T, Park SJ, Ishihara K, Hirano T (2002) Tyrosine 759 of the cytokine receptor gp130 is involved in Listeria monocytogenes susceptibility. *Genes Immun* 3:136-143.
- Kang H, Remington JS, Suzuki Y (2000) Decreased resistance of B cell-deficient mice to infection with Toxoplasma gondii despite unimpaired expression of IFN-gamma, TNF-alpha, and inducible nitric oxide synthase. *J Immunol* 164:2629-2634.
- Kaufmann SH, Emoto M, Szalay G, Barsig J, Flesch IE (1997) Interleukin-4 and listeriosis. *Immunol Rev* 158:95-105.
- Kayagaki N, Yan M, Seshasayee D, Wang H, Lee W, French DM, Grewal IS, Cochran AG, Gordon NC, Yin J, Starovasnik MA, Dixit VM (2002) BAFF/BLyS receptor 3 binds the B cell survival factor BAFF ligand through a discrete surface loop and promotes processing of NF-kappaB2. *Immunity* 17:515-524.
- Keats JJ, et al. (2007) Promiscuous mutations activate the noncanonical NF-kappaB pathway in multiple myeloma. *Cancer Cell* 12:131-144.
- Kennedy NJ, Kataoka T, Tschopp J, Budd RC (1999) Caspase activation is required for T cell proliferation. *J Exp Med* 190:1891-1896.
- Kerksiek KM, Busch DH, Pilip IM, Allen SE, Pamer EG (1999) H2-M3-restricted T cells in bacterial infection: rapid primary but diminished memory responses. *J Exp Med* 190:195-204.
- Kerksiek KM, Ploss A, Leiner I, Busch DH, Pamer EG (2003) H2-M3-restricted memory T cells: persistence and activation without expansion. *J Immunol* 170:1862-1869.
- Laemmli, U.K. 1970. Cleavage of structural proteins during the assembly of the head of bacteriophage T4. *Nature* 227: 680-685.
- LaRosa DF, Stumhofer JS, Gelman AE, Rahman AH, Taylor DK, Hunter CA, Turka LA (2008) T cell expression of MyD88 is required for resistance to Toxoplasma gondii. *Proc Natl Acad Sci* 105:3855-3860.
- Lawrence T (2009) The nuclear factor NF-kappaB pathway in inflammation. *Cold Spring Harb Perspect Biol* 1:a001651.

- Li Y, Hu J, Vita R, Sun B, Tabata H, Altman A (2004) SPAK kinase is a substrate and target of PKCtheta in T-cell receptor-induced AP-1 activation pathway. *EMBO J* 23:1112-1122.
- Lighvani AA, Frucht DM, Jankovic D, Yamane H, Aliberti J, Hissong BD, Nguyen BV, Gadina M, Sher A, Paul WE, O'Shea JJ (2001) T-bet is rapidly induced by interferon-gamma in lymphoid and myeloid cells. *Proc Natl Acad Sci* 98:15137-15142.
- Lim JH, Ha UH, Woo CH, Xu H, Li JD (2008) CYLD is a crucial negative regulator of innate immune response in Escherichia coli pneumonia. *Cell Microbiol* 10:2247-2256.
- Lim JH, Jono H, Koga T, Woo CH, Ishinaga H, Bourne P, Xu H, Ha UH, Xu H, Li JD (2007a) Tumor suppressor CYLD acts as a negative regulator for non-typeable Haemophilus influenzae-induced inflammation in the middle ear and lung of mice. *PLoS One* 2:e1032.
- Lim JH, et al. (2007b) Tumor suppressor CYLD regulates acute lung injury in lethal Streptococcus pneumoniae infections. *Immunity* 27:349-360.
- Liu L, McBride KM, Reich NC (2005) STAT3 nuclear import is independent of tyrosine phosphorylation and mediated by importin-alpha3. *Proc Natl Acad Sci* 102:8150-8155.
- Livak,K.J. and T.D.Schmittgen. 2001. Analysis of relative gene expression data using real-time quantitative PCR and the 2(-Delta Delta C(T)) Method. *Methods* 25: 402-408
- Lorber B (1997) Listeriosis. *Clin Infect Dis* 24:1-9.
- Luft BJ, Hafner R, Korzun AH, Leport C, Antoniskis D, Bosler EM, Bourland DD, III, Uttamchandani R, Fuhrer J, Jacobson J, . (1993) Toxoplasmic encephalitis in patients with the acquired immunodeficiency syndrome. Members of the ACTG 077p/ANRS 009 Study Team. *N Engl J Med* 329:995-1000.
- Luft BJ, Remington JS (1992) Toxoplasmic encephalitis in AIDS. *Clin Infect Dis* 15:211-222.
- Luo D, Szaba FM, Kummer LW, Plow EF, Mackman N, Gailani D, Smiley ST (2011) Protective roles for fibrin, tissue factor, plasminogen activator inhibitor-1, and thrombin activatable fibrinolysis inhibitor, but not factor XI, during defense against the gram-negative bacterium Yersinia enterocolitica. *J Immunol* 187:1866-1876.
- Lutjen S, Soltek S, Virna S, Deckert M, Schluter D (2006) Organ- and disease-stage-specific regulation of Toxoplasma gondii-specific CD8-T-cell responses by CD4 T cells. *Infect Immun* 74:5790-5801.
- Mahoney DJ (2008) Both cIAP1 and cIAP2 regulate TNFalpha-mediated NF-kappaB activation *Proc Natl Acad Sci* 105:11778-83
- Makarova KS (2000) A novel superfamily of predicted cysteine proteases from eukaryotes, viruses and Chlamydia pneumoniae *Trends Biochem Sci* 25(2):50-2

- Manicassamy S, Gupta S, Huang Z, Sun Z (2006) Protein kinase C-theta-mediated signals enhance CD4+ T cell survival by up-regulating Bcl-xL. *J Immunol* 176:6709-6716.
- Marsland BJ, Kopf M (2008) T-cell fate and function: PKC-theta and beyond. *Trends Immunol* 29:179-185.
- Marsland BJ, Nembrini C, Grun K, Reissmann R, Kurrer M, Leipner C, Kopf M (2007) TLR ligands act directly upon T cells to restore proliferation in the absence of protein kinase C-theta signaling and promote autoimmune myocarditis. *J Immunol* 178:3466-3473.
- Marsland BJ, Nembrini C, Schmitz N, Abel B, Krautwald S, Bachmann MF, Kopf M (2005) Innate signals compensate for the absence of PKC-{theta} during in vivo CD8(+) T cell effector and memory responses. *Proc Natl Acad Sci* 102:14374-14379.
- Marsland BJ, Soos TJ, Spath G, Littman DR, Kopf M (2004) Protein kinase C theta is critical for the development of in vivo T helper (Th)2 cell but not Th1 cell responses. *J Exp Med* 200:181-189.
- Mason NJ, Liou HC, Hunter CA (2004) T cell-intrinsic expression of c-Rel regulates Th1 cell responses essential for resistance to Toxoplasma gondii. *J Immunol* 172:3704-3711.
- Massoumi R (2009) Down-regulation of CYLD expression by Snail promotes tumor progression in malignant melanoma *J Exp Med* 206:221-32
- Massoumi R (2010) Ubiquitin chain cleavage: CYLD at work. *Trends Biochem Sci* 35:392-399.
- Massoumi R, Chmielarska K, Hennecke K, Pfeifer A, Fassler R (2006) Cyld inhibits tumor cell proliferation by blocking Bcl-3-dependent NF-kappaB signaling. *Cell* 125:665-677.
- Montoya JG, Liesenfeld O (2004) Toxoplasmosis. *Lancet* 363:1965-1976.
- Mowen KA, Glimcher LH (2004) Signaling pathways in Th2 development. *Immunol Rev* 202:203-222.
- Mullarky IK, Szaba FM, Berggren KN, Parent MA, Kummer LW, Chen W, Johnson LL, Smiley ST (2005) Infection-stimulated fibrin deposition controls hemorrhage and limits hepatic bacterial growth during listeriosis. *Infect Immun* 73:3888-3895.
- Nijman SM (2005) A genomic and functional inventory of deubiquitinating enzymes *Cell*. 123(5):773-86
- Pamer EG (2004) Immune responses to Listeria monocytogenes. *Nat Rev Immunol* 4:812-823.
- Perkins ND (2007) Integrating cell-signalling pathways with NF-kappaB and IKK function. *Nat Rev Mol Cell Biol* 8:49-62.
- Pfeffer K, Matsuyama T, Kundig TM, Wakeham A, Kishihara K, Shahinian A, Wiegmann K, Ohashi PS, Kronke M, Mak TW (1993) Mice deficient for the 55 kd tumor necrosis factor

receptor are resistant to endotoxic shock, yet succumb to *L. monocytogenes* infection. *Cell* 73:457-467.

Plitas G, Burt BM, Nguyen HM, Bamboat ZM, DeMatteo RP (2008) Toll-like receptor 9 inhibition reduces mortality in polymicrobial sepsis. *J Exp Med* 205:1277-1283.

Reiley WW, Jin W, Lee AJ, Wright A, Wu X, Tewalt EF, Leonard TO, Norbury CC, Fitzpatrick L, Zhang M, Sun SC (2007) Deubiquitinating enzyme CYLD negatively regulates the ubiquitin-dependent kinase Tak1 and prevents abnormal T cell responses. *J Exp Med* 204:1475-1485.

Reiley WW, Zhang M, Jin W, Losiewicz M, Donohue KB, Norbury CC, Sun SC (2006) Regulation of T cell development by the deubiquitinating enzyme CYLD. *Nat Immunol* 7:411-417.

Rieser E, Cordier SM, Walczak H (2013) Linear ubiquitination: a newly discovered regulator of cell signalling. *Trends Biochem Sci* 38:94-102.

Sabil SD, Jones RG, Deenick EK, Liadis N, Elford AR, Vainberg MG, Baerg H, Woodgett JR, Gerondakis S, Ohashi PS (2007) CD4+ and CD8+ T cell survival is regulated differentially by protein kinase Ctheta, c-Rel, and protein kinase B. *J Immunol* 178:2932-2939.

Salek-Ardakani S, So T, Halteman BS, Altman A, Croft M (2005) Protein kinase Ctheta controls Th1 cells in experimental autoimmune encephalomyelitis. *J Immunol* 175:7635-7641.

Samavati L, Rastogi R, Du W, Huttemann M, Fite A, Franchi L (2009) STAT3 tyrosine phosphorylation is critical for interleukin 1 beta and interleukin-6 production in response to lipopolysaccharide and live bacteria. *Mol Immunol* 46:1867-1877.

Schaeffer EM, Debnath J, Yap G, McVicar D, Liao XC, Littman DR, Sher A, Varmus HE, Lenardo MJ, Schwartzberg PL (1999) Requirement for Tec kinases Rlk and Itk in T cell receptor signaling and immunity. *Science* 284:638-641.

Shiloh MU, MacMicking JD, Nicholson S, Brause JE, Potter S, Marino M, Fang F, Dinauer M, Nathan C (1999) Phenotype of mice and macrophages deficient in both phagocyte oxidase and inducible nitric oxide synthase. *Immunity* 10:29-38.

Soete M, Fortier B, Camus D, Dubremetz JF (1993) Toxoplasma gondii: kinetics of bradyzoite-tachyzoite interconversion in vitro. *Exp Parasitol* 76:259-264.

Stevens L, Htut TM, White D, Li X, Hanidu A, Stearns C, Labadia ME, Li J, Brown M, Yang J (2006) Involvement of GATA3 in protein kinase C theta-induced Th2 cytokine expression. *Eur J Immunol* 36:3305-3314.

Sun SC (2008a) Deubiquitylation and regulation of the immune response. *Nat Rev Immunol* 7:501-11

Sun SC (2008b) New insights into NF-kappaB regulation and function. *Trends Immunol* 10:469-78

- Sun SC (2010) CYLD: a tumor suppressor deubiquitinase regulating NF-kappaB activation and diverse biological processes. *Cell Death Differ* 17:25-34.
- Sun Z, Arendt CW, Ellmeier W, Schaeffer EM, Sunshine MJ, Gandhi L, Annes J, Petrzilka D, Kupfer A, Schwartzberg PL, Littman DR (2000) PKC-theta is required for TCR-induced NF-kappaB activation in mature but not immature T lymphocytes. *Nature* 404:402-407.
- Suzuki Y, Orellana MA, Schreiber RD, Remington JS (1988) Interferon-gamma: the major mediator of resistance against Toxoplasma gondii. *Science* 240:516-518.
- Suzuki Y, Yang Q, Yang S, Nguyen N, Lim S, Liesenfeld O, Kojima T, Remington JS (1996) IL-4 is protective against development of toxoplasmic encephalitis. *J Immunol* 157:2564-2569.
- Tan SL, Zhao J, Bi C, Chen XC, Hepburn DL, Wang J, Sedgwick JD, Chintalacharuvu SR, Na S (2006) Resistance to experimental autoimmune encephalomyelitis and impaired IL-17 production in protein kinase C theta-deficient mice. *J Immunol* 176:2872-2879.
- Thuille N, Wachowicz K, Hermann-Kleiter N, Kaminski S, Fresser F, Lutz-Nicoladoni C, Leitges M, Thome M, Massoumi R, Baier G (2013) PKCtheta/beta and CYLD are antagonistic partners in the NFkappaB and NFAT transactivation pathways in primary mouse CD3+ T lymphocytes. *PLoS One* 8:e53709.
- Urbanik T, Kohler BC, Boger RJ, Worns MA, Heeger S, Otto G, Hovelmeyer N, Galle PR, Schuchmann M, Waisman A, Schulze-Bergkamen H (2011) Down-regulation of CYLD as a trigger for NF-kappaB activation and a mechanism of apoptotic resistance in hepatocellular carcinoma cells. *Int J Oncol* 38:121-131.
- Utermohlen O, Dangel A, Tarnok A, Lehmann-Grube F (1996) Modulation by gamma interferon of antiviral cell-mediated immune responses in vivo. *J Virol* 70:1521-1526.
- Watford WT, Hissong BD, Durant LR, Yamane H, Muul LM, Kanno Y, Tato CM, Ramos HL, Berger AE, Mielke L, Pesu M, Solomon B, Frucht DM, Paul WE, Sher A, Jankovic D, Tsichlis PN, O'Shea JJ (2008) Tpl2 kinase regulates T cell interferon-gamma production and host resistance to Toxoplasma gondii. *J Exp Med* 205:2803-2812.
- Xu P (2009) Quantitative proteomics reveals the function of unconventional ubiquitin chains in proteasomal degradation *Cell* 1:133-45
- Xu S (2010) IL-17A-producing gammadeltaT cells promote CTL responses against Listeria monocytogenes infection by enhancing dendritic cell cross-presentation *J Immunol* 10:5879-87
- Zarnegar BJ (2008) Noncanonical NF-kappaB activation requires coordinated assembly of a regulatory complex of the adaptors cIAP1, cIAP2, TRAF2 and TRAF3 and the kinase NIK. Zhang J, Stirling B, Temmerman ST, Ma CA, Fuss IJ, Derry JM, Jain A (2006) Impaired regulation of NF-kappaB and increased susceptibility to colitis-associated tumorigenesis in CYLD-deficient mice. *J Clin Invest* 116:3042-3049.

Zhang Z, Fuentes NL, Fuller GM (1995) Characterization of the IL-6 responsive elements in the gamma fibrinogen gene promoter. *J Biol Chem* 270:24287-24291.

Declaration

Hiermit erkläre ich, dass ich die von mir eingereichte Dissertation zum Thema:

Regulation of nuclear factor kappa-light-chain-enhancer of activated B cells (NF-κB) by protein Kinase C theta (PKC-θ) and cylindromatosis (CYLD) in murine listeriosis and toxoplasmosis

selbstständig verfasst, nicht schon als Dissertation verwendet habe und die benutzten Hilfsmittel und Quellen vollständig angegeben wurden.

Weiterhin erkläre ich, dass ich weder diese noch eine andere Arbeit zur Erlangung des akademischen Grades doctor rerum naturalium (Dr. rer. nat.) an anderen Einrichtungen eingereicht habe.

Magdeburg, den 27.08.2013

Nishanth Gopala Krishna

Curriculum vitae

Persönliche Daten

Name	Gopala Krishna Nishanth
Adresse	503, Fermersleber Weg 45A 39112 Magdeburg
Geburtsdatum	16.12.1980
Geburtsort	Hyderabad, AP, India
Familienstand	Verheiratet
Telefon	0049-391-5585468
E-Mail	<u>nishanth.gopala@med.ovgu.de</u>

Hochschulausbildung

1999 - 2001	Bachelor of Science, von Osmania University , Hyderabad, Indien
2001 - 2003	Masters of Science, von Osmania University, Hyderabad, Indien

Beruflicher Werdegang

2003 - 2007	Wissenschaftlicher Mitarbeiter des Centre for Cellular and Molecular Biology, Hyderabad, Indien
seit 2007	Wissenschaftlicher Mitarbeiter des Instituts für Medizinische Mikrobiologie , Otto-von-Guericke- Universität Magdeburg.